

POLITECNICO DI TORINO

Faculty of Engineering

DMEAS

Master's degree in biomedical engineering

Master Thesis

**Design, prototype development and
testing of an antibody-drug conjugate
using a novel colchicine derivative**

ACCADEMIC YEAR 2019/2020

POLITECNICO DI TORINO

Faculty of Engineering

DMEAS



Supervisor

Prof. Jacek Adam Tuszynsky

Prof. Afsaneh Lavasanifar

Candidate:

Antonio Vitale

ACCADEMIC YEAR 2019/2020

Acknowledgement

I would like to express my deepest gratitude to.

- My supervisor Prof. Jacek Adam Tuszynski for giving me the opportunity to work on one of his important projects. Thanks to this work experience I learnt a lot about how to pursue a work goal acquiring different notions every day. Furthermore, I really appreciated his wise advices about my project as well as his kind reliability. Finally, I cannot thank him enough for his endless essential help and motivation throughout such a unique historical period due to all the problems related to the Covid-19 pandemic.
- My supervisor Dr. Afsaneh Lavasanifar for giving me the opportunity to chase my studies in her lab among with all the given advices about my work.
- My Co-supervisor Dr. Mohammad Reza Vakili for introducing me to the thrilling chemistry world, guiding me during the whole period of experiments.
- My kind lab mates Dr. Forughalsadat Sanaee, Sams Sadat, Igor Pavia, Waleed Neyaz, Parnian Mehinrad for their support and help all the time that I needed.
- Dr. Vishwa Somayaji for his help with the $^1\text{HNMR}$ spectrometry.
- My houseowners Wojciech and Gillian for have become my first Canadian friends in this adventure. I really enjoyed the time spent together breaking up the concrete and most of all your help during the initial sad moments.
- All my friends that shared with me these five years period of university studies or the ones before. Particularly, I would like to thank some of them. My housemates for being my second family, spending with me all the beautiful party moments as well as the challenging periods during the exam's preparation. My close friend Simona for all the patience proved and for listening to all my thoughts. Silvia for have been my personal tester for all the recipes made in these years. Finally, my oldest friends Enrico and Dario, the "dictator" and the "boy with a concert in his head" respectively, whom knowing me longer, they helped me to do not take the life always too seriously.

- My unique girlfriend Alessandra, who I met only four years ago and is changing my life. Even if I was on the other side of the world, I felt always at home with you and I which I could feel the same emotions very soon again. You knew me better than anyone else in these years, living with me many adventures and life goals always together. Especially, I would like to thank you for cheering me up every day with you words, kindness and endless love.
- I finally thank my father, mother and my little brother for having always believed in me, providing constant love, affection and comprehension. I couldn't have been who I am today without your constant presence.

Contents

1. Abstract.....	6
2. Introduction	7
2.1 Cancer Outline	7
2.3 Colchicine	30
2.4 Compound CR-42-024.....	35
2.5 Introduction to ADC	39
2.6 Antibody characteristics	42
2.7 Payload.....	46
2.8 Taxonomy of Linker	48
2.9 Conjugation site and strategies	52
2.10 Summary of ADC fundamental parameters.....	57
2.11 Polyethylene glycol (PEG)	60
2.12 Thesis Proposal	61
3. Materials and Methods.....	63
3.1 Introduction.....	63
3.2 Materials.....	63
3.3 Methyl carbamate deprotection	64
3.4 CCI-NH ₂ /linker conjugation	66
3.5 Direct conjugation.....	68
3.6 Antibody drug conjugation	70

3.7 Measuring the drug amount on antibody by UV/Vis spectrometry	72
3.8 In vitro cellular uptake	73
3.9 <i>In-vitro</i> release study	75
3.10 <i>In-vitro</i> cytotoxicity study	75
3.11 Analysis apparatus	76
3.12 Statistical analysis	77
4 Results.....	78
4.1 Characterization of synthesized products.....	78
5 Discussion and Conclusion.....	94
6 Future directions	96
7. References	98

1. Abstract

From the Paul Ehrlich's idea of the "magic bullet", developed more than 100 years ago, outstanding findings pushed many researchers and companies to getting into the ADCs technology. The modular structure of the ADCs based on three major constituents, a monoclonal antibody (mAb), a linker molecule and a cytotoxic payload, theoretically allows the appropriate efficacy and controlled therapeutic toxicity for the treatment of many cancers and not only. Nowadays, many other diseases are also treated with this strategy. Today, seven ADCs are marketed and several hundred are advancing through different preclinical and clinical stages of development.

A deep analysis of the ADC class of treatments it has been reported by the introduction chapter of this thesis. Many recent techniques have been mentioned, explaining the pivotal points for a complete theme comprehension.

After that, the main purpose of this Master thesis work was to design, synthesize and test in-vitro a novel antibody-drug conjugate (ADC) using Panitumumab as a biological molecule and a new produced colchicine derivative molecule, named CCI-001 as a payload. First, several reactions have been carried out in order to obtain the chemical conjugation between the CCI-001 with a heterobifunctional pegylated linker, taking advantages of two different strategies. Two of the obtained products, CCI-NH₂ and L+D₁, were then deeply characterized by several analytical methods. The therapeutic index of these obtained new molecules was found improved when compared to the CCI-001. Particularly, showing a tremendous increase in hydrophilicity compared to the standard one. Moreover, the cytotoxicity of these new molecules as well as for the final ADC was assessed in three different cell lines, finding a preserved cytotoxicity in a nanomolar concentration range. However, no one of the ADC treated cell lines reached the 50 % of the cell viability. With the purpose of explain this behaviour, the uptake of the standard antibody was monitored thanks to the conjugation with a fluorescent dye. EGFR receptor dependent attitude was confirmed, leading to some final thoughts to explain the unexpected ADC lack in cytotoxicity.

2. Introduction

The present chapter introduces the essential notions to fully understand the theory behind this Master's thesis work. In further detail, section 2.1 carries out a survey of the cancer disease, in the interest of EGFR hallmark and a deep characterization of Pancreatic cancer disease reporting its rationale as well as the current standards of care since it has been chosen as a target disease in this work. Whereas, section 2.2 dissects the Microtubule targeting agents, stressing the Colchicine molecule along with one of its derivative called CCI-001, because of the direct exploitation of this molecule in this work. After that, this chapter describes the class of antibody drug conjugates (ADC) treatment, with focus on their core principles as well as a short summary of their preparation strategy since the purpose of this work regards the design of a novel ADC molecule.

2.1 Cancer Outline

As a consequence of the current medicine development, supported by the better understanding in human physiology as well as the latest findings in the microbial and viral fields, nowadays almost no one of the diseases that were widely spread in ancient times (like Cholera or Tuberculosis) is still dangerous. On the other hand, today cancer disease is the second among the Non-Communicable Diseases (NCDs) for the number of fatalities and DALYs in the world. Only in 2017, there were around 24.5 million incident cancer cases worldwide and 9.6 million cancer deaths, furthermore it caused more than 233.5 million of DALYs [1]. The largest increase in cancer incident cases between 2007 and 2017 occurred in middle SDI countries, with a 52% increase. The drivers that give rise to the cancer incidence involve environmental risk factors (like radiation or pollution exposure), lifestyle (lack in physical activity) or genetic predisposition. However, despite the encouraging results reached in the treatments of some tumours, one third of cancer patients are still terminal. Because of this lack in decisive standard therapy, cancer disease is one of the most studied target for the development of several new drugs.

2.1.1 Cancer nature

As Dhobzansky discusses in his work, the cancer cell can be said to be “for something”, it is a crude survival, as better option to avoid extinction [2]. In this characterization, and because it promotes survival, cancer is an alternative form of life, one that is latent, and coded in all eukaryotic cells, which gives rise as a solution to the problem of alleged existential threats. Thus, the alteration of the existing status quo, as mentioned above, led by many root causes, which can be preventable or not preventable, competes in the development of cancer [3]. Regardless of that, the common outcome of the former and the latter factors results in DNA cellular changes. At that point, if these changes are too large or if the cell isn't strong enough to fix them itself, a cancer disease starts in terms of uncontrolled growth and cell division. This new-born cells are unspecialized when compared to the healthy ones, causing tissues lack of functionality where they arise. While the worst-case scenario results in a condition incompatible with life. Over the years many definitions have been reported in order to define the broad cancer condition. Hanahan and Weinberg, in 2000, recognized six key features that mark cancer, such as the presence of own growth signals, resistance to antigrowth signals, apoptosis escape, high tissue invasiveness and metastasis, sustained angiogenesis and limitless replicative potential. Moreover, genetic instability plays a pivotal role in the aetiology of this group of diseases. One important point to consider is that, even if there is a set of molecular alterations or behaviours that may be common for all cancers, the cells transformed under the control of these common features do not necessarily result in the same evolutionary path or the same final phenotype neither. This consequent cancer heterogeneity, especially for the differences of molecular targets, is an open problem for the development of a curative therapy. Nowadays, chemotherapy, radiation and surgery are the standard of cares for cancer treatment, as monotherapy or a as combination of the three. In order to overcome the cancer heterogeneity, the former deals with a combination of drugs, oral or intravenously administered, the latter uses high-energy particles or waves, such as x-rays, gamma rays, electron beams, or protons, to destroy or damage cancer's DNA. However, the systemic delivery of such potent cocktails of drugs as well as the high potency of radiations carry several drawbacks, affecting the even the healthy cells. Moreover,

due to the lack in the treatment specificity, the malign cells can easily rearrange their genomic information in order to become resistant against this treatments. Besides, as reported in the Heng-Duesberg model, an accelerated macroevolution is the central trait of cancer, resulting in the rapid emergence of resistant variants, as would “adaptive resilience” as an ancient trait. Thus, a novel promising approach to treat this elaborate condition is the “personalized medicine”. This approach involves new agents that can selectively target some cancer biomarkers, mainly those that drive the cancer. So that, Epidermal Growth Factor receptor (EGFR) as well as the hormone receptor are just two among hundreds of suitable targets due to their amplification/mutation in the cancer cells. Even if this therapy is not truly personalized in an individual sense, it can be applied to a large subset of patients, that overexpress the same detectable hallmarks in their tumour. Encouraging results reached in this direction deal with recombinant humanized monoclonal antibodies, such as trastuzumab for HER2-positive breast cancer, in addition to more complex devices like the antibody drug conjugates (ADC).

2.1.2 EGFR a promising target for cancer treatment

As just mentioned, every tumour cell has an alteration at the genome level, which may be detected by changes in the cell phenotype, either in the cell interior or on the cell surface. This means that, each cancer cell is always covered by an array of biologically active surface molecules, that acting also as receptors for specific ligands, may result in signal transduction to the cell’s genetic machinery. Most often, this signal transduction leads to an increase in tumour division and cell spreading [4]. The Growth factor receptors, an important family of these cancer hallmarks, consist of four members of membrane-spanning receptors such as EGFR1, HER2, EGFR3 and EGFR4. In particular, the EGF receptor (also called HER-1) is a single chain transmembrane glycoprotein with six different specific ligands, such as EGF, TGF- α , amphiregulin, β -cellulin, HB-EGF and epiregulin. After the ligand binds to a single-chain EGFR, the receptor forms a dimer, which triggers the autophosphorylation of the C-terminal tail. The autophosphorylation is the first among a multi-step intracellular signaling pathways, which play prominent role in normal cellular growth. Even if not all the theory behind the EGFR mechanism of action it has been well elucidated, it was possible to understand some

basic functions of this important cellular receptor, drawing a relation with the related cell activity, as shown in Figure 1. The followed list of pathways provides a general outlook of the EGFR mechanism of action, without going too into details since it is not the primary aim of this work [5]:

- The activation of the serine/threonine mitogen-activated protein (MAP) kinase cascade is involved with cell division. Closer, the MAP cascade is composed by the subsequent activation of Shc/Grb2/Sos/Ras/Raf/MEK1/2/Erk1/2 resulting in the expression of transcription factors such as Ell-1 and *c-fos*.
- Cell division can be promoted also through the activation of lipid kinase phosphatidylinositol-3kinase (PI3K). A positive feedback loop between Gab1 and PI3K leads to anti-apoptotic signaling through the transcription factor (NF)-kB by the activation of protein kinase B (PKB) and PKC. Both

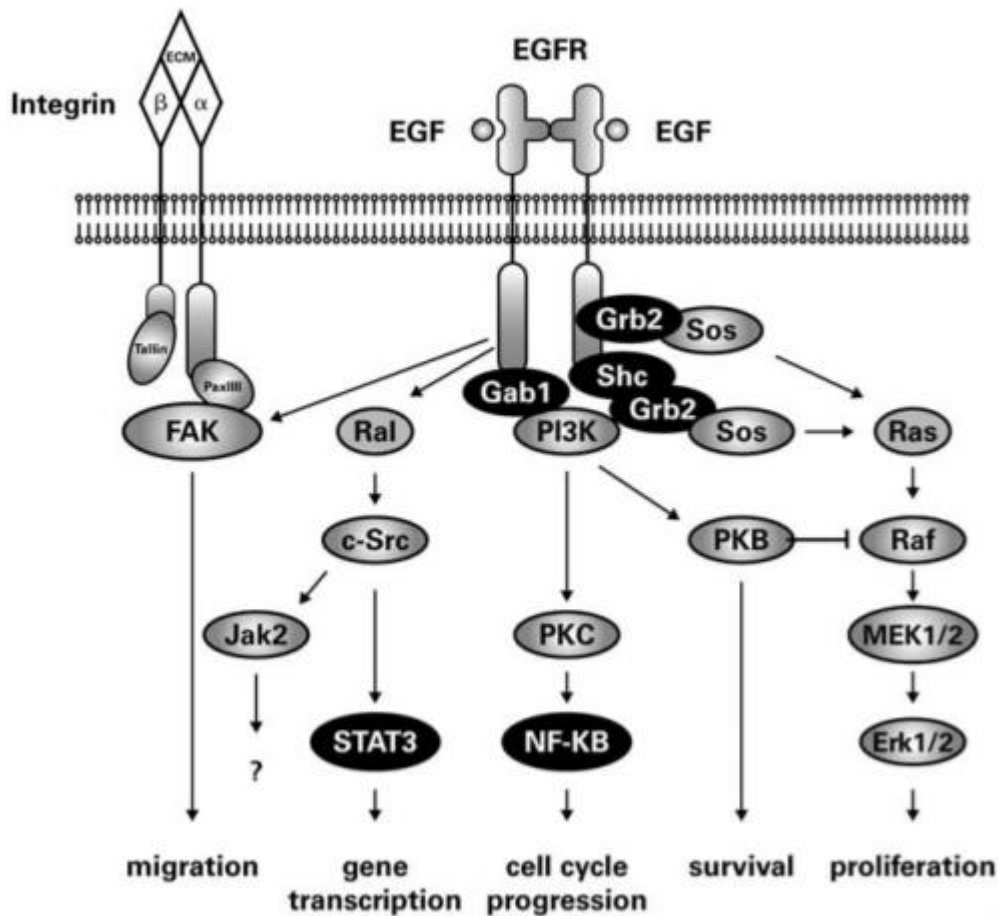


Figure 1. Main pathway cascades for the EGFR.

last listed protein kinases pathways are also deeply implicated in several tumour behaviours.

- Being strictly related to the induction of the signal transducer and activator of transcription (STAT) family of transcription factors, the activation of the c-Src cascade covers a very important role in the growth as well as in the transformation of cancer cells. For instance, the STAT3 activation is implicated in the resistance of tumour cells against cytotoxic therapy.
- Even if the activation of the PLC γ pathway bears a central role in the cell motility boosting, resulting in tumour invasion and metastasis, the involvement of the MEK signaling is still required in order to have a proper trigger.
- To conclude, pro-angiogenic factors are related to the activation of STAT3 and MEK pathways, resulting in the production of vascular endothelial growth factor (VEGF).

Despite the predominant EGFR blockade has a cytostatic outcome, treatments using cetuximab (an anti-EGFR monoclonal antibody) as a monotherapy has been shown to induce apoptosis in endothelial cells of xenograft models of prostate and pancreatic carcinoma. On the other hand, there is plenty of literature on how the EGFR blockade can lead to an increase efficacy when coupled with chemotherapy and radiation therapy. However, even the process behind this supporting mechanism is still under study. On the other hand, the cancer cells anti-recovery effect which takes place after EGFR blockade treatment results well established [5].

Nevertheless, mutations and genetic alterations occurred at many genes and microRNAs (miRs) may result in aberrant signaling pathways, that are implicated in several human diseases, such as psoriasis, Alzheimer's disease, schizophrenia and many tumour phenotypes. In particular, in this last field of application, the alteration in EGFR signaling pathways results in cancer cell proliferation, activating invasion and metastasis, developing drug resistance, blocking apoptosis and increasing the angiogenesis as well [6]. The mRNA expression of this receptor, tested thanks to real time PCR, is widely found in every tumour type, but considerable expression, including also the co-expression with HER-2 receptor, is a distinctive mark correlated with more advanced disease, poor survival and

metastasis in pancreatic cancer, which is one of the conditions in which this thesis is focused on [7].

Given the wealth of information regarding the structure and function of this receptor and its importance in human cancer, the EGFR signal pathway has proven to be an ideal target for the rational design of anti-cancer agents. Hence, two classes of EGFR antagonists are now in clinical use, such as anti-EGFR monoclonal antibodies and small-molecule EGFR tyrosine kinase inhibitors. The former, such as cetuximab, binding with the extracellular domains of the receptor (ECDs), can discontinue its function. The latter such as erlotinib, competes reversibly with ATP to bind to the intracellular catalytic domain of EGFR tyrosine kinase, inhibiting the EGFR autophosphorylation and the subsequent signaling [8]. Specifically, this work gives special emphasis to the anti-EGFR monoclonal antibodies, that in theory recognize EGFR exclusively and are therefore highly selective for this molecular structure. Even though, in practice the EGF receptor and the downstream signal pathway are largely affected by genomic modifications that may result in acquired resistance of treatments.

2.1.3 Pancreatic Cancer

The pancreas is a six to eight inches long gland organ located in the abdomen. It fits in the gastrointestinal tract, within which it plays an essential role in the transformation of the food in free accessible energy for the cells. Mainly, the pancreas has two functions, an exocrine one (performed by acinar cells) and an endocrine one (performed by α , β , δ , ϵ cells). The former represents the cells for the 95% of the whole pancreas weight and produce pancreatic enzymes to aid the digestion, the latter comprises hundreds of thousands of endocrine cells known as islets of Langerhans that plays important hormone regulatory function, secreting molecules such as insulin and glucagon, that are essential for the blood sugar level homeostasis. Due to its important function, diseases that affect this organ certainly result in disorders for the whole body. Leaving out the rare genetic diseases, the most common pathologies for this organ are chronic/acute pancreatitis, diabetes and pancreatic cancer. There are different types of pancreatic cancers. They are divided into two main groups, according to the different pancreas cellular phenotype. The

former is made by mutated exocrine cells, and accounts for the most cases, the latter includes neuroendocrine tumours started in the neuroendocrine cells. Therefore, pancreatic ductal adenocarcinoma (PDAC) is the most common type, because of its over 90% expression, among all pancreatic cancer patients. To date, pancreatic cancer is the fourth most common cancer worldwide with a 5-year overall survival of less than 8%, owing to its two common traits of this condition are aggressive nature and early metastasis. Nowadays, surgery and chemotherapy are the two therapies available for this condition, but they are inadequate. Surgery is runnable on less than 20% of patients. So far, the current first-line chemotherapy, such as cytidine analogues, the poly-chemotherapeutic protocol FOLFIRINOX, or gemcitabine plus nab-paclitaxel, respectively act almost as a palliative solution, since are limited by intrinsic or acquired chemoresistance. Despite experimental evidences assert that the involvement of the tumour microenvironment is crucial in the chemoresistance, as recent data show that CAFs contribute to gemcitabine failure metabolizing this agent. On the other hand the whole underlying mechanisms are poorly understood [9]. Moreover, PDAC tumour also express a high level of radioresistance, resulting in tumour progression even during therapy. Here again, the mechanisms in charge seem to be multifactorial, since both the hypoxic tumour environment as well as an over expression of key regulators of the DNA damage response appear to be implicated. Unfortunately, ample evidence reports that the incidence of PDAC is expected to rise until doubling, both in terms of new diagnoses and in terms of PDAC-related deaths in the U.S. as well as in European countries, within the next ten years. A certain reason for this is based on the magnitude of different risk factors, except for the overall ageing, associated with this malignancy. Briefly, they can be summarized in cigarette smoking and exposure (1.74-fold increased risk), type II diabetics (1.8-fold increased risk), increased body mass index and alcohol consumption (1.55-fold and 1.46-fold increased risk respectively).

2.1.4 Biological hallmarks of pancreatic cancer adenocarcinoma (PDAC)

The risk factors just described as well as other macro- and microenvironmental stimuli, such as tissue damage, inflammatory, or stress conditions are the primary triggers in a process called acinar-to-ductal metaplasia (ADM). The high level of

acinar cells plasticity provides the basis for this process, in which acinar cells transdifferentiate to more epithelial (ductal-like) phenotypes. In the first instance, due to the acquired “progenitor cell-like” phenotype, the acinar cells are more vulnerable to proto-oncogenic hits. Hence, two key mutations occur at the proto-oncogene KRAS and at the phosphoinositide 3-kinase (PI3K). The former comes out in up to > 90% of PDAC tumours resulting in acceleration of tumour-promoting potential, the latter results also elevated in PDAC leading to increased tumour cell survival [10-11]. However, the whole understanding of the PDAC transcriptomic landscape is still poor due to the presence of many more uncommon alterations such as the germline mutations in DNA damage repair genes (e.g. breast cancer early onset genes 1/2 (BRCA1/2), and ataxia telangiectasia mutated protein serine/threonine kinase ATM) or the somatic mutation in DNA mismatch repair regulator genes [12]. Furthermore, epigenetic (re-)programming is firmly related to tumour progression and metastasis formation [13]. Lastly, the heterogeneity of this malignance is further enhanced by the distortion in non-coding RNAs likewise by DNA methylation and histone post-translational modification. So far, diverse trials have been carried out in order to define distinct subtypes, thanks to the immunohistochemistry, with the goal of grouping patients towards personalized treatment strategies. Despite encouraging findings in this field, nowadays there is still no prerequisites in the application of classification for clinical application. To make things more complicated, the high heterogeneity of PDAC increases upon therapeutic intervention. Moving on the PDAC environment, which Figure 2 reports a schematic representation, it is characterized by some recurrent traits such as the extensive desmoplastic stroma, hypoxia and desmoplasia, macrophages recruitment and the systemic frequencies of monocytes and granulocytes. The first one of these peculiarities is prevalently composed by extensive desmoplastic stroma (up to 90% of the tumour volume) that is originate from cancer-associated fibroblasts (CAFs), which can be either myofibroblastic or inflammatory phenotypes. Specifically, pancreatic stellate cells play a central role in the development in this pervasive abnormal extracellular matrix (ECM). In this way, because the expression of focal adhesion kinase 1 (FAK1) in PDAC is a significant step in the ECM building process, it is a suitable target for therapeutic intervention [14]. As far as Hypoxia is concerned, due to its origin from desmoplasia-associated

hypervascularization, it is tightly interlinked with desmoplasia. Together these two conditions represent a barrier against T cell infiltration and activation as well as a trigger for a strong accumulation of myeloid cells [15-16]. Finally, monocytes and granulocytes lead to an important immunosuppressive function, preventing the T cell function [17].

Another PDAC hallmark is its fast and easy progression to metastatic disease. Even if the exact causes are still poorly understood, three corroborations seem to play an active role in this process such as many tumour micro- and macroenvironment parameters, blood glucose concentration and pre-existing future target factor released by the primary tumour mass [18-19]. The first one among these features is finely tuned by the epithelial-to-mesenchymal transition (EMT). Briefly, this transformation, expressed by the quasi-mesenchymal PDAC subtype, is an attribute associated with poor prognosis due to the rapid metastasis formation. Furthermore, together the common source and the quasi-staminal nature of the PDAC cells compete in the high degree of clonality inside the metastasis. Furthermore, the inverse process, called reacquired epithelial state, seems to be crucial in order to colonize other tissues [20]. Finally, in most pancreatic ductal adenocarcinomas, the overexpression of a specific tubulin isotype called β III-tubulin, which will be well reviewed later, possibly accounts for the suboptimal response of these tumours to microtubule-stabilizing agents, suggesting that microtubule dysfunction is an early feature of this disease [21].

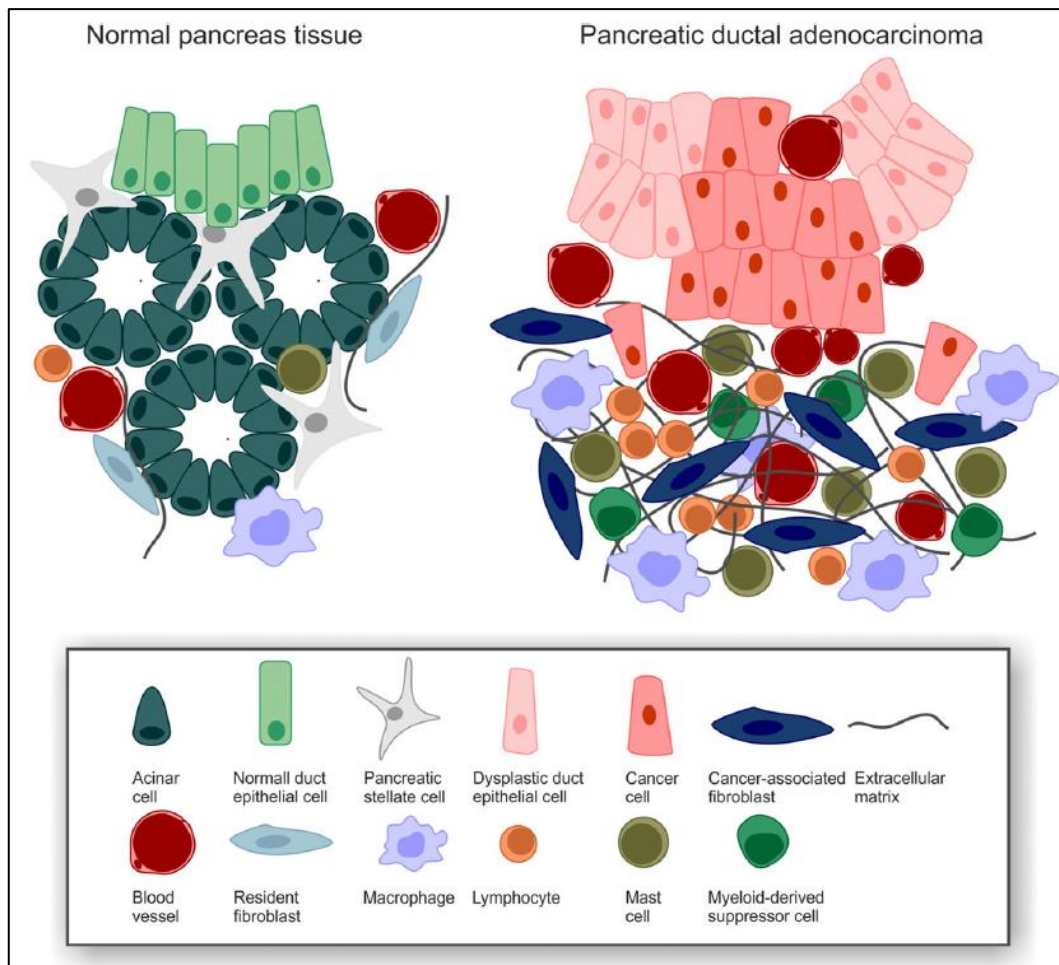


Figure 2. PDAC desmoplasia tumour microenvironment [9].

2.1.5 Role of EGFR in pancreatic cancer

As mentioned before, the rapid and frequent metastasis formation is a distinctive feature in pancreatic cancer, with relevance in PDAC subtype. Even if the importance of this state is commonly well appreciated to be linked to the high PDAC mortality, not too much is known about the molecular mechanism that governs such aggressive invasive behaviour. The EGFR family of receptors plays a pivotal role in many malignant transformations and its involvement has been tested prominent especially in the worst cases of PDAC, in which overexpression of EGFR occurs in over half of all pancreatic cancers. Specifically, it is associated with more advanced conditions, poor survival and high rate of metastasis formation. Several EGFR related mechanisms are responsible for these typical outcomes. For instance, EGFR expression leads to Src-dependent phosphorylation of p130^{CAS}, where CAS is a focal contact-localized scaffolding protein linked to cell migration

and invasion. CAS is the first promoter for the Ras-associated protein (Rap1) signalling, which is an important molecular structure linked to cancer cell migration. Ectopic expression of Rap1GAP inhibits migration in pancreatic carcinoma cells and serves as a metastasis suppressor. However, due to Rap1 very low GTPase activity, it relies on GTP hydrolysis by GTPase-activating proteins (GAPs), which has been identified to be lacking in pancreatic carcinoma. Even though suppressing Rap1 expression blocks EGFR-induced metastasis without affecting primary tumour growth [22]. Moreover, CAS has a prominent role also in the binding with other effectors, giving rise to several intracellular pathways all connected with cell migration response.

The EGFR overexpression is strictly linked to the mutation in the KRAS (Ki-ras2 Kirsten rat sarcoma viral oncogene homolog). As mentioned before, almost the whole PDAC samples harbour oncogenic mutations in the KRAS gene. However, the expression of mutant KRAS doesn't lead to the development of cancer by itself, therefore animals with mutant KRAS overexpression form tumours only after a long latency or pancreatitis induction. This means that there is the need of a secondary event to initiate pancreatic tumour genesis. From intense study on patient samples of transition acinar-to-ductal metaplasia (ADM), EGFR has been tested as upregulated. Thus, EGFR provides the inside-outside signaling that allows the beginning of the signal transduction, under the control of the mutated KRAS gene. For this reason, EGFR when treated with the mAb cetuximab, that binding to EGFR external domain, doesn't work anymore as signaling bridge [23]. However, EGFR inhibition has been shown to be minimally effective in PDA patients, because it is linked only with the tumour genesis not with tumour therapy with the purpose to avoid the tumour progression. In order to have some clinical effects in this way, the monoclonal antibodies have to be used in a multi approach therapies, for instance a phase II trials with cetuximab and radiotherapy indicated that this mAb has a radiosensitizer nature, enhancing the effects of the irradiation, while displayed minimal toxicity [24].

2.1.6 Immunotherapy as a treatment for PDAC

Recently, in order to overcome the poor results achieved with the standard PDAC therapy, since there has not been significant progress with targeted treatments, more attention has been paid to immunotherapy. Normally, the immune system plays an active role in controlling the body, thanks to its effector cells such as natural killer cells (NK) and cytotoxic T cells. These two classes of effectors can recognize the mutated cancer cells and destroy them before development of clinical disease [25]. However, owing to their malignant transformation process the cancer cells may develop specific bypass mechanisms to escape immune response, becoming 'invisible' for the aforementioned immune effector cells, in a dynamic process called immunoediting. According to several current evidence, PDAC results in weak immunogenic nature due to its extreme mutagenicity conduct and innate aggressive behaviour. Several aspects of the PDAC play an active role in the weakness of the immunotherapy approach such as over/down surface molecule expression, external cells infiltration and the execution of specific processes. The first aspect involves mainly the abundant expression of programmed death ligand 1 (PD-L1) and the downregulation of antigen presenting cells (MHC). The former causes T-cell apoptosis, the latter escapes from cell-mediated immunity by downregulating expression of major histocompatibility antigen (MHC) [26-27]. As far as external cells infiltration is concerned, PDAC cells produce granulocyte-macrophage colony-stimulating factor (GM-CSF) which leads the infiltration of myeloid derived cells to the tumour microenvironment, suppressing the antigen specific T-cell response [28]. Finally, through a peculiar process called 'immune privilege', PDAC cells are also able to generate immune tolerance by downregulating Fas receptor signaling to escape immune effector cells attack, while the overexpression of Fas ligand is used to induce apoptosis of activated antitumor cytotoxic T cells [29].

Immunotherapy implementing immune checkpoint inhibitors has boosted cancer treatment in the last years, bearing in mind the outstanding success reached by trastuzumab in breast cancer therapy [30]. Thus, according to recent researches, monoclonal antibodies (mAbs) tested as promising targeting tools in order to treat the immune evasion for several solid tumours, which is led by some

immunomodulatory receptors. However, after some encouraging starting results, mAb did not demonstrate a significant activity. Thereby, Ipilimumab, an anti-CTLA4 antibody, was found to be safe, although did not demonstrate to be effective against tumour growth, when tested during a phase II study [31]. Likewise, an anti-PD-L1 antibody, that acts as immune checkpoint inhibitor for BMS-936559, showed no responses in 14 patients who had been previously treated for PDAC, though significant tumour regression were observed in other solid tumours such as melanoma and lung cancer [32]. The main feature of the immunosuppressive PDAC microenvironment is its massive stromal content and the excessive deposition of extracellular matrix, including hyaluronan, mentioned before [33]. In order to cope to this abnormal deposition, a combined approach with human hyaluronidase 20 with gemcitabine and nab-paclitaxel, tested in early phase clinical trials, revealed promising results [34]. However, stromal myofibroblasts genetically deleted in mouse models led to disease exacerbation with diminished animal survival, due to the enhanced regulatory T cell-mediated immunosuppression [35]. The last shield against the (re-)activation of anti-PDAC immunity is at cellular level, because of massive infiltration by myeloid cells, such as MDSCs, resulting in exclusion of CD88+ T cells [29].

In summary, due to its extremely complex nature, all the single agent strategies reported in order to improve the overall clinical outcome, appear to be more challenging than other cancer entities. Consequently, the most promising strategies would incorporate combinations of different approaches, such as the union between immunotherapy with chemotherapy or radiotherapy [36].

2.1.7 Chemotherapy as a treatment for PDAC

As reported before, advanced/metastatic disease at presentation together with genetic heterogeneity and unique microenvironmental features are the potential barriers for resistance to cytotoxic chemotherapy. This means that efforts are still required in order to overcome this dismal outcome of patients with PDAC.

Along this line, the PDAC overexpression of endothelial growth factor (VEGF), a protein in charge of the pathogenesis and spread of pancreatic cancer, has been

studied in multi-therapeutic approaches. Despite a combination of gemcitabine plus bevacizumab (a VEGF inhibitor), when tested in phase III clinical study, failed to show any significant clinical benefit when compared to single-agent gemcitabine [37].

On the other hand, as far as the heterogeneity is concerned, the PDAC genetically various nature makes hard for the conventional therapies achieves good results. Due to the target to different cellular processes, lead to the success of treatment without affecting the normal cell, which may lead to unacceptable side-effects.

As far as the PDAC genetic heterogeneity is concerned, conventional therapies that target different cellular processes fail to distinguish between cancerous and normal cells leading to unacceptable side-effects. A new promising targeted approach that may be useful, in order to bring the light on the chemotherapeutic agents, depends on the PDAC abnormally fragmented mitochondria. Basically, mitochondria are essential to the oncogenicity of PDAC, since this malignancy requires mitochondrial oxidative phosphorylation to fuel its growth. PDAC fragmented mitochondria are correlated with more oxidative phosphorylation. Thus, oral leflunomide, an FDA-approved arthritis drug can foster the mitochondrial fusion, promoting a 2-fold increase in Mfn2 expression in tumours [38].

2.2 Microtubules and microtubule affecting dugs

Microtubules (MTs) along with actin and intermediate filaments are the principal components of the eukaryotic cell's cytoskeleton. They are necessary for a lot of fundamental cell functions such as carrying out cell division, motility, cell form and morphogenesis, intracellular vesicle trafficking, secretion and surface specialization. The first biophysical evidence of MTs presence was carried out, thanks to their implication in the mitotic spindle of living cells, by Schmidt in 1939. Subsequently, microtubules were discovered by transmission EM studies (Manton and Clarke, 1952; Fawcett and Ported, 1954). The term tubulin, the monomer of microtubules, was coined by Mohri in 1968. Since its discovery, significant contributions have been reported increasing the interest for this biological structure and paving the way for the beginning of the biochemistry era [39]. Due to their deep

implication in several fundamental processes, both for the healthy as well as in the pathological conditions, microtubules are an auspicious target for many novel treatments carrying out by the tubulin-binding agents such as Vinca alkaloids and Taxanes as well (TBAs). Specifically, understanding the existence of different tubulin isotypes, novel more effective and safer treatments are achievable, avoiding the known TBAs toxicity. A focus has been reported on the colchicine molecule, examining how recent works starting from its standard molecular structure, were able to obtain a new colchicine molecule with improved features able to overcome its natural limitation. The understanding of how molecular changes can affect the final outcome is a central point in this work since a novel modified colchicine molecule, which bears an increased affinity toward the β III-tubulin isotype it has been used as a payload in this work.

2.2.1 Microtubule and Microtubule polymerization

Microtubules are dynamic protein polymeric structures composed of a single type of globular protein named tubulin. They are assembled into a cylindrical hollow structure, with internal diameter of about 12 nm and external one about 25 nm and can achieve 50 μ m of length. Each tubulin dimer linked head-to-tail forms a protofilament arranged in parallel. Usually the microtubule structure is composed of a set of 13 of these protofilaments, assembled around a hollow core. The univocal

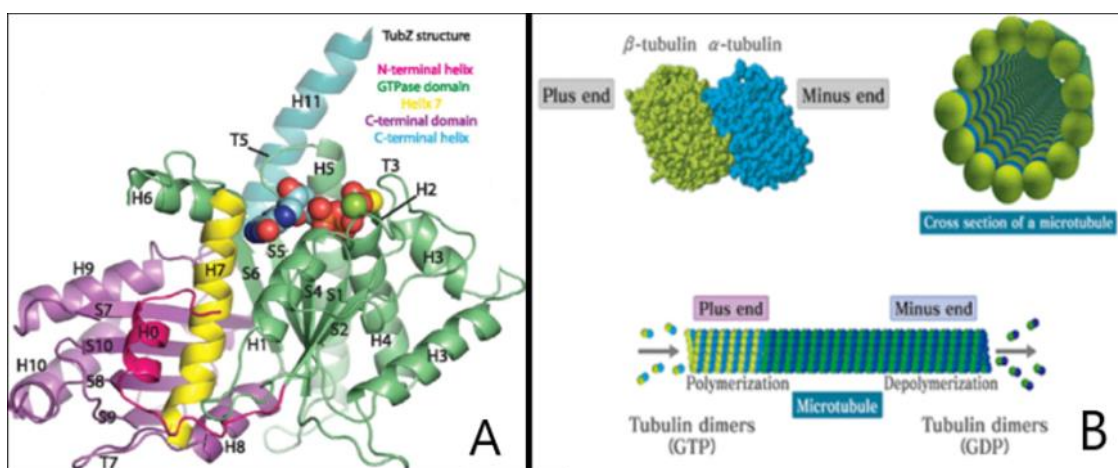


Figure 3. Tubulin X-ray crystallography structure description (A), simple polymerization of microtubules scheme (B).

dimers orientation within the microtubules gives them intrinsic polarity, since the slow-growing α -tubulin faces the minus end, while the fast-growing β units the plus end, Figure 3B. Tubulin is made of α and β tubulin polypeptides (55 kDa each one). Analysing this structure, can be concluded that α - and β - tubulin monomers have a very high level of structural similarity, no differences can be noted at 6 Å resolution, since each monomer is composed by a core of two β -sheets surrounded by a helix. Specifically, each monomer shows three functional domains, as reported in Figure 3A [40]. First, there is the amino-terminal domain, the nucleotide binding region, made of six parallel β -strands (S1-S6) alternating with six helices (H1-H6) and six loops (T1-T6) that directly connected the early structures. At last, helix H7 completes the binding site. After that, together the 3 helices (H8-H10) and β -sheets (S7-S10) form the intermediate taxol-binding domain that will be further investigated in the next paragraph. Finally, the two antiparallel helices (H11-H12) represent the carboxy-terminal domain, which is the motor protein binding site. Moreover, a third type of tubulin (γ -tubulin) forms ring structures that contain 10 to 13 γ -tubulin molecules specifically localized to the centrosome, where it plays a pivotal role in initiating microtubule assembly starting from the minus ends.

Considering the polymerization process of microtubules, the nucleation-elongation mechanism, powered by the hydrolysis of GTP, builds a microtubule core made of tubulin with stoichiometrically-bound GDP and a Pi leaving it, Figure 3B.

Two main mechanisms drive the GTP hydrolysis inside the microtubules, the treadmilling and the dynamic instability. The former involves both the ends on the same microtubule, since leads the offset state between the net growth at one microtubule end, where tubulin molecules bound to GTP, and the net shortening at opposite end, in which tubulin molecules bonding to GDP are continually lost from the minus end [41]. The latter, explained by Tim Mitchison and Marc Kirschner in 1984, deals with the presence or absence of the GTP-containing-tubulin at the microtubule end, the loss of the cap (GTP hydrolysis) leads to the depolymerization process. Both ends can either grow or shorten according to the addition rate of GTP-bound tubulin molecules. As long as the GTP-bound tubulin molecules addition rate is faster than GTP hydrolysis, the microtubule is able to growth, otherwise if the rate of polymerization slows, the GDP-bound tubulin will dissociate, resulting

in rapid depolymerization and shrinkage of the microtubule [42]. More specifically this last mechanism is composed of four main subphases:

- The phase of microtubule growth and shortening
- The “catastrophe” phase, which is characterized by the frequency of transitions from growth or pause to shortening
- The “rescue” phase, which is characterized by the frequency of transitions from shortening to growth or pause

The short half-lives as well as the high dynamic turnover of the microtubule’s dynamic instability play an essential role during mitosis, through the formation of the mitotic spindle. Because of the microtubules involvement in separating the chromosomes they can be used as a therapeutic target to prevent cellular division, predominantly in those “cellular division dependent” diseases like tumours.

Emerging evidence suggests that tubulins as well as microtubule-associated proteins may play an active role in a range of cellular stress responses, thus conferring survival advantage to cancer cells. In light of this, several molecules have been used in cancer chemotherapy to selectively inhibit rapidly dividing cells such as colchicine and colcemid; or also to block cell division, like taxanes, thanks to their binding ability to bind to the β -tubulin [43]. Moreover, it has been reported that also chemotherapeutic agents that do not bind to tubulin can also affect microtubule stability, since microtubules are interlinked with several primarily cellular functions.

2.2.2 Tubulin isotypes and β III-tubulin

Altered tubulin isotype expression is the most widely characterized microtubules alteration reported in cancer and has been observed in both solid and haematological tumours. When compared to α -tubulin isotypes, β -tubulin isotypes have been studied more deeply due to its largest availability of isotype-specific antibodies, the fastest β -tubulin isotypes molecular dynamic and the fact that the TBAs must bind to the β -tubulin subunit to exert their toxic effect. Specifically, β -tubulin has 7 different isotypes (β I, β II, β III, β IVa, β IVb, β V and β VI). They share

high sequence homology, they are encoded by different genes and distinguished by their unique carboxy terminal tail as well [44]. Despite the high sequence homology of these isotypes, genetic analyses enlightened unequivocal evidence for isotype-specific functions in vivo such as meiosis and the final cell shape of platelets. While the former is up to beta-tubulin isotype (encoded by β Tub85D gene), the latter is handled by the beta-tubulin isotype β VI (encoded by TUBB1 gene). Another isotype of tubulin, the beta-tubulin isotype β III (encoded by TUBB3 gene), yields neural migration in mice and plays also a fundamental role in the multidrug resistant mechanism (MDR).

Thanks to the immunohistochemically detectable expression of TUBB3, high β III-tubulin expression has been reported in many tissues, both normal tissues and tumour ones. In normal tissues, it has been founded especially inside the brain neurons as well as the endothelium of blood vessels, on the other hand, when founded in different tumour types, it has been associated with poor patient survival as well as poor response to microtubule-targeting anti-cancer drugs like taxanes. Specifically, it is overexpressed in various brain tumours (85%–100%), lung cancer (35%–80%), pancreatic adenocarcinoma (50%), renal cell carcinoma (15%–80%), and malignant melanoma (77%) [45].

The alteration in expression of the β III-tubulin occurs both at gene level and at protein level, leading to an increased gene transcription and enhanced mRNA stability. However, tubulin final expression is not only settled by the mRNA levels, since many others post-translational mechanisms such as tumour suppressor miR-100 and the miR-200 family as well as epigenetic mechanisms [44]. Several different varieties of cell stress, reported in many cancers, trigger an alteration in β III-tubulin expression, hence led to chemotherapeutic resistance, such as [44]:

- Hypoxic conditions induce β III-tubulin expression through three main factors such as direct binding of HIF1 α (hypoxia-inducible factor heterodimer α) to the E box motif within its 3'UTR, the basal β III-tubulin expression level and the proximity to necrotic tumour regions.
- Oxidative stress conditions, which are ruled by direct interactions between β III-tubulin and glutathione S-transferase as well as by unknown co-

operative mechanisms between β III-tubulin and DNA damage repair enzyme excision repair cross-complementation group-1 (ERCC1). Therefore, thanks to its cys239, β III-tubulin can act as redox switches, since the oxidation of this residue inhibits microtubule assembly and stability.

- Metabolic stress, which is linked to uncontrolled cell proliferation without adequate nutrients, is ruled by β III-tubulin and its implication in glucose stress responses.
- Autophagy activity, thus is intrinsically linked with metabolic stress responses, is strictly influenced by TBAs, since they act as suppressor for microtubule dynamics.
- Cell death signaling, which is a complex network of proteins, may modulate its effect interacting with tubulin, since the binding can reduce the apoptotic potential of cancer cells. For instance, semaphorin 6A (a pro-survival factor), deals with β III-tubulin leading to a resistance for a broad range of chemotherapy agents.

These results suggest the central position of β III-tubulin as a pro survival factor in cancer. This means that this specific isotype has the potential to refine personalized medicine becoming a promising drug target. However, despite this encouraging findings, pharmaceutical agents which can specifically bind to β III-tubulin are almost unexplored [46].

2.2.3 Connection between β III-tubulin expression and drug resistance

Generally, the expression of β III-tubulin is associated with drug resistance as well as poor prognosis in patients, but at high cell level it could be toxic by itself. Particularly, the overexpression of this tubulin isoform is one of the two resistance mechanisms associated with the taxane-resistant tumour phenotype. The initiator of taxanes family, named paclitaxel, fails in a stable binding with the β III-tubulin since this isotype bears an Arg²⁷⁷ instead of a Ser²⁷⁷ as the others tubulin isotype does. Moreover, also the increased microtubules dynamic generated by this tubulin isotype, it makes the microtubules more resistant to the stabilisation of microtubule dynamics operated by taxanes. On the other hand, depolymerizing agent like colchicine, due to its different binding site called colchicine binding site (CBS), it

is not limited by the β III-tubulin presence. In order to exclude the different mode of action for the depolymerizing agents as a possible strategy to evade the treatment resistance led by the overexpression of the β III-tubulin, it has been seen that, even for the vinorelbine, which is a microtubule-destabilizing agents, there is a substantial loss in the efficacy since it bind to the Vinca alkaloid binding site instead of the CBS [47].

On this way seems clear that the presence of punctual variations inside this specific tubulin isoforms are a good starting point in order to develop more specific drugs molecules (or reorganized existing ones) able to provide a target therapy since the expression specific expression of this tubulin isotype in malignant tissue decreasing the MT characteristic systemic cytotoxicity. Moreover, this strategy has relevance for the development of a powerful secondary line of treatment against cancer cell lines that have developed drug resistance after standard chemotherapeutic treatments, with paclitaxel, since it has been established an increased sensitivity to molecules such as colchicine and vinblastine for this resistant cell lines [48]. Cell This new generation of treatments, targeting the β III-tubulin can treat also the beforementioned severe conditions linked to this tubulin isotype.

2.2.4 Expression of β III-tubulin in pancreatic cancer

Human pancreatic tumours and pancreatic cancer cells express high levels of β III-tubulin, especially in advanced PDAC patient tissue specimens. Moreover, aberrant β III-tubulin expression seems to be correlated with activation of KRAS as well as upregulated during the transformation stages of pancreatic intraepithelial neoplasia (PanIN) to, which is the precursor of PDAC. In order to define the functional role of this tubulin isotype, using the gene-silencing approach, researchers have determined its implication in several cancer promoting aspects. In the first place, suppress β III-tubulin expression led to a drop in clonogenic potential, hence in ability to form colonies, of pancreatic cancer cells both in absence and presence of chemotherapeutic drugs. Particularly, muting β III-tubulin in non-tumour genic HPDE cells didn't affect cell viability or growth, proving the fundamental involvement of β III-tubulin in pancreatic cancer cells. Furthermore, β III-tubulin

suppression leads to a marked increase in apoptosis, which is further sustained in presence of chemotherapy drugs [49].

2.2.5 Taxol®

Taxol, a small molecule approved in 1992 by FDA, but first isolated by Wall and Wani from the bark of the tree *Taxus Brevifolia* 20 years early, was the forerunner of the taxanes family [50]. It was proposed as a novel cancer treatment, with the generic name paclitaxel, due to its unique mechanism of action, resulting in a clear role in improving the outcome for cancer patients. High resolution mass spectrometry, the ultraviolet (λ_{max} MeOH, 272 nm, ϵ 4800) and the infrared spectra (ν_{max} CHCl₃ 1680 cm^{-1}) were in accord with the detected Taxol's molecular formula C₃₁H₃₆O₁₁, while Figure 4 displays the correct molecular structure.

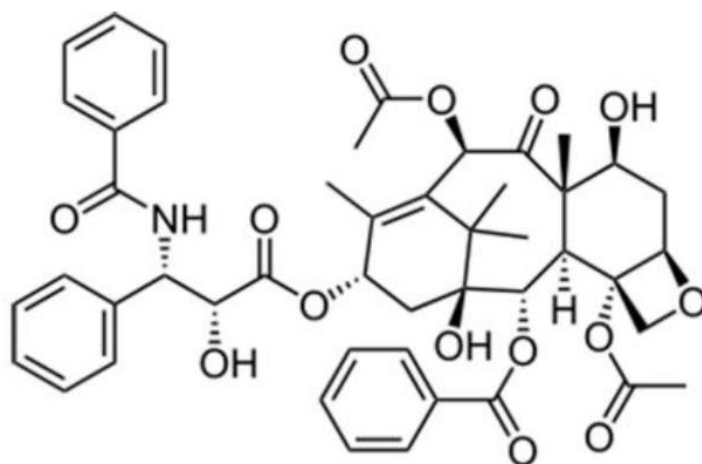


Figure 4. Molecular structure of Taxol.

Taxol® possessed impressive activity against the relatively resistant murine B16 melanoma and a panel of human solid tumours carried as xenografts in mice. For these reasons, today Taxol molecule has been further developed leading to others semisynthetic molecules such as Taxotere® and Cabazitaxel.

The mechanism of action of Taxol® has been carried out almost ten years after its isolation by the Horwitz laboratory in 1979 [51]. This study revealed that Taxol has the capacity to increase the polymerization of stable microtubules. Three amino acid residues have been found to be active in the interaction of Taxol with β III-

tubulin such as the amino acid residues 217-231, the M-loop (residues 273-285) and the N-terminal 31 amino acids. Particularly, the drug reorganized the microtubule cytoskeleton leading to the inhibition of cell proliferation and migration as well. The formation of stable microtubule bundles in cells are a hallmark of Taxol treatment. Due to its singular mechanism of action, the taxol took part of the microtubule-stabilizing agent family. Moreover, Taxol shows two different outcomes depending on its concentration. Cells are blocked in mitosis at higher concentration ($>10\text{nM}$), while aberrant mitosis leads to cells death and suppression of microtubule dynamics at lower drug concentration [⁵²].

2.2.6 Vinca alkaloids

The Vinca alkaloids, displayed by Figure 5, are a microtubule destabilizing family of drugs with specific spindle inhibitor mechanisms. In 1957, the Vinblastine (VLB), extracted from the plant known as the Madagascar periwinkle, was the first molecule belonging to this class, after that other molecules have been discovered such as vincristine, vinorelbine and colchicine, and most of them have been successfully served in clinical use as chemotherapy agents. Explicitly, Vinca alkaloids inhibit cell proliferation by binding to microtubules, which leads to a mitotic block and apoptosis. However, they can also affect the division of healthy cells, leading to common side effects such as neurotoxicity for vincristine and digestive system toxicity for vinblastine. In terms of molecular structure, the Vinca alkaloids family share some common features among which a vindoline ring connected to a catharanthine ring through carbon-carbon bonds [⁵³]. Vinca alkaloids exert their anti-mitosis function binding two sites per mole of tubulin dimer in a distinct position compared to those of the taxanes, colchicine and GTP. Specifically, low concentration of Vinca alkaloids ($<1\ \mu\text{mol}$) leads to a potent kinetic suppression of tubulin exchange binding at the high-affinity sites at the microtubule end. On the other hand, high drug concentration ($>1\ \text{to}\ 2\ \mu\text{mol}$) causes

the slay of microtubules into spiral aggregates or spiral protofilaments, driving to microtubule disintegration.

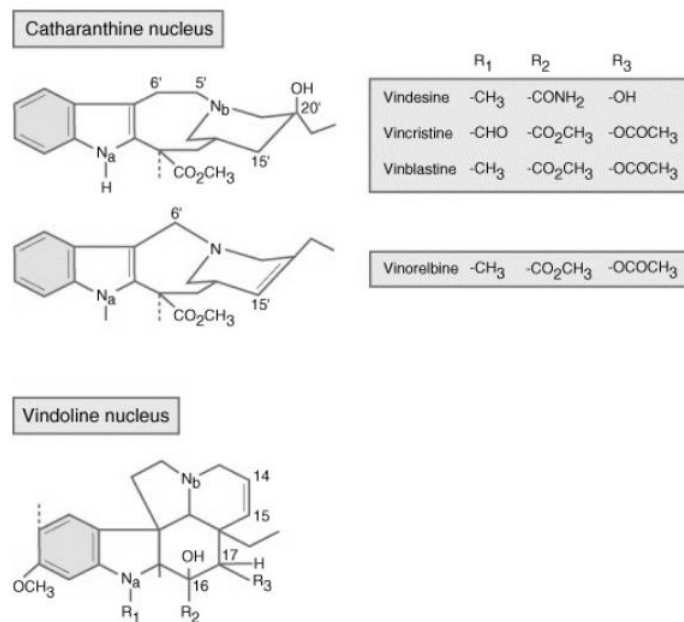


Figure 5. Common molecular structure components of Vinka alkaloids.

2.3 Colchicine

Colchicine has been already used 3000 years ago as a cure upon the extraction from its plant form called *Colchicum autumnale*, nowadays this molecule is a well characterized, Figure 6A. This molecule shows a similar mechanism with the vinca alkaloids, displaying two different outcomes in accordance to its concentration.

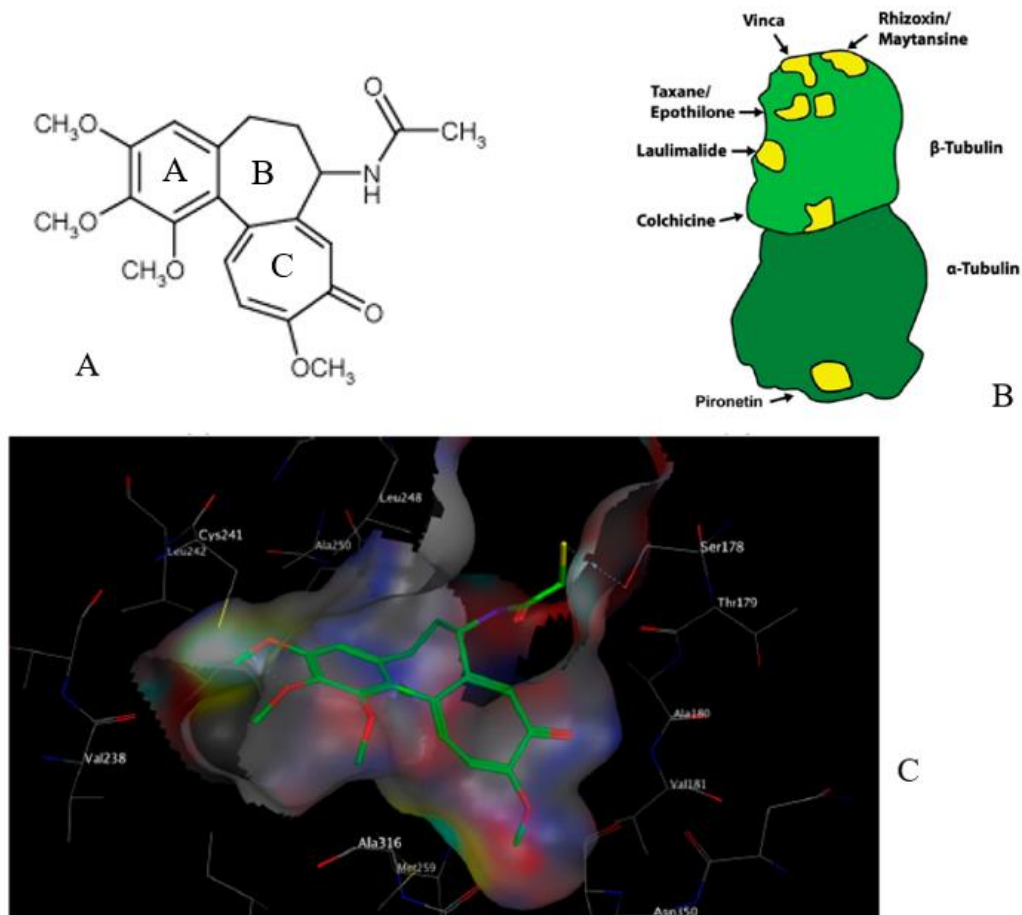


Figure 6. A: Molecular representation of the colchicine molecule. B: Schematic representation of colchicine and other tubulin affecting agents binding site on the tubulin dimer. C: Model of N-deacetyl-N-(2-mercaptoacetyl) colchicine (DAMA)-colchicine bounding between $\alpha\beta$ tubulin dimer.

Interesting, colchicine has no affinity to bind directly to the microtubule ends, while it can join with free tubulin, developing the TC complex that can associate with the

ends of a microtubule, sterically blocking further addition of the tubulin dimers at the growing ends of microtubules [54]. Nonetheless, the TC complex doesn't completely prevent the tubulin addition to microtubules but can only slow down the conjugation of new tubulin. To conclude the analysis of the mode of action, the loss of the microtubule GTP cap occurs at high colchicine concentrations, inducing the microtubules depolymerization. On the other hand, at low concentration it can induce the microtubules stabilization. Thanks to its behaviour of tubulin affecting agent, colchicine is currently used to treat Bechet's disease, familial Mediterranean fever, recurring pericarditis and as a gout medication as well. Moreover, the inhibition of a nucleotide-binding domain (NOD)-like receptor protein 3 (NLRP3) inflammasome protein complex paves the way for a novel, tubulin independent, colchicine application as a promising atherosclerosis-associated inflammation treatment, proving additional features for this ancient drug molecule [55].

Another advantage of targeting the CBS is the angiogenesis inhibition since this physiological process is one of the lead driving process in the solid tumour development process. However, this latter effect takes place only at concentrations near or even more than the maximum tolerated dose for the standard colchicine molecule. Despite the cheap availability of this molecule, its effective application as a chemotherapeutic agent is restricted by its high toxicity, the high interaction with the P-gp efflux pump, which lead to drug resistance and the narrow therapeutic index since once injected as a free drug, it can be absorbed equally from both healthy and tumour cells. This high cytotoxicity is given by its ability to accumulate intracellularly many-fold over the concentration added to the culture medium [56]. In high doses, it can cause hepatocellular failure, marrow failure, disseminated intravascular coagulation and late central-nervous-system dysfunction, but most of all it is harmful for the gastrointestinal tract. However, as said before, the colchicine tricyclic alkaloid molecule structure can be easily modified in order to modulate different outcomes.

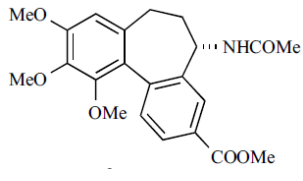
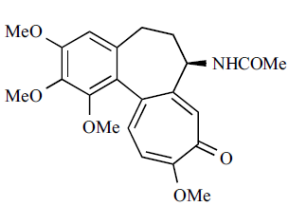
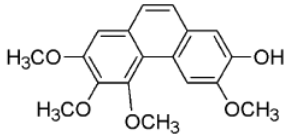
2.3.2 Colchicine structure-activity relationship (SAR)

Looking closely at the colchicine tubulin mechanism of action it can be seen how, once the colchicine molecule binds to the $\alpha\beta$ -tubulin dimer, it leads to a substantial

change in the shape of the polypeptide's dimer. The primary effect of this conformational change is the impair interaction between the lateral $\alpha\beta$ -tubulin dimers, which is fundamental to allow the normal microtubules assembly process [57]. Each one of the three carbon rings in the colchicine molecule plays an active role for the final effect. It has been described the pivotal participation of the 3,4,5-trimethoxyphenyl A ring in the interaction with the colchicine binding site (CBS), conferring the known strength of this interaction. Specifically, a 3.5 Å X-ray structure of the $\alpha\beta$ tubulin dimer, complexed with the DAMA colchicine, Figure 6C, revealed the formation of a strong hydrogen bond between the tubulin Cys-241 and the DAMA-colchicine A ring. On the other hand, the seven membered B ring doesn't has an active role in the molecule binding function, however, it plays a crucial role in retaining the stereochemistry of the colchicine molecule, enabling the correct molecular folding required for the right placement of the C ring inside the CBS. The latter, called tropolone ring, forming the hydrogen bond between the Thr-179 and Val-181 α -tubulin monomer, it bears for the tubulin assembly inhibitory function thanks to its oxygen atom. Figure 7 and Table 1 provide more detailed description of this relationship between the structure modifications of the colchicine molecule and its final function. Since the structure activity relationship (SAR) of this molecule has been deeply investigated, several different derivatives, produced modifying the B and C rings, showed improved therapeutic efficacy or better binding features compared to the unchanged molecule.

Table 1. Brief summary of the colchicine most important groups involved in its therapeutic activity.

Molecular group	Mechanism	Example molecule
Trimethoxy phenyl (A ring)	Stabilizer for the TC complex anti-tubulin activity [58]. Sets the correct molecule conformation [59].	

	Synthetic modifications of this ring lead to loss of biological activity	
Tropolone (C ring)	<p>The 10-methoxy group can be replaced with halogen, alkyl, alkoxy or amino groups without affecting tubulin binding affinity, while steric bulk substituents decrease the activity [60].</p> <p>Seven-membered tropolone can be exchanged with an aromatic phenol without affecting the affinity with tubulin.</p>	<p>Allocochicine</p> 
Seven-membered (B ring)	<p>Non primarily crucial for tubulin binding ability.</p> <p>Sets some properties such as activation energy reversibility and quantum yield of the drug-tubulin complex.</p>	<p>Unnatural 7R-colchicine (without any tubulin binding activity) [61].</p> 
Dihedral angle between the A and C rings	<p>A planar or nearly planar settlement does not result in an active molecule. I.e. combretastatin A-4 [62].</p> <p>High activity has been established for angles between 30° to about 60°. Molecules with angles larger</p>	

	or smaller than these values are less active [63].	
--	--	--

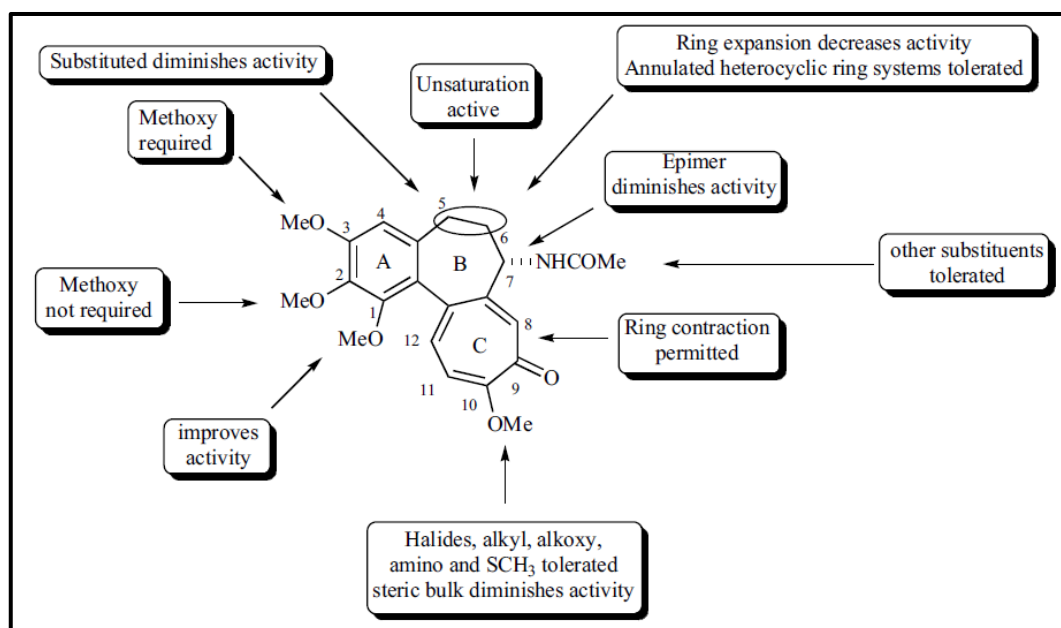


Figure 7. Colchicine ring characterization. Brief summary of the colchicine structure activity relationship.

Another important point is the strong interaction between the P-gp efflux pump, a 170 kDa transmembrane protein, and the colchicine molecule. For this reason, some cancer cells, which usually overexpress this protein, can easily eliminate the colchicine molecule. Conformational changes in this protein occur after binding its substrate. In this way, expanding its transmembrane helical domain, this protein allows the transport outside the cell of its ligands, even more than one at a time. Particularly, the hydrophobic interactions play a central role in a colchicine efflux by p-gp for resistant cancer cell cultures [64]. For this reason, the introduction of polar substituents at the C-10 position of colchicine by replacing 10-oMe group with OH, Cl, NH₂ or NH-substituted groups could reduce the colchicine efflux [61]. In this way, two promising molecules, bearing a chlorine group or a primary amine at the C-10 position show an improved behaviour [65]. The resulting decrease in the P-gp interaction is made possible thanks to a different binding orientation in the P-gp cavity given by H-bonding and ionic interactions within the Ala-987 and Gln-725 residues on the outer side of the transmembrane protein cavity. However,

despite achieving lower P-gp affinity, they show a decrease in cytotoxicity when tested on HCT-116 cell line, displaying IC_{50} values of 6.0 μM and 0.04 μM respectively. Values that seem not promising when compared with the IC_{50} of the standard colchicine on the same cell line (0,05 μM).

From the last consideration seems evident how a small change made on the colchicine molecular structure can improve one parameter making another worst. In light of this, an effective change on the molecule, which can be worth of an intensive study in order to reach an optimized final product concerns the design of a βIII -specific colchicine derivative since as profoundly explained before this isomeric tubulin form is deeply implicated in differ cancer mechanisms.

2.4 Compound CR-42-024

Seventy derivatives of existing microtubule-affecting compounds have been designed using a high-performance computing cluster, synthesized in two series (CH and CCI) and tested for them cytotoxicity in vitro by J.A. Tuszynski et al, Experimental Oncology, University of Alberta. The objective was to obtain a βIII tubulin selective binding ability and higher cytotoxicity against cancer cells compared to the standard colchicine molecule. The study's screen consisted in: in silico/in vitro function, in vitro cytotoxicity and finally the lead compounds were examined in vivo. For the CH series, compound CH35 showed better results, improving cytotoxicity compared to the standard colchicine molecule as well as the other derivatives against several cancer cells but having lower lethality on the normal ones [66]. However, compound CH35 wasn't eligible to be patented. With reference to the CCI series, CCI-001 and CCI-42-23 were found to be patentable but thanks to a superior predicted ADMET profile, the CCI-001 has been identified as a lead compound, demonstrating the following properties [67]:

- Anti-mitotic in vitro at nM concentration.
- Anti-motile, preventing cell migration at pM levels and possibly anti-angiogenic in mouse models.
- No specific organ toxicity. Additionally, when tested against normal human fibroblast cell line, it showed relatively low cytotoxicity effect.

- In vivo toxicity as low as 0.05 mg/kg. On the other hand, colchicine (LD50 1,7 mg/kg), taxol (MTD = 50 mg/kg), gemcitabine (MTD = 120 mg/kg) and cisplatin (9 mg/kg) show higher values.
- Efficacy better than some licensed standard of care products.

CCI-001 is high effective on cancer cell lines in vitro and is more cytotoxic than paclitaxel, which doesn't display anti-angiogenic ability at all. A SAR rationale for these previously described compounds is reported in Figure 9, while Figure 8 reports the molecular structure for the two previously cited promising compounds CH35 and CCI-001.

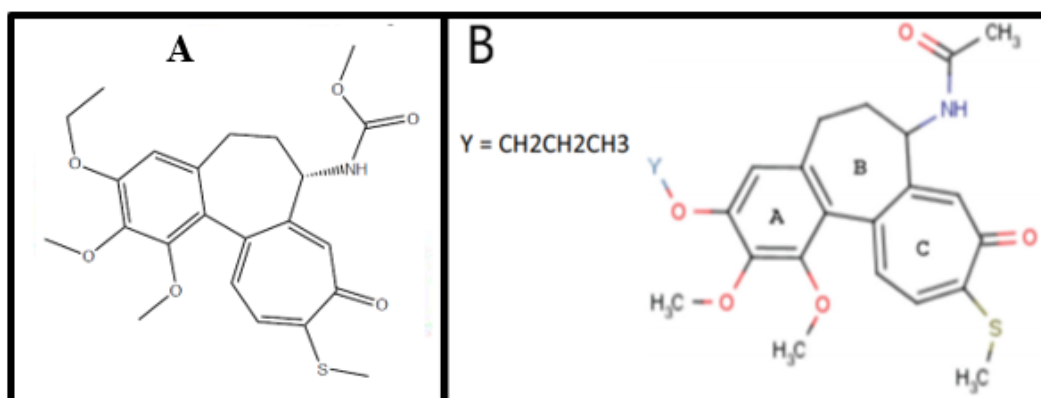


Figure 8. A: CCI-001 molecular structure representation. B; CH-35 molecular structure representation.

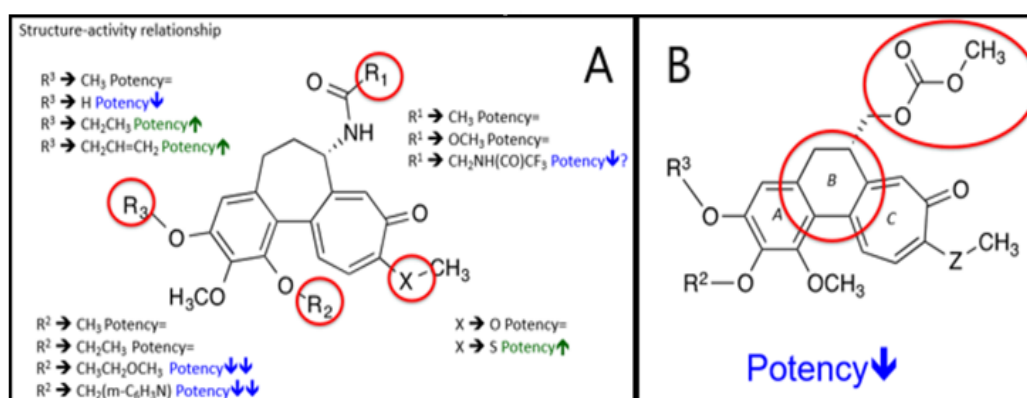


Figure 9. A: SAR of Colchicine molecule. B: SAR of 6-carbon B-ring variants.

Being a colchicine derivative, CCI-001 has a similar mechanism of action. CCI-001 treatment causes an increase in proportion of cells in G2/M phase leading to the induction of apoptosis in a dose-dependent manner. Moreover, prolonged exposure to CCI-001 induces microtubule depolymerization and causes loss of microtubule integrity.

The better result carrying by the CCI-001, which even increasing the affinity toward the β III-tubulin, displaying -48.4 as predicted binding free energy, still doesn't present loss in other characteristics when compared to the standard colchicine molecule. Nevertheless, when was compared with all major anti-tubulin agents (Paclitaxel, Laulimalide, Vinblastine, Combretastatin and Taccalonolide) in regard to their effects on taxol-resistant breast cancer cells, it exhibited the best GI50 values (between 0.5 and 3 nM), even if cell viability was still present at high concentrations. The resistance was due to the presence of the beforementioned Pgp intramembrane protein. It was determined that CCI-001 is a weak substrate for p-glycoproteins. Hence, this could be a possible contribution factor to drug resistance, although this is many times less pronounced than in the case of the parent compound. Subsequently, a new treatment strategy that involved the combination between CCI-001 and 3BP was found to be more effective even against resistant cell lines. For instance, a significant effect also has been observed on paclitaxel resistant SK-BR-3 breast cancer cell lines. The way for further improvements of this novel drug molecule seems promising. However, despite all the reported good qualities, the CCI-001 high hydrophobicity as well as its very low (nanomolar) effective concentration, make the systemic use of this molecule challenging. A first trial in order to increase the uptake and improve the administration as well resulted in a micellar formulation containing the CCI-001 as a payload. A polymeric combination of PEO_{5k}-b-PBCL_{7.9k} it has been used, obtaining an encapsulation efficiency of 94.5 % and increase the solubility 24.7-fold times when compared to the standard free drug.

2.4.1 CCI-001 as a promising treatment

As a possible solution to increase cancer specificity and selectivity by a narrowing the molecular target selection, the CCI-001 colchicine derivative has shown very

positive results when used as a treatment agent for many dozens of tumour cell lines.

- Most of all it has been revealed as most effective against bladder cancer and pancreatic cancer due to the characteristic high expression of β III-tubulin in both these two cancer families [67]. In addition, CCI-001 showed high efficacy also against cell lines that are resistant to Gemcitabine (an antineoplastic chemotherapeutic agent), when tested on bladder cancer cell lines, as reported by Figure 10. Another important result observed was the CCI-001 highly synergistic effect with cisplatin when given as a conjunction therapy. This provides another clinical avenue to further pursue CCI-001, which may allow the level of cisplatin to be reduced while maintaining efficacy in the treatment of metastatic bladder cancer patients. On the other hand, CCI-001 is antagonistic when given in conjugation with Gemcitabine. A very high in vitro treatment efficacy was also assessed for two pancreatic cancer cell lines called MiaPaCa-2 and Panc-1 showing IC50 of 4.42 nM and 3.28nM respectively.

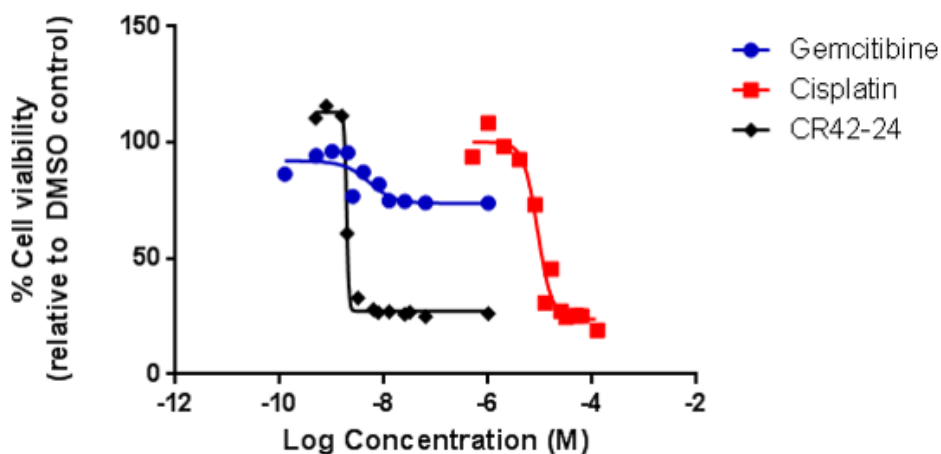


Figure 10. UMUC-3 (a human Bladder Transitional Cell Carcinoma Derived) Gem-Cis Cytotoxicity.

- It has been demonstrated, using both mass spectrometry performed on hGBM (human glioblastoma patient specimen) and in silico modelling, a favourable binding energies between TUBB4 (a protein involved in cell

membrane trafficking) and the glucose transporter GLUT1, which is overexpressed in patient-derived human glioblastoma multiform (GBM).

2.5 Introduction to ADC

As a new class of immunoconjugates, the antibody drug conjugates (ADCs) offer a new promising way of targeted treatment for various diseases. Primarily developed for oncology applications. After the initial success, they are starting to be employed also for non-oncological indications such as ophthalmology and as anti-inflammatory therapeutics [68-69]. In the field of cancer treatment, they show a significant opportunity to overcome the drawbacks related to classical chemotherapy treatments, such as side effects of systemic therapy, acquired drug resistance or relapse, but also they constitute a new way to deliver the future wave of radiopharmaceuticals [70-71]. The value of the global market for ADCs is estimated to be expanding at a compound annual growth rate in excess of 20% and expected to reach \$15 billion by 2030. Notably, more than \$5 billion has been invested in this ADC sector, and partnership activity has increased at an annual rate of 30%. Tumour-specific monoclonal antibody (mAB), a cytotoxic drug (usually too toxic to be used alone) and a specialized chemical linker make up together the ADCs typical structure, which is shown in Figure 11. Infinity adjustments are

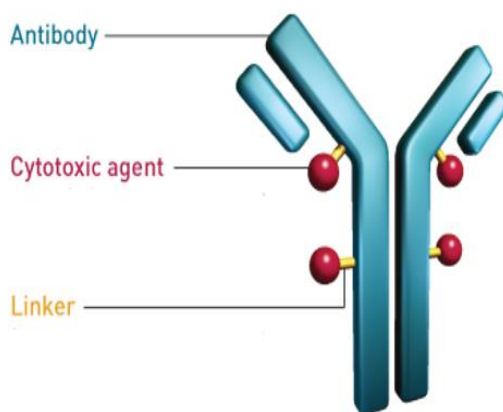


Figure 11. Schematic structure of a basic antibody drug conjugate.

doable playing with these three main blocks since thousands of different drug molecules, recombinant antibodies and suitable chemical linker structure are

discovered every day. Each of these structure bears several properties which must to be finely regulated in order to have a well-known and a final ADC that works properly. Moreover, this trilateral structure can be enriched by the addition of other molecules with the aim of reaching specific behaviours. For instance, a PEG molecule inside the linker structure as a spacer as well as the use of bulk polymeric nano molecules are just two examples of the ADC adjustability. Lastly, starting from the ADC strategy, the collection of viable approaches can become even larger if other biomolecules are considered as building block instead of the antibody such as antibody fragments or small peptide. The following chapters, providing a brief summary of the theory behind the ADC design and applicability, will be useful in order to better understand the experimental work done in this thesis.

The result of the ADC characterization and preclinical studies is the delivery to the market of eight approved by the FDA clinically tested ADCs, as shown in Table 2 [72]. At the same time, more than 100 ADCs are currently in different stages of clinical development, and there are hundreds of ongoing clinical trials involving ADCs as reported in ClinicalTrials.gov and by PubMed. An early proof-of-concept can be achieved relatively rapidly in a Phase I study, with an appropriate biomarker and patient selection, hence commercial organizations are willing to invest in these novel therapeutic modalities. Despite these encouraging findings, there are some limiting factors such as cell phenotype heterogeneity within a tumour and a high cost associated with the scale-up of GMP-level production. Furthermore, it is worth to mention that the ADC production require a long path and a multi-step process, in which each phase plays a significant role for the good success of the final ADC. Moreover, the development of antibody-drug conjugates would not have been possible without collaboration, discussions and many informal exchanges of ideas between peers as well. Many conferences have been arranged across the world in order to provide an appropriate platform to engage and discuss new ideas, such as the world ADC organized by Hanson Wade in San Diego.

Table 2 Up to date clinically available ADCs and providers.

Drug	Maker	Condition	Trade name
Gemtuzumab ozogamicin	Pfizer/Wyeth	Relapsed acute myelogenous leukemia (AML)	Mylotarg
Brentuximab vedotin	Seattle Genetics, Millennium/Takeda	relapsed HL and relapsed sALCL	Adcetris
Trastuzumab emtansine	Genentech, Roche	HER2-positive metastatic breast cancer (mBC) following treatment with trastuzumab and a maytansinoid	Kadcyla
Inotuzumab ozogamicin	Pfizer/Wyeth	relapsed or refractory CD22-positive B-cell precursor acute lymphoblastic leukemia	Besponsa
Polatuzumab vedotin	Genentech, Roche	relapsed or refractory (R/R) diffuse large B-cell lymphoma (DLBCL)	Pilivy
Enfortumab vedotin	Astellas/Seattle Genetics	adult patients with locally advanced or metastatic urothelial cancer who have received a PD-1 or PD-L1 inhibitor, and a Pt-containing therapy	Padcev
Trastuzumab deruxtecan	AstraZeneca/Daiichi Sankyo	adult patients with unresectable or metastatic HER2-positive breast cancer who have received two or	Enhertu

		more prior anti-HER2 based regimens	
Sacituzumab govitecan	Immunomedics	adult patients with metastatic triple-negative breast cancer (mTNBC) who have received at least two prior therapies for patients with relapsed or refractory metastatic disease	Trodelvy

2.6 Antibody characteristics

Following the development of hybridoma technology by Köhler and Milstein (1975), combined with serological techniques and analytical tools, monoclonal antibodies were used to dissect the surface structure of human cancer cells, thus paving the way for the identification of cancer cell surface antigens suitable for targeting by antibodies. Generation of monoclonal antibodies from many species, including humans, is required in order to avoid the negative consequences due to the innate response of the body's immune system, as was common with the first generation of ADCs since they used murine monoclonal antibodies. To do this, a specific approach has been developed, [73]. Nowadays, the rise of monoclonal antibody technology, with its increased specificity, longer half-lives, more predictable overall pharmacokinetic and pharmacodynamic behaviours than their small molecule inhibitor counterparts, paved the way for new approaches in cancer treatment.

Basically, the antibodies are Y-shaped complex proteins structures, which consist of four polypeptides chains. Each polypeptide chain is assembled by different amino acids joined thanks to the peptide bond, a chemical bond where the carboxyl group of one molecule reacts with the amino group of the other molecule, releasing a molecule of water (H₂O). The immunoglobulin class derives from antibody's heavy-chain variety (γ , μ , α , ϵ , δ) [74]. The most common subtype used is the IgG due to its long half-life, around one week *in vivo*. Figure 13 reports the IgG antibody

molecule general structure enlightened its composition. Briefly, a characterization of the antibody molecule can be done as follow [75]:

- **Heavy chain:** each antibody has two identical heavy chains of about 50 kDa, which are essential in order to carry on the antibody activity mediation function.
- **Light chain:** each antibody has two light chain of about 25 kDa, which the end part of these is responsible of the antigen binding function.
- **Fab fragment:** composed of one constant and one variable domain of each of the heavy and the light chain, the Fab fragment thanks to its specific 3D conformation is directly responsible for the antigen binding specificity on the cell surface. In fact, 3D changes in this important terminal structure will lead to a loss in antigen binding affinity.
- **Fc region:** situated in the tail region of antibody, it allows the binding with the immune system effectors such as neutrophils or T-cells line family.

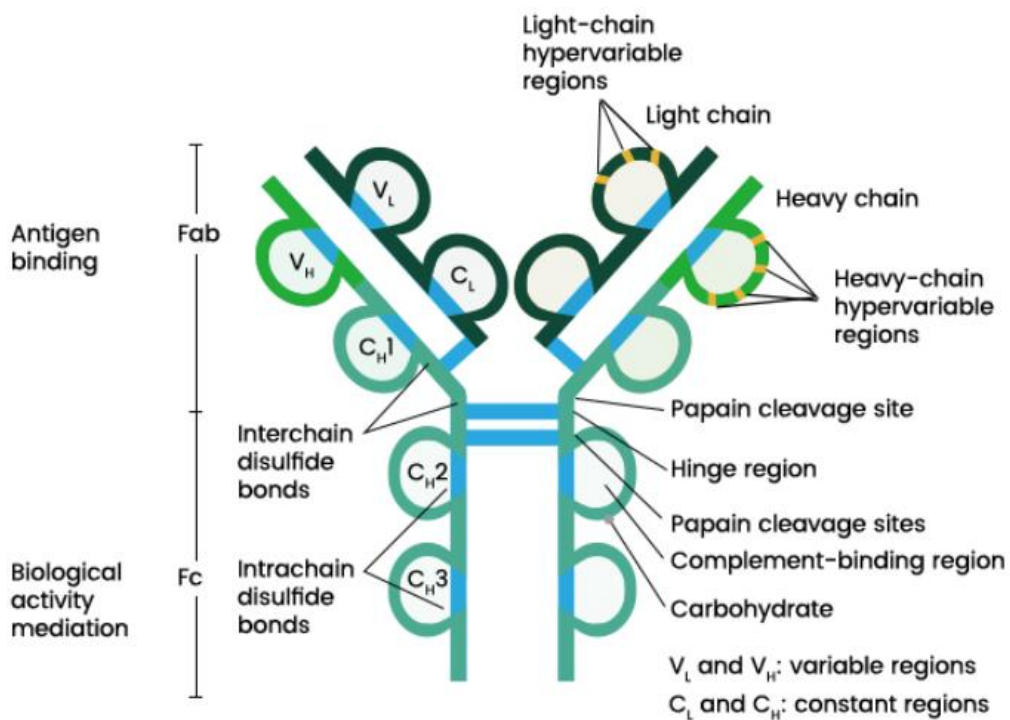


Figure 12. Antibody structure diagram [75].

The entire IgG structure is bind together thanks to the presence of 4 disulfide bounds, two between the heavy chains and two between the light and the heavy chains, as reported in Figure 12.

As far as the IgG antibody is concern, they can persist for the very long periods inside the body after that some external triggers such as bacteria, viruses, neutralises bacterial toxins aloud their initial production. Moreover, when complexed with macrophages they can enhance their effectiveness. In this way, it has been reported that an antibody can induce antibody-dependent cell-mediate cytotoxicity (ADCC) and complement-dependent cytotoxicity (CDC). The former is critical in monoclonal antibody (mAb)-mediated cancer therapy, the latter could be the causes of higher toxicity of the ADC.

As far as this work is concerned, the main mAb concerns the ability to finely recognize the presence, if existing in an adequate concentration, of a specific antigen (target) on the cell surface, which could allow the subsequent binding mediated internalization. Substantially, the monoclonal antibody in the ADC structure acts as a key, able to reduce a lot the drug cytotoxicity, when compared to a simple drug systemic administration. However, the complete off-target effect neutralization is only theoretically available.

2.6.1 Panitumumab

It is obvious that, being different proteins, each antibody has a unique mechanism of action. The following discussion reports the behaviour of a specific antibody called Panitumumab since it will be the biological protein employed in this work. Panitumumab is a recombinant, fully humanized, immunoglobulin G2 monoclonal antibody that targets the epidermal growth factor receptor (EGFR). It has been approved by the U.S. Food and Drug Administration (FDA) and the European Medicines Agency (EMA) for the treatment of patients with EGFR-expressing metastatic colorectal carcinoma (mCRC) after failure of standard chemotherapy.

As previously discussed, the EGFR phosphorylation is the first stage among a vast cascade of events that lead to the cancer growing. Since now, panitumumab thanks to its specific binding affinity with this membrane receptor, has shown two cytotoxic effects. First, binding the EGFR extracellular domain, by competing with

endogenous ligands like the EGF molecule, preventing the subsequent receptor phosphorylation, it stops the whole cascade of events that happen after the normal receptor phosphorylation [76]. Particularly, panitumumab's binding epitope on the EGFR receptor accounts for P349, P362, D355, F412 and I438. Two of the previously listed epitope (D355 and K443) are shared with the EGF binding site. As far as the binding affinity for EGFR, panitumumab shows a value near 0.05 nM, binding the cellular receptor with more than 8fold greater affinity than that of cetuximab, which is another anti-EGFR monoclonal antibody. According to the most recent researches, at K_D concentrations between 1 and 10 nM, panitumumab can reach its optimal anti-EGFR tumour targeting, accumulation and retention.

Because of its IgG2 nature, panitumumab isn't in the position to induce NK cell-driven ADCC or cytotoxic T-cell tumour infiltration, as does cetuximab instead. However, it can lead to some immunostimulatory action via neutrophil driven ADCC and monocytes [77].

Another important thing to bear in mind is that due to its considerable size, the antibody ability to penetrate through the cell membrane is always less when compared to the penetration efficacy of a small peptide chain, for instance a single-chain fragment variable (scFvs), which has usually a molecular weight around 30kDa. Furthermore, this last molecular entity, thanks to the absence of the Fc region shows reduced immunogenicity.

To conclude, panitumumab has two different *in vivo* mechanisms of clearance. When administrated at doses below 2 mg/kg it is internalized into the cells with followed lysosome degradation once internalized within the cells. At doses above 2 mg/kg the clearance is mediated by the reticuloendothelial system (RES) [78].

2.6.2 Panitumumab and Colorectal cancer

Approved for the treatment of EGFR-expressing (K)RAS-unselected chemo refractory mCRC by the US FDA and the EMA in 2004 and 2007 respectively, to date more than 240,000 patients received panitumumab-containing therapy [79]. According to the recent updates, panitumumab is indicated for RAS wt mCRC as a monotherapy after failure of fluoropyrimidine-, oxaliplatin-, and irinotecan-

containing chemotherapy regimens, in combination with FOLFOX or FOLFIRI in first-line, and in combination with FOLFIRI in second-line mCRC^[77].

Recently, it has been proposed also another outcome, suggesting how panitumumab can further inhibit tumour proliferation through the EGFR internalization and via protein destabilization, resulting in reducing cell's proliferation, without any proper apoptosis^[80]. Interestingly, even if some works report how the inhibition of the EGF signal pathway through monoclonal antibody is ineffective against patients whose tumours do not harbour Kirsten rat sarcoma (KRAS) mutations, on the other hand an equal number of publications state the undistinguished effectiveness of the antibody treatment^[80-81]. For sure there is a difference in treatment outcome between panitumumab administered in vivo or in vitro. In fact, when used in vivo it is not effective against colorectal cancer patients with a mutation in KRAS. However, the total understanding of the panitumumab exact mechanism of action is far to be known since even some patients with wild-type KRAS can develop a resistance against this biomolecule.

2.7 Payload

The payloads employed in the ADC approach can be characterized as follows: small molecules, plant-, animal- or microorganism-derived, usually hydrophobic^[82]. A first generation of drugs used in the development of ADCs derived from clinically validated chemotherapeutic agents, such as doxorubicin and methotrexate. Nevertheless, after they showed promising results in preclinical trials, they produced poor results in vivo analysis due to the low therapeutic index and low antitumor activity at reasonable doses.

Afterwards, cytotoxic payloads, such as auristatin or maytansine derivatives, being 100- to 1000-folds more potent in vitro than the chemotherapeutic agents, have been used to improve the performance of the second generation of ADCs.

Nowadays, the third generation of ADCs is becoming available for testing and it involves more homogeneous ADCs with well-characterized DARs and desired cytotoxicity developed by site-specific conjugation methods.

Based on the existing examples, an assumption can be made that the available payloads employed in ADC approaches belong to the following three main classes: (1) the DNA-damaging (cyclopropylpyrrolo[e]indolones (CPIs), Calicheamicin (ozogamicin), Duocarmycin and Benzodiazepine (PBD)) [17- 18], (2) the microtubule inhibitors (Thailanstatin A and Pladienolide B, Maytansinoids and Colchicine derivatives) [19- 20] and (3) the antifolate agents (such as methotrexate and trimethoprim) [21-22].

2.7.1 Drug-to-antibody ratio (DAR)

The drug-antibody ratio (DAR) must be well defined in order to have a reproducible and scalable ADC production process. Experimental works revealed that the optimal DAR for most ADCs is 4 drug molecules per antibody to ensure a compromise between cytotoxicity and pharmacokinetic stability of ADCs.

High DAR values are directly dependent to the in vitro potency of ADCs, but this could lead to faster clearance or potential immunogenic reactions in some cases instead [83-84]. Pfizer has reported that conjugation to highly exposed sites such as the C-terminal of the heavy chain results in high hydrophobic ADCs, resulted in high clearance. On the other hand, conjugation to “hidden” sites such as the C-terminal of the kappa chain, comes from ADCs with lower hydrophobicity and lower clearance. The DAR could be influenced using different linkers, since the linker polarity can play a relevant role in the conjugation of large hydrophobic molecules. All in all, higher DAR has two main problems: 1) Conjugation liabilities, that lead to the increase of aggregation and 2) PK liabilities. These two problems are interconnected because they are driven by hydrophobicity [85].

To overcome the limitations that DAR generates by the endogenous hinge cysteine residues of the mAb, reaching a maximum number of payloads at ~8, an intermediary dendritic or polymeric linker can be adopted between the antibody and the payload. This last approach, as mentioned before, shows how broad could be the adjustability of the final ADC molecule.

As will be better explained later, the initial ADC DAR value is not a fixed number, on the contrary it can quick change under several conditions such as time, environmental presence of enzymes or changes in pH and most of all the specific

chemistry of the linker as well. In order to characterize the temporal evolution of this very important measure, several analyses can be carried out. In this way, the hydrophobic interaction chromatography (HIC) and the UV-spectroscopy can result in a viable strategies. The former provides the exact percentage rate between different clusters of conjugation in the same pool of ADC, but it requires a very specific and expensive apparatus. The latter, thanks to a simple absorbance detection and following the Lambert-Beer law, it gives one number as the average between all the different clusters of DAR.

2.8 Taxonomy of Linker

The linker bears several very important features in every ADC. It is a chemical structure, most of all linear, composed of different chemical motifs which support specific behaviours. The goal of the linker is to bind together the cytotoxic drug and the antibody, through specific mechanisms, preventing the splitting outside the targeted cell. To get this done, there are mostly two classes of linkers available: cleavable ones and non-cleavable ones. The former plays an active part in the degradation process once the ADC has been internalized inside the cell, the latter involves a solution that requires the antibody degradation inside the cell in order to allow the drug to be effective.

From the beginning of the ADC technology, a lot of different linkers with different chemical structures, cleavable mechanisms and efficacy have been proposed. Whatever is the linker chemistry, for an ADC to be selective and potent, the linker technology employed should strive to achieve the following three pivotal goals:

- **High stability circulation.** Which means that the employed linker should not be reactive with all the components outside the cell. For instance, the plenty of enzymes, carbohydrates and proteins which are abundant in the systemic circulation. In this way, the stability circulation is strictly linked to the target specificity of the final ADC.
- **High water solubility** in order to favour the bioconjugation and prevent the formation of inactive ADC aggregates. Moreover, Pfizer has shown that the place of conjugation on the antibody also plays a pivotal role in this

mechanism. It has been seen that a conjugation at the level of C-terminal of the heavy chain results in ADCs with higher hydrophobicity than the same ADCs assembled by the conjugation at the C-terminal of the kappa chain. This behaviour is due to the “shielded” nature of the last site, and leads to a lower hydrophobicity and lower clearance of the compound [86]. Linker polarity is a central characteristic required in order to face ADCs aggregation issues. Ample evidence has been reported in this regard involving such aspects as linker modification as extended PEG units, charged amino acids, phosphate and sulphate groups, and ternary ammonium salts.

- **Allow efficient release of highly cytotoxic payload-linker metabolite** (if the linker is cleavable). In fact, if on one hand the linker stability is required in order to avoid any off-target effect, on the other hand, the hydrolysis of the linker is essential once reached the desired destination in order to have the treatment. Moreover, another important point is the ability of the deconjugated linker + drug molecule to still be cytotoxic, as it was the standard drug molecule. In fact, being a total new molecule, because of the chemical conjugation between the linker and the payload, the final therapeutic behaviour could be different than the one of the payload alone.

Given the plenty of different linker solutions, the next subparagraph will delve into their mechanisms, without tacking in consideration the non-cleavable ones since there have not been used in this thesis work.

2.8.1 Reducible disulfides linkers

Disulfides are the most prominent class of a chemically cleavable motif found in ADC linkers. They are stable at physiological pH, but in a rich glutathione (GSH) environment like cytosol, they are sensitive to nucleophilic attack from thiols. The difference in the reduction potential between the cytoplasm and the plasma is assessed as a working mechanism in this approach.

Moreover, high levels of GSH have been found in the tumour environment due to the associated oxidative stress, allowing the extracellular drug release as well.

This linker technology was coupled mainly with Maytansinoids because of their thiol appendage. An average DAR of 3–4 is permitted this way. In 2008 researchers at Genentech and Immunogen assessed the effects of α -methyl substitution on disulfide linker stability. They found that a linker with one methyl-group on each side of the disulphide was the most active alongside a non-cleavable analogue [87-88]. Gemtuzumab ozogamicin (Mylotarg ®) is a FDA approved ADC that takes advantage of this conjugation method [89].

A novel disulphide-carbamate technology linker has been designed in order to enable the conjugation with a wider range of potential payloads. In this manner, Thomas H. Pillow et al have produced a direct connection between the thiol of a maytansine drug (pyrrolobenzodiazepine (PBD)) with the thiol of a cysteine-engineered antibody, thanks to the incorporation of self-immolative spacer to connect the disulfide linker to an amine-containing drug. They have also demonstrated that the stability of this complex is affected by changing the location through cysteine mutants. All conjugates had DAR values of 1.8 to 2.0. This study also provided a comparison among the efficacy and toxicity of this novel disulfide-linker to that of a peptide-linked version, using a mice human non-Hodgkin lymphoma tumour xenograft relatively resistant to MMAE ADCs.

The release mechanism is based on the degradation of the antibody followed by disulfide reduction in the cytosol by cellular reductants such as GSH. When contemplated in vitro, the release mechanism of this class of linkers has been established to be due also to the presence of two enzymes called Thioredoxin 44 (TRX) and glutaredoxin (GRX) [90].

2.8.2 Enzyme cleavable linkers

Dipeptide/glycosidase/phosphatase-cleavable linkers belong to the enzyme cleavable linkers class. Nowadays they represent the leading linker design in the ADC field, as exemplified by Adcetris, a marketed ADC. After the failure of the two tetrapeptides, Gly-Phe-Leu-Gly and Ala-Leu-Ala-Leu, due to their slow release kinetics, a new generation of dipeptide-cleavable linkers have been found with Phe-Lys-PABC and Val-Cit-PABC, in which the PABC spacer is the para amino benzyl alcohol. They are more selective and potent than acid-cleavable hydrazine-

containing ADC, because of the cathepsin B presence in lysosomes. Moreover, it is easy to perform some residue additions, for instance in the Val-Cit linker, in order to dramatically increase the linker stability (Glu-Val-Cit has the highest stability indeed), and the linker selectivity towards the cathepsin B (through the substitution of the Val moiety with the cyclobutane-1,1-dicarboxamide (cBu) ones) [91-92].

The β -Glucuronidases (β -glucuronidase and β -galactosidase) instead are hydrolytic lysosomal enzymes in the glycosidase class that catalyse the breakdown of β -glucuronic acid residues in polysaccharides. Furthermore, these enzymes are secreted by some tumours in the necrotic area.

This extracellular activity has been used for the development of β -glucuronidase-cleavable prodrugs as early as 1988, leading to the first β -glucuronidase-cleavable linkers applied to ADCs by Seattle Genetics in 2006. The generated conjugates were highly stable in isolated rat plasma (half-life of 81 days). Moreover, they were potent in vitro and highly active in mice. The characteristic DAR was = 8 without forming high aggregation that could reduce the hydrophilicity and the in vivo efficacy [93]. Since a high level of extracellular β -glucuronidase is present in the microenvironment of solid tumours, ADCs with glucuronide linkers can lead to drug release outside of the targeted cancer cells [94].

Meanwhile, the β -Galactosidase is an analogue of β -glucuronidase in its hydrolytic activity, but it is over-expressed in certain tumour types and is able to hydrolyse the β -galactoside. According to many studies, when a β -Galactosidase cleavable linker is used with trastuzumab and MMAE, it is more potent than the Val-Cit-PABC analogue [95]. Moreover, this linker-payload combination has been shown to be more efficient than the approved drug trastuzumab emtansine (T-DM1) for the treatment of HER2+ mammary tumours in mice.

The hydrophobicity masking entity of the β -glucuronidase linker has been assessed in the development of highly-loaded homogeneous ADC by Warren Viricel et al, in order to overcome the limited DAR 2-4, decrease non-specific uptake, protection against payload metabolism, enlarge the efficacy in low-target expressing tumours and allow the use of moderately potent drugs as ADC payloads.

Phosphatase-cleavable linkers were completely unknown until 2015. They are hydrolysed by the lysosomal acid pyrophosphatase and acid phosphatase into their parent alcohols in the lysosome. The natural substrate's high hydrophilicity and the alkyl alcohol payload easy release are the two main assets of this class of linkers. Phosphatase cleavable linkers have been presented by Merck in a seminal 2016 paper with the purpose of to release steroids upon internalization into hematopoietic cells. Subsequently, these authors tested this new class of linkers also for the ADC strategy [96]. The “cleavability” of a phosphate containing linkers is unsuitably slow when they are tested in a lysosomal extract.

2.9 Conjugation site and strategies

The choice of a suitable conjugation site on the antibody's chains for the covalent attachment of the linker and payload has a great influence on the stability of the final ADC. For instance, the conjugation to a large antibody provides the linker less accessible to chemical and enzymatic triggers. Consequently, the plasma stability increases, and target cell release rates slow down. On the other hand, the common goal among the totality of conjugation methods is to reach the highest homogeneity possible. Therefore, a pool of heterogeneous antibodies could be composed of two classes, the loaded antibodies, characterized by different DAR, and the unloaded ones. Obviously, this latter class, binding with the same antigens of the loaded antibodies, reduces the efficacy of the treatment. In other words, the homogeneity of ADCs is a crucial determinant of their potency and safety. To sum up the practices involved in this purpose, there are two main families of techniques, the chemicals conjugation and the enzymatic ones. In this way there will be characterized only the chemical strategies since the theory as well as the mechanisms under the enzymatic conjugation techniques will not bear a crucial role in this specific work. Moreover, a specific focus will be carried on the click chemistry approach.

2.9.1 Chemical conjugation

Even if the conjugation via lysine or thiols have been the first strategies exploited in this field, owing to their large availability on the antibody structure and the simple driving chemistry under the binding of the linker, during the last ten years they have been replaced by other up to date techniques.

There are about 80 lysine residues on a typical antibody structure, and about 10 residues are chemically accessible. Moreover, some lysine residues, that are also critical in the antibody-antigen interactions. If they were modified, this would lead to a change in binding affinity. Consequently, high heterogeneity of the final ADC, that results in an undefinable DAR, has been the attribute of this method. As described above, DAR and its distribution critically impact PK/PD, and cytotoxicity of the ADCs as well.

On the other hand, the cysteine coupling relies on a specific reaction between cysteine residues of the antibody and a thiol-reactive functional group installed on the linker. The presence of the free thiols on the antibody is accorded by the selective reduction of the four interchain disulfides, since they are not crucial for the structural stability of the IgG. Three reagents have been developed for the use in this approach. The first is the bis-sulfone reagent, which undergoes bis-alkylation to conjugate both thiols of the two cysteine residues that were obtained through the reduction of native disulfide bonds. After that, it undergoes a series of Michael and elimination reactions to the conjugate payload [97]. ADC with this strategy results in the FDA-approved ado-trastuzumab emtansine. The second reagent for the generation of Cys-bridged ADCs is dibromo-maleimide, resulting in ADCs with the average DAR4. The last reagent is a dibromopyridazinedione with two clickable sites. Basically, this reagent is unique because two compounds can be attached per disulfuride bond, meaning eight compounds can be attached per antibody [98]. This appealing approach opens the opportunity of attaching two drugs with different modes of actions or with synergistic behaviour, overcoming the ADC drug resistance.

To sum up these techniques that involve the thiol's remarkable reactivity, they result in a better DAR, from 2 to 8, and higher heterogeneity in comparison with the lysine ones. However, for this approach further improvements are still required in order to strengthen the final DAR and the circulation stability. In fact, as will be

discussed soon, the cysteine-maleimide linkage is instable in the circulatory system, because of the reactivity of the thiol group, resulting in the premature release of toxin before cell internalization [99]. Although recent advances have been made in this area, a strong drive to develop novel reagents for reliable, chemoselective, stable and irreversible thiol labelling remains. Thus, during the last years, many studies have been developed in order to provide better strategies of conjugation.

The state of the art in this thiol reactive conjugation family have been carried out thanks to the development of two novel site-specific conjugation technologies, named TIOMABs and unnatural selenocysteine incorporation.

The former, firstly introduced by Junutula and co-workers in the 2008, through the introduction of two new cysteine residues (one per heavy chain), allowed a selective mAb attachment following the thiol's chemistry [100]. The resulting modified antibody named THIOMAB, displayed highly homogeneous DAR (almost always two), and no perturbation of the IgG 3D folding. Moreover, even if high doses of ADCs usually result in a deficiency of toleration rate, important doses, of the THIOMABs tested in rats, keep adequate tolerability. In other words, the homogeneous composition of this conjugate is the driving feature in the minimization of the systemic toxicity. The latter, tested by X. Li and co-workers, consists in the engineered monoclonal antibodies with one or more translationally selenocysteine residue, which is a non-canonical amino acid (NCAA), structurally similar to the classic cysteine, but contains a selenium atom instead of the sulfur one [101]. The high selenocysteine reactivity allows to afford homogeneous ADCs with 2/4 DAR. The resulting selenomab-drug conjugates are highly stable and profoundly potent both in vivo and in vitro. Nevertheless, unnatural amino acid-based methodology usually requires appropriate procedures that involve biological agents for the genetic engineering process, and after all, the incorporation of non-natural amino acids could be cause of undesired immunological response.

2.9.2 Click chemistry and Thiol-maleimide mechanism

The reported definition for a chemical reaction in order to be eligible as belonged to the family of “click chemistry” requires that the chemical reaction must be *modular, wide in scope, give very high yields, generate only inoffensive products*

that can be removed by nonchromatographic methods, and be stereospecific. The required process characteristics include simple reaction conditions (ideally, the process should be insensitive to oxygen and water), *readily available starting materials and reagents*, the use of *no solvent or a solvent that is benign* (such as water) *or easily removed*, and simple product isolation. Purification if required must be by nonchromatographic methods, such as crystallization or distillation, and the product must be stable under physiological conditions [102].

Belonging to this specific “click” reactions family, the Michael addition reactions are a special type of conjugate addition in which the strong nucleophilic attack on the β -carbon of an α,β -unsaturated carbonyl results in a negatively charged enolate intermediate, that subsequently yields the Michael adduct, by protonating the catalyst, as displayed in Figure 13 A. Michael addition reaction is a simple, robust, and highly effective reaction that can result in C–C bond formation under relatively facile reaction conditions. As far as the sub-group called thiol-Michael addition reactions is concerned, typical acceptors are electron-deficient molecules such as acrylates, methacrylates, vinyl sulfones, and maleimides. Particularly, the thiol-Maleimide bond has a crucial role.

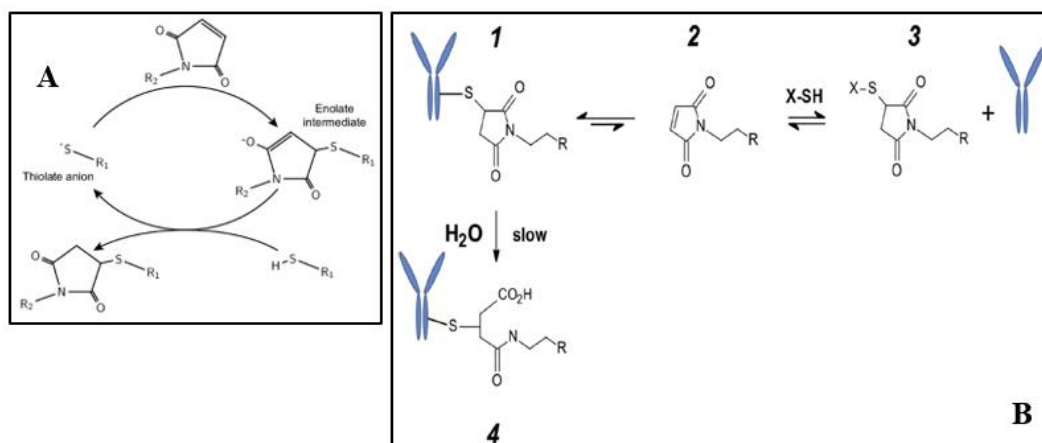


Figure 13. A: Standard cycle of maleimide-thiol Michael reaction.
 B: Retro Michael reaction from 1 to 3 and different outcome which can lead to the ring opening and subsequent conjugate stabilization.

It has been largely used in many biological systems such as cross-linking of hydrogels, the fluorescent labelling of molecules and for the beginning generations

of linkers for biological molecules. The high reactivity of carbon-carbon bond in maleimides is seen to be due to two main factors: (i) the bond angle distortion and the ring strain and (ii) the carbonyl groups being in the *cis*-conformation [103].

From the ADC point of view, the maleimide-thiol reactivity is useful in order to have a high specific chemical conjugation taking advantage of the cysteine amino acids on the antibody. However, after a promising start, where this linkage was stable, there have been clear evidences about its reversibility. Specifically, the leading causes of this instability are related to:

- Plasma exposure since some thiol containing molecules such as GSH or albumin can compete with cysteine for the maleimide bond.
- A site-dependant solvent accessibility, which plays an important role in order to define the hydrolyzation rate of the thioether bond.
- An oxidative process, which if it is stopped to a partial oxidation to a sulfoxide could retain the ADC potency, otherwise, if full sulfur oxidation to form a free sulfonate analog occurs, the payload will be discharged.

On the other hand, it has been noticed that the maleimide ring can be permanently stabilized, preventing the plasma-linked hydrolysis. This specific mechanism, named ring-opening generally showed a significant improvement in efficacy as compared to their ring-closed counterparts, with a half-life of 7 day for the unhydrolyzed one and more than 2 weeks for the ring-open form. This phenomena is linked to a series of different reasons, which are still object of study such as:

- Positively charged amino acid residues lead to rapid succinimide ring hydrolysis in the linker.
- Different chemical and physical techniques. The conversion from the maleimide ring to a ring-open form was reached by:
 - Enhancing the buffer pH to 9.2 for 14h.
 - Mechanical ring stretching
 - Proximity to electron withdrawing groups on the maleimide N-substituent
 - Presence of PEG chain near the maleimide functional group.

Figure 13 reports a representation of the previously discussed maleimide pathways, to whom it has been essential an entire workflow of analysis such as plasma incubation followed by affinity-based capture and characterization of the isolated ADC by HIC for the DAR assessment and LC-MS in order to monitoring the changing in molecular weight [104- 105].

2.10 Summary of ADC fundamental parameters

The vastity of adjustable parameters which concerns the ADC manufacturing make their manufacture a challenging process. The following list provides a schematic explanation about several critical parameters that must be addressed in order to develop targeted drugs with broad applicability for clinical cancer medicine. Meanwhile, singular a description will be provided for each of the followed parameters in order to clarify their specific function. Seems clear how a common thread among all these parameters is the final toxicity.

- **Non-target tissue uptake.** Being more crucial *in vivo*, this outcome it has not completely understood. In fact, only modest accumulation of ADCs occurs at the target (tumour) site (~0.1% of administered dose per gram of tumour) in humans. Therefore, the major fraction of ADCs remains in circulation or is distributed to normal tissues and may be subject to uptake and catabolism, resulting in toxicity in normal cells. Even a low expression of the target antigen on the non-tumoral cells membrane can lead to an increase in off-target uptake. Most of ADCs under clinical development suffer from this unspecific uptake issue. Besides the target-antigen expression, even the rate of internalization, recycling/trafficking kinetics of target antigen, intrinsic sensitivity to the payload and *in vivo* distribution of ADCs to normal cells/tissue may potentially determine ADC toxicity. Figure 14 provides a clear overview among different nonspecific routs for the ADC absorption [106-107].
- **Absence of immunogenicity.** Fortunate, with the rise of chimeric and humanized mAbs, the immunogenicity it has been quite always prevented, maintaining the high affinities for tumour associated antigens.

- **Inefficient drug release from the mAb within tumour masses.**
- Release of drug with low potency:
- **Inappropriate linker stability.** Playing a pivotal role in ADC efficacy and tolerability, it is measured in terms of half-lives. The linker stability has been carefully studied, resulting in a plenty of different techniques which bear different pros and cons.
- **Control over the ADC stoichiometry**

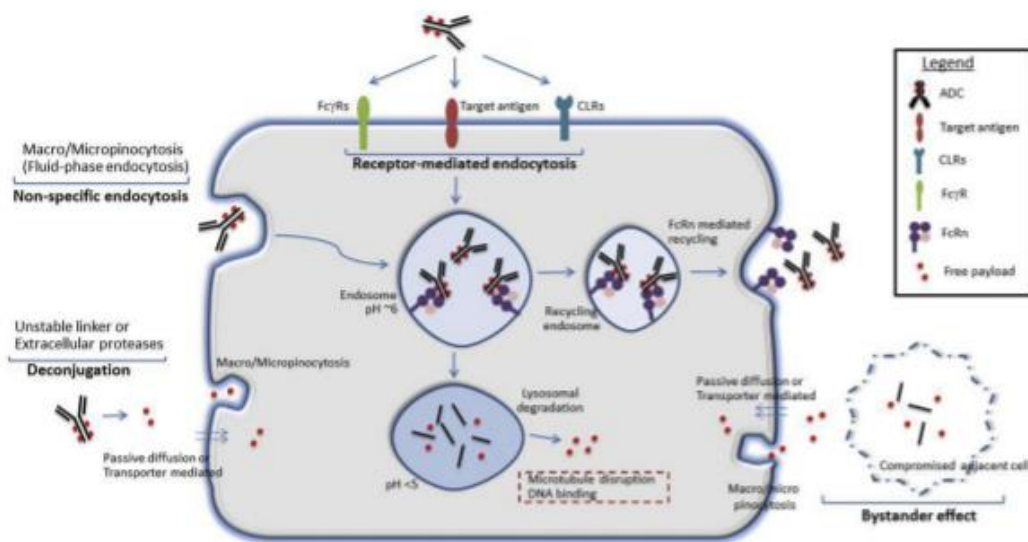


Figure 14. Other receptors which bind conserved Fc regions of IgG antibodies such as Fc gamma receptors (FcγRs), neonatal Fc receptor (FcRn) and C-type lectin receptors (CLRs) may also contribute to target-independent internalization/trafficking of ADCs in normal cells. Non-specific endocytic mechanisms such as micropinocytosis or micropinocytosis could also contribute to internalization of intact ADC or free payload (released extracellularly due to linker-drug instability or extracellular protease activity). Free payload may also enter normal cells by other mechanisms such as passive diffusion (if membrane permeable), non-specific endocytosis or specific transporters (if substrate for membrane transporters)-mediated uptake. In addition, antigen-positive target cells are also able to mediate toxicity by releasing payload into the local environment that is subsequently taken up by antigen-negative normal cells (bystander effect) by either passive diffusion, transporter-mediated uptake or by other non-specific endocytosis mechanisms [107].

2.11 Polyethylene glycol (PEG)

This chemical structure worth the last mention since it has been chosen as a structural component in this work due to its wide applicability and plenty of good properties. The structure of PEG is commonly expressed as $H-(O-CH_2-CH_2)_n-OH$. PEG is also called polyethylene oxide (PEO) or polyoxyethylene (POE) according to its molecular weight. In the 1859, A.V. Lourenço and C.A. Wurtz independently isolated products that were polyethylene glycols.]. As regards the fate of PEG in the body, absorption of PEG across gastrointestinal tract and skin decreases with the increase in MW with almost 50% of absorption observed with PEG 400. Today is well understood that PEG is prone to (per)oxidation and resulting degradation of the polymer chain [108]. The initial step in the PEG degradation inside the body is the formation of esters and formaldehyde, which they will be further oxidized to carboxylates, as reported by Figure 15A [109]. In this way, also the physiologic presence of ROS inside the body can lead to a faster PEG oxidative degradation [110].

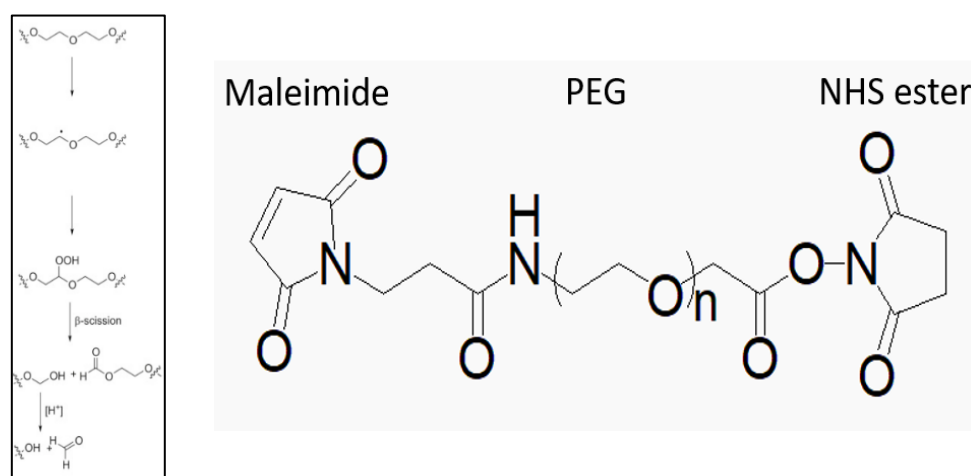


Figure 15. A: degradation process of PEG chain inside the body. B: heterobifunctional PEG containing linker used in this

As far as the physical properties are concerned, PEG molecules display a very high solubility in water as well as in many organic solvents including aromatic hydrocarbons. Moreover, according to the MW it is colourless, odourless and viscous with a freezing point from -10 C (up to 700), while polymerized compounds are wax-like solids with melting point up to 67 C (MW > 1000). Others important

features such as its neutral, lubricating and non-volatile nature increase the popularity of this molecule in many fields. Lastly, its high structure flexibility, biocompatibility, non-irritating nature, and non-immunogenic. As aforementioned, because PEG holds such many properties it is used in a lot of different applications for instance chemical ones, industrial ones, commercial and recreational ones and lastly, very important uses concern the biological field, and every day researches benefit from this molecule for new frontier practices. Specifically, in the biopharmaceutical field, PEG acts as a solubilization enhance factor upon synthetical chemical molecules, like drugs, that usually display poor water solubility. As a result, liquid PEGs (PEG 200 to PEG 600) can be used as water miscible solubilizers in oral liquids and parenterals, while high MW PEGs have been used for microencapsulation of active drugs. Most notably, PEG conjugated therapeutic help in passive targeting to the tumour, enhancing the overall circulating time of the conjugated drug.

With this idea several ADCs have be developed during recent years. Patrick J. Burke et al in their approach have tried various PEG chain lengths, up to PEG24. Finding a clear relationship between the PEG chain length and the *in vivo* efficacy. Longer PEG chains resulted in slower clearance, with a threshold length of PEG8 beyond which clearance was not impacted. Conjugates bearing PEG of enough length to minimize plasma clearance provided a wider therapeutic window relative to faster clearing conjugates bearing shorter PEGs. This result suggests that PEG8 is enough to shield the hydrophobic moieties of the drug-linker and consequently minimize the nonspecific cellular uptake. As PEG length decreased from PEG8 to PEG4 the clearance doubled from 9.0 to 18.8 mL/kg day [111].

2.12 Thesis Proposal

2.12.1 Work steps overview

1. Modify the CCI-001 molecular structure, deprotecting the amine group by the selective methyl carbamate cleavage.

2. Reach the covalent conjugation between the CCI-001 amine derivative and a MAL-PEG-NHS heterobifunctional linker.
3. Find an effective procedure in order to obtain the direct conjugation between the CCI-001 with the MAL-PEG-NH₂ heterobifunctional linker thanks to the synthesis of unsymmetrical ureas bond.
4. Characterize through different specific analysis such as ¹H-NMR mass spectrometry and FTIR the reactions products.
5. Obtain a selective and reproducible bond between the engineered drug/linker molecule (L+D) with the recombinant, fully human monoclonal antibody (Panitumumab), resulting in the production of an antibody drug conjugate.
6. Study the *in-vitro* release of the produced ADC, using two different *in-vivo* mimetic dissolution buffers.
7. Trace the *in-vitro* Panitumumab internalization behaviour within different cell lines, taking advantages of the conjugation with the Cy5.5 fluorescent dye.

2.12.2 Specific objectives

1. Assess the *in-vitro* behaviour and the cytotoxicity of Panitumumab conjugated CCI-NH₂ after the administration in colorectal and pancreatic cancer cell lines.
2. Study the newly produced CCI-001 amine derivative and the CCI-001 amine derivative/linker *in-vitro* potency using the same cell lines.
3. Analyse the *in-vitro* release profile of the final ADC.

3. Materials and Methods

3.1 Introduction

The present chapter contributes to the fully understanding of the technical work attempted during this master thesis work, with the purpose of elucidate the laboratory techniques carried out during the operate.

3.2 Materials

Maleimide-polyethylene glycol- N Hydroxysuccinimide (MAL-PEG8-NHS, MWt 618 Da, 97%) was purchased from Broadpharm (San Diego) and maleimide-PEG-amine (MAL-PEG1K-NH₂, MWt 114 kDa, 97%) was purchased from Nanocs, Inc (USA). Bis(trimethylaluminum)-1,4-diazabicyclo[2.2.2]octane adduct (DABAL—Me₃) was purchased from Sigma-Aldrich Canada. CCI-001 (colchicine derivative, 3 g) was kindly provided by professor Tuszynski research group (U.o.A, Physics department). Rituximab (Rituxan ®, anti CD20 monoclonal antibody) and Panitumumab (Vectibix ®, anti EGFR monoclonal antibody) were generous supplied from Cross Cancer Institute. Spectra/por dialysis tubes (MWCO, 1KDa 3.5kDa, 12-14 kDa) were purchased from Spectrum. Cy5.5 NHS dye was purchased from Lumiprobe (Hallandale Beach, Florida). Silica gel columns for flash chromatography (24g and 12g) were purchased from Teledyne ISCO (USA). All other chemicals and reagents used were of analytical grade.

3.2.1 Cell culture

Cell culture media DMEM, cell culture media DMEM + F12, fetal bovine serum (FBS) and penicillin- streptomycin-L-glutamine were purchased from GIBCO Life Technologies INC (Burlington, ON, Canada). HCT-116 (colorectal cancer, EGFR+) and SW-620 (colorectal cancer, EGFR-) were received from the laboratory of professor Lavasanifar. PANC-1 (pancreatic cancer, EGFR+) was kindly donated by Cross cancer institute.

3.3 Methyl carbamate deprotection

The CCI-001 amine derivative (which for shortness will be called CCI-NH₂ from now on) was obtained in acceptable yield ($\approx 30\%$) only after several hydrolysis trials, synthesized by Table 3, while the complete description that follows involves only the successful procedure, Figure 16 entry 6. Briefly, CCI-001 (350 mg) and methanol (1 ml) were first mixed in a round bottom flask until total solubilization of the drug powder. 5M HCl (67 ml) was added to the previous mixture. The final solution was placed on magnetic stirring, refluxed and TLC controlled until reaction completion after 18-24h. The flask was cooled at room temperature once the reaction was terminated. The final product was purified thanks to a multi-step procedure. In short, the reaction solution was transferred inside a 500 ml separation funnel and dichloromethane (CH₂Cl₂, 20 ml) was added in order to extract the unreacted drug molecules since the desired amine derivative at high acidic pH was more soluble in the water phase. The remaining water phase was neutralized using sodium hydroxide (NaOH, 50 ml) until pH 14. The amine derivative, which at this pH value was more soluble inside the organic phase was extracted several times using CH₂Cl₂ until the colour of extracted phase was not yellow anymore. During the final extraction steps, sodium chloride (NaCl, 4g) was added in order to enhance the product separation from the organic phase, which otherwise was trapped inside a micelles of products inside the solution. After that, the organic mixture was chemically dried out with anhydrous MgSO₄. Finally, the dried solution was

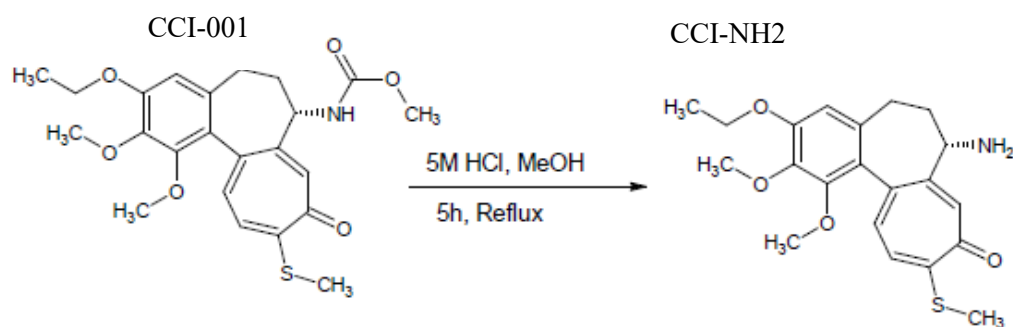


Figure 16. Deprotection reaction in order to achieve the amine deprotection.

evaporated using a rotary evaporator, setting the water bath temperature at 40 °C. The final product was obtained as a brownish powder.

Table 3. Summary of all the trials carried out for the CCI-NH₂ achievement.

Trials	Condition	Drug (mg)	Solvent system	Time and Temperature (°C)	Results	Ref
1°	Microwave	9	MeOH, THF, 2M LiOH (1:1:1, 1,6 ml)	10 mins 100	NO	[¹¹²]
2°	Microwave	10	MeOH, THF, 2M LiOH (1:1:1, 2 ml)	10 mins 120	YES	[¹¹²]
3°	Microwave	11	MeOH, 2LiOH (1;1, 2,5 ml)	11 mins 120	YES	[¹¹²]
4°	Sand bath	150	MeOH (10 ml) 2M HCl (10 ml)	72 h 90	NO	
5°	Reflux	150	THF (10 ml) 5M HCl (30 ml)	6 h	NO	
6°	Reflux	350	MeOH (1 ml) 5M	5 h	YES	

			HCl (30 ml)			
7°	Reflux	100	MeOH (1 ml) 5M HCl (30 ml)	48 h	NO	
8°	Room temp	20	CH ₂ Cl ₂ (equimolar) 1M TFA	48 h	NO	
9°	Reflux	30	EtOH (3,3 ml) DD Water (0,7 ml) 4.5M KOH	24 h	NO	[¹¹³]

3.4 CCI-NH₂/linker conjugation

The preparation of a new molecule through the chemical conjugation between the synthesized CCI-NH₂ and the NHS-PEG7-MAL linker, which for shortness will be named L+D_1 from now on, was accomplished after several surveys, which are reported in Table 4. The following subsections will be focussed on the two strategies which both led to the successful outcome.

3.4.1 Reaction in dry THF

The complexed new molecule made by the conjugation between CCI-NH₂ with the NHS-PEG7-Mal was accomplished thanks to a multi steps procedure designed with dr. Reza Vakili, summarized by Table 4 entry 2. Briefly, the obtained CCI-NH₂ (20 mg) was dissolved in 1 mL of THF (HPLC grade) in a small glass vial. An equimolar amount of NHS-PEG7-Mal (32 mg) linker was weighed in a separate small size vial. The drug solution was added to the linker vial and stirred overnight with the vial cap on. The day after the solution level in the vial was marked with a sharpie, after that the vial was filled with DD water (2 mL) and the new volume level inside the vial was marked again. The complete THF evaporation, which was

assessed after one night checking the marks on the glass vial. Finally, the reaction mixture was centrifuged in order to remove all the aggregations. At the end, the mixture was placed inside the freeze drying in order to remove the solvents. The dried residue was solubilized in ethyl acetate (2 mL) and purified by silica gel chromatography eluting with EtOAc/MeOH as a mobile phase.

3.4.2 Reaction in DMF

The conjugation between CCI-NH₂ and the NHS-PEG7-Mal linker, Table 4 entry 3 was achieved using a modification of a previously published procedure [114]. To summarize, in a small glass vial containing a magnetic stirrer bar, anhydrous DMF (0,7 ml), CCI-NH₂ (15 mg) and diisopropylethylamine (DIPEA) (1.5 equivalent; 58 μmol; 10 μL) were allowed to mix together for 30 minutes. Later NHS-PEG7-Mal linker (1.1 equivalent, 25 mg) was added. The reaction vial was wrapped with aluminium foil and the mixture was stirred at room temperature overnight under argon. The following morning 20-fold volume excess of DD water was added to the reaction allowing the stirring for other 30 minutes. At the end, the mixture was placed inside the freeze drying in order to remove the solvents. The dried residue was solubilized in ethyl acetate (2 mL) and purified by silica gel chromatography eluting with EtOAc/MeOH.

Table 4. Trials attempted for the chemical conjugation between CCI-NH₂ and the NHS-PEG7-MAL linker.

Trials	Condition	Reagents (mg)	Solvent system	Time and Temperature (°C)	Results
1°	Stirring Room temp	CCI-NH ₂ (25 mg) linker (40 mg)	Dry CH ₂ Cl ₂ DD Water	72h	YES

2°	Stirring Room temp	CCI-NH2 (20 mg) linker (32 mg)	Dry THF	10 mins 120	YES
3°	Stirring Room temp Dark and Inert condition	CCI-001 (15 mg) linker (25 mg)	DMF (0.7 ml) DIPEA (30 ml)	5 h	YES

3.5 Direct conjugation

Many trials, summarized in Table 5, with different nucleophilic substances have been carried out in order to reach the direct conjugation between the CCI-001 and

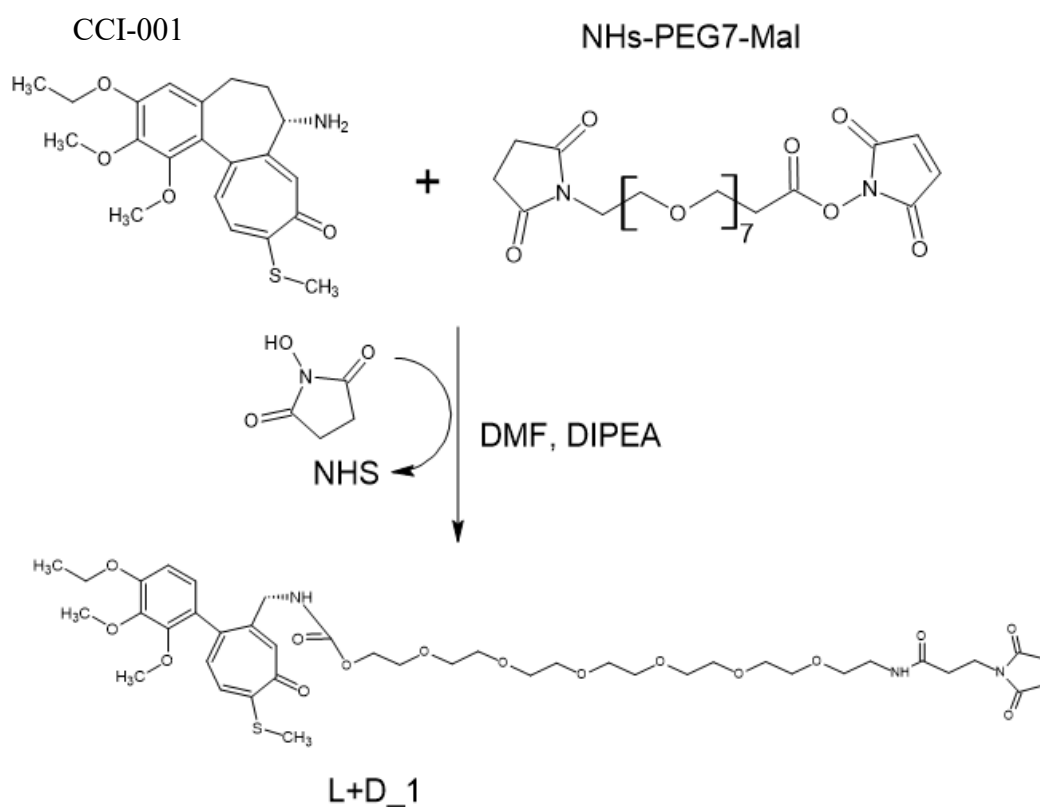


Figure 17. Conjugation between CCI-NH2 and NHS-PEG7-Mal linker reaction scheme.

the NH₂-PEG-Mal linker, removing the intermediated step of the amine deprotection. Specifically, the strategy reported by the entry 1° took advantage of a very weak organometallic compound called DABAL-Me₃ (Bis(trimethylaluminum)-1,4-diazabicyclo[2.2.2]octane adduct).

Table 5. Attempted trials for achieve the conjugation between CCI-001 and the NH₂-PEG-MAL without carbamate deprotection.

Trials	Condition	Reagents	Solvent system	Time and Temperature (°C)	Results	Ref
1°	Sonication Reflux	CCI-001(45 mg) DABAL-Me ₃ (26 mg) linker (100 mg)	Dry C ₇ H ₈	1 h (40 °C) 2 h (90 °C)	NO	[¹¹⁵]
2°	Reflux	CCI-001 (30 mg) DABAL-Me ₃ (60 mg) linker (115 mg)	Dry THF	18 h	Unk	[¹¹⁶]
3°	Reflux	CCI-001 (25 mg) linker (63 mg) DMAP (1.3 eq.)	THF	72 h	NO	[¹¹⁷]
4°	Reflux	CCI-001 (30 mg) linker (70 mg)	ACN	72 h	NO	[¹¹⁸]
5°	Reflux	CCI-001 (25 mg) linker (63 mg)	IPA	72 h	NO	[¹¹⁹]

mg) TEA (1
equivalent)

3.6 Antibody drug conjugation

The conjugation between the previously synthesized L+D_1 with the monoclonal recombinant antibody Panitumumab involved a click chemistry reaction between the Maleimide functional group on one end of the linker with the introduced sulfhydryl groups on the lysine of antibody, thanks to the iminothiolane reagent (2-IT) used during the antibody activation step [120]. This important step is reported by Figure 18. Three batches of ADC, named ADC1, ADC2 and ADC3, have been produced using the following procedure, using different amount of L+D_1 have been used each time. As far as the following description is concerned, it stands for the third batch of ADC produced. As a first thing, different buffers required for the procedure were made up as follows: Buffer A (PBS 1X pH 7.4), Buffer B (50 mM triethanolamine, 150 mM NaCl, 2,5 mM EDTA, adjusting the pH until 8), conjugation Buffer (PBS 1X, 2.5 mM EDTA, pH 7.4). First, one day before starting the reaction, the antibody solution, at the concentration of >30 mg/mL, was poured inside a dialysis bag (C/O 12 kDa) and placed in a cold room in order to allow the buffer exchanging from the storage buffer to buffer B. A fresh 2-IT solution in Buffer B was prepared at the final concentration of 1 mg/mL. The antibody solution was removed from the dialysis bag and poured inside a glass vial with a small magnet. The protein concentration was adjusted until more than 5 mg/mL using Buffer B. 20:1 molar ratio (2-IT:mAb) was added from the 2-IT stock solution. After the last step the protein concentration was slightly less than 5 mg/mL. Then, the reaction solution was stirred (very gentle) at room temperature for 1h under dark condition in order to prevent the oxidation of the newly added thiol groups. In the meantime, the L+D_1 was dissolved inside the conjugation Buffer at the final concentration of 1 mg/mL. After one hour the antibody solution was poured inside a dialysis bag (C/O 12 kDa) in order to remove the unreacted 2-IT. The system was wrapped again with aluminium foil and placed inside a cold room in order to prevent the antibody unfolding. Buffer B was used as dissolution medium since the EDTA property of preventing the thiols oxidation. The last step lasted for 2 hours

exchanging the dissolution medium two times. At the end of the 2 hours, the free thiols concentration on the antibody was assessed thanks to the Ellman's test according to the published protocol [121]. Shortly, a DTNB stock solution 10 μ L have been made with a final concentration of 50 mM sodium acetate and 2 mM DTNB (5,5'-Dithiobis(2-nitrobenzoic acid)) using DD water as a solvent and quickly refrigerated. Another stock was made with final concentration of 1M Tris adjusting the pH until 8.0. So that, 50 μ L of the DTNB solution, 100 μ L of Tris solution and 845 μ L of DD water were combined together directly inside the cuvette, and after setting the back ground with the UV spectroscopy, 5 μ L have been taken from the activated antibody solution and combined with the previously working solution. After extensive mixing, the absorbance at 412 nm was detected in order to estimate the free thiol group concentration inside the antibody solution. At the end of the two hours, the activated antibody solution was transferred from the dialysis bag to a small glass vial containing a magnetic stirrer and the protein concentration was helved adding enough volume of conjugation Buffer. According to the previously detected thiol concentration, 6-fold molar excess of the L+D_1 have been added inside the glass vial and left to react for 4 hours at room temperature. After reaction completion, 2-mercaptoethanol (BME) was added to quench the reaction, neutralizing the unreacted thiol groups. Specifically, the amount of BME added was 2-fold molar excess of the summation between the moles of 2-IT and the moles of L+D_1. One hour after the neutralization reaction, the reaction solution was placed inside a dialysis bag (C/O 12 kDa) and in a cold room for the purpose of removing all the unreacted chemicals employed during the last steps. After 24 hours and several exchanges of dissolution media (PBS 1X pH 7.4), the antibody solution was "sterilized" using a 0.22 μ m syringe filter. The solution characteristic DAR was determined thanks to the UV/Vis spectrometry according the procedure reported for this type of analysis, which will be discussed by the following sub paragraph [122]. Finally, the ADC solution was stored in fridge.

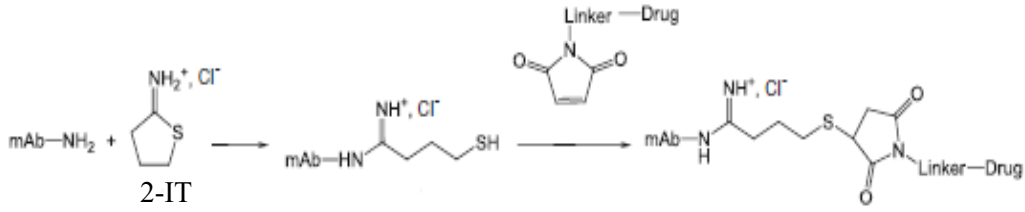


Figure 18. Iminothiolane-based conjugation.

3.7 Measuring the drug amount on antibody by UV/Vis spectrometry

The protein concentration as well as the average number of drugs conjugated to the antibody (drug antibody ratio or DAR) inside the antibody-drug conjugate solution was calculated thanks to the UV/Vis spectroscopy analysis and using the Lambert-Beer law, Figure 19. Taking advantage of the extinction coefficients of the antibody and the drug together with the measured absorbances of the ADC solution, the DAR can be determined. In order to better understand this procedure, all the calculations steps have been described schematically. First, the drug absorption maximum ($\lambda(D)$) has been found, reading the cuvette with the sample after taking the blank. The panitumumab adsorption maximum was assumed to be 280 nm as usual for this family of proteins. After that, the extinction coefficients (ϵ) of the antibody and the drug at 280 nm and $\lambda(D)$ have been calculated by the reverse Lambert-Beer equation using an absorbance value inside the linear range. As a third step, the absorption spectrum of the ADC sample was obtaining and the absorbances at both 280 nm and $\lambda(D)$ were taken. Finally, the average DAR of the ADC solution was calculated solving two simultaneous equations, reported in Figure 19, with the aim of find the individual concentrations of antibody and drug, c_{mAb} and c_{drug} . Then, the average DAR was expressed dividing c_{drug} by c_{mAb} .

$$A = \epsilon c \ell, \quad \begin{aligned} c_{mAb} &= \left(A_{280} \epsilon_{drug}^{\lambda(D)} - A_{\lambda(D)} \epsilon_{drug}^{280} \right) / \left[\left(\epsilon_{mAb}^{280} \epsilon_{drug}^{\lambda(D)} - \epsilon_{mAb}^{\lambda(D)} \epsilon_{drug}^{280} \right) \ell \right] \\ c_{drug} &= \left(A_{280} \epsilon_{mAb}^{\lambda(D)} - A_{\lambda(D)} \epsilon_{mAb}^{280} \right) / \left[\left(\epsilon_{drug}^{280} \epsilon_{mAb}^{\lambda(D)} - \epsilon_{drug}^{\lambda(D)} \epsilon_{mAb}^{280} \right) \ell \right] \end{aligned}$$

Figure 19. Mathematical formula for the DAR estimation.

3.8 In vitro cellular uptake

Fluorescence detected thanks to a plate reader (Synergy Readers, Hybrid Multi-Mode Plate Readers) was used to evaluate the summation between the cell superficial absorbance and the uptake of fluorescent-labelled Panitumumab against two human cancer cell lines, the HCT-116 (EGFR+) and SW-620 (EGFR-), labelling the antibody with a Cy5 dye.

3.8.1 Antibody labelling

Panitumumab (MWt. 147 kDa) was labelled with Cy5 NHS ester at an applied 1:20 molar ratios following the instructions reported by the published procedure [¹²³] Briefly, the pure panitumumab antibody solution was buffer exchanged overnight in a dialysis bag (C/= 12 kDa) using a slightly alkaline media pH 8.3 as a dissolution buffer. The day after, the protein solution was diluted until 4 mg/mL inside a small glass vial containing a magnetic stirrer. Cy5 NHS ester was dissolved in 250 μ L of DMSO and the appropriate volume was added to the protein's solution (0,23 mg; 70 μ L). The reaction, reported by Figure 20, lasted for at least 4 hours at room temperature (or overnight inside a cold room) under dark condition. The conjugate was then purified from free dye by size exclusion chromatography on Sepharose CL-6B column using PBS pH 7.4 as the mobile phase. The eluent was collected in 16 fractions of 2 mL each, from the column. Each fraction was subjected to UV-plate reader in both absorbance (Pierce BCA Protein Assay Kit by Fisher scientific) and fluorescence analysing the plate at 600/700, to assess the protein and the dye concentration respectively. These analysis were carried out in order to find which ones of the collected fractions were the ones with the antibodies.

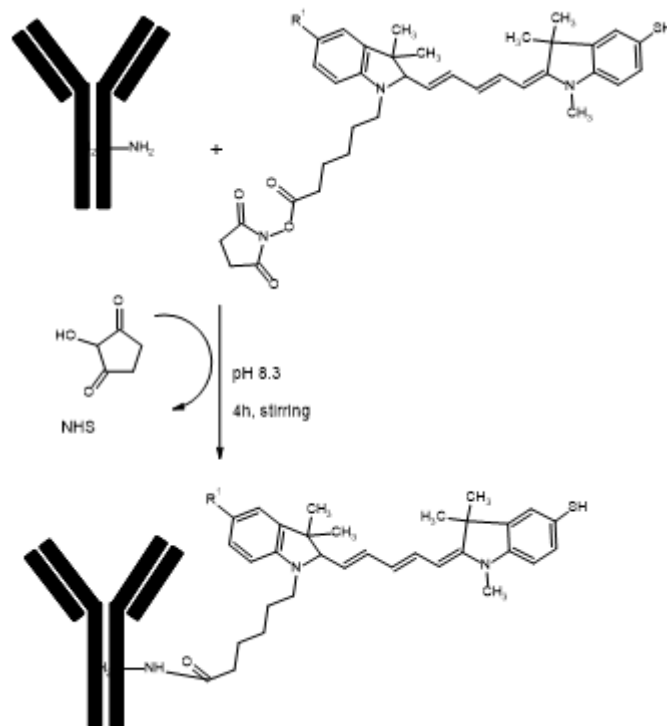


Figure 20. Scheme of the conjugation reaction for the fluorescent dye attachment to panitumumab.

3.8.2 Internalization assessment

The cell lines were grown in 75 cm² culture flasks until a confluence of ~ 80% was achieved. The medium was then aspirated, and cells were washed with PBS (pH 7.4). The cells were dislodged using 0.25% of trypsin–EDTA solution and, if needed, kept at 37 °C for a few minutes to detach them completely. The trypsin was then deactivated using a small volume of FBS-containing growth medium. The suspended cells were collected in a Falcon tube and centrifuged at 500g for 5 min. The resultant pellet was resuspended in medium, and the cells were counted using a hemocytometer. 500.000 cells for each cell line have been poured in each well, adding 1 mL of medium. Two 12-well plates were seeded according to this procedure, placing the plates at 37 °C for 24 h in a humidified CO₂ incubator. After the 24 h inside each well a 40% of the existing media volume was added in volume of labelled panitumumab, reaching a final dye concentration of 10 µg. Two and height hours later, the medium was aspirated, and the cells were first washed twice

with PBS, then detached with 300 μ L of trypsin. Half of the trypsin solution volume from each well was poured in a different black 96-well plate spot, placing each cell line in quadruplicate. At that point, the internalized dye quantity was detected reading the fluorescence thanks to the UV plate reader. The reading was carried on using 600 nm as excitation emission and 700 nm as detection. In order to exclude the influence of the trypsin fluorescence, one well of the black 96-well plate was filled with pure trypsin.

3.9 *In-vitro* release study

Release of L+D_1 from the chemically conjugated panitumumab was determined in two different PBS 1X based buffers, one containing the same concentration of bovine serum albumin (BSA) of the blood (4.5 g/dL) and the other one with a pH 4.7 in order to simulate the lysosomal environment. The release procedure was designed in the way that the ADC solution (2 mL) was transferred into a dialysis bag (MWt C/O 3.5 kDa) and placed into the buffer system. The release study was performed at 37 °C in a shaking water bath (VWR®). At selected time intervals, 110 μ L of solution were taken from the inside the bag and replaced with 110 μ L of fresh PBS 1X. Each sample was analysed by UV plate reader using a standard curve of free L+D_1. The amount of L+D_1 released was calculated by subtracting the amount of L+D_1 inside the dialysis bag from the initial amount of L+D_1.

3.10 *In-vitro* cytotoxicity study

The cytotoxicity of CCI-001, CCI-NH2, L+D_1, ADC1 and ADC2 was tested against the HCT-116, SW-620 and Panc-1 cell lines using 3-(4,5- dimethylthiazol-2-yl)-2,5-diphenyltetrazolium bromide (MTT) assay. The growing condition for all the three cell lines were the same except for the different media used with the Panc-1 cell line. So that the following description will be referred to the two cell lines which were cultivated with DMEM. Briefly, the cells were grown in DMEM media supplemented with 10% FBS and 1% P/S (Penicillin and Streptomycin) antibiotics and maintained at 37 °C with 5% CO₂ in a tissue culture incubator. After the detaching procedure the cells were seeded in each well of a 96 well plate according

different ratios depending on the specific cell line. HCT-116, SW-620 and Panc-1 were seeded with 2000, 4000 and 5000 cells per well respectively. Each of the treatments was dissolved in an appropriate volume of DMSO in order to reach the concentration of 51.2 μM . It is important to notice that, this concentration, in the case of the treatments with L+D_1 stood for the effective CCI-NH₂ concentration, so that a correction factor was applied in order to consider the increase in MWt due to the linker presence, multiplying all the previously concentrations for 2.5. From this most concentrated stock other nine stocks have been made with serial dilution. At the time of treating the cells, the 2% in volume of the estimated treatment media has been taken from each DMSO stock in order to have a constant 1% DMSO concentration in each well, excluding the DMSO contribute to the final detected cell toxicity. A 2% in DMSO of the treatment media volume was added even inside the wells which correspond to the treatment control. After 48, 72 and 92 hours of incubation, MTT solution (20 μL ; 5 mg/mL) was added to each well and the plates were then incubated for another 3 hours. Then, the media inside was discarded and 100 μL of DMSO were added in each well to dissolve the formazan crystals. The cell viability was detected by measuring the optical absorbance at 570 nm (using Synergy Hybrid plate reader). The mean absorbance of each treatment was determined and converted to the percentage of viable cells relative to the control. The software graph prism 8 has been used to analyse the data, using the log (inhibitor) vs. response model and plotted the log(inhibitor) vs. normalized response. Moreover, the IC₅₀ value and the final sigmoid were obtained for each treatments at each time point.

3.11 Analysis apparatus

Thin layer chromatography (TLC) on silica gel (0.25 mm of thickness) UV₂₅₄ sensible plastic sheets with different mobile phases solutions has been used during the synthesis section of the work in order to give a quick answer as to how many components are in a mixture. Moreover, TLC has been also used to support the identify of a compound in a mixture when the R_f of a compound is compared with the R_f of a known compound when run on the same TLC plate.

Molecular chemical structures were analysed and confirmed by ^1H nuclear magnetic resonance ($^1\text{H-NMR}$) using a 600-MHz Bruker spectrometer (Bruker Instruments, Inc., Billerica, MA, USA). All NMR samples had a volume of 0.6 mL. The data were processed using the Bruker software TopSpin 3.5. All samples, including the reagents, were dissolved in deuterated chloroform (CDCl_3) at a concentration of 2-7 mg/mL.

Exact molecular weights were assessed thanks to mass spectrometry.

Clear confirmation on the functional groups, which characterize the produced molecules, was obtained thanks to the FTIR analysis. Specifically, the apparatus was a Nicolet Continuum FTIR Microscope made by Thermo Scientific, USA. All the samples were prepared as cast films and 32 scans with a resolution of 4 were made.

3.12 Statistical analysis

Statistical analysis was performed using either Student's *t* test or one-way ANOVA. The significance level (α) was set at 0.05. All experiments were conducted in triplicate unless mentioned otherwise in the text. In tables or graphs data points are represented as mean \pm standard deviation (SD).

4 Results

4.1 Characterization of synthesized products

4.1.1 Thin layer chromatography (TLC)

All the reactions were monitored by TLC. Different mobile phases have been used since the various products polarity. Table 6 reports the R_f values and mobile phases condition used during the monitoring. The displayed R_f values, reported for some of the successful reactions only, stand for the final products R_f value. On the other hand, where the desired product wasn't obtained at all, the reported R_f value is the same of the reagent (CCI-001). One important consideration to keep in mind regards the nature of the silica gel plate used. Since silica is a slightly acidic compound, any basic moiety, especially amines (the obtained aromatic amine derivative in this case) tend to "stuck" inside the silica covered plate or column and do not come out from the base line, as reported in Figure 21 A. Even increasing the mobile phase polarity, adding more MeOH didn't work. So that, a better strategy to obtain the amine derivative movement on the silica plate involves the neutralization/basification of the silica layer before loading the compound by wetting the column with TEA or ammonia (1-2% v/v) inside the mobile phase. Figure 21 B reports the different outcome after the basification of the plate.

Table 6. Summary of the TLC analysis condition for the synthesis reactions carried out.

Entry	Reaction	Outcome	Mobile phase	R _f value
1°	Methyl carbamate deprotection	Desired product obtained	EtOAc: MeOH 80:20 v/v + NH ₃	0.43
2°	Direct conjugation	Desired product not obtained	EtOAc: CH ₂ Cl ₂ 60:40 v/v	0.61

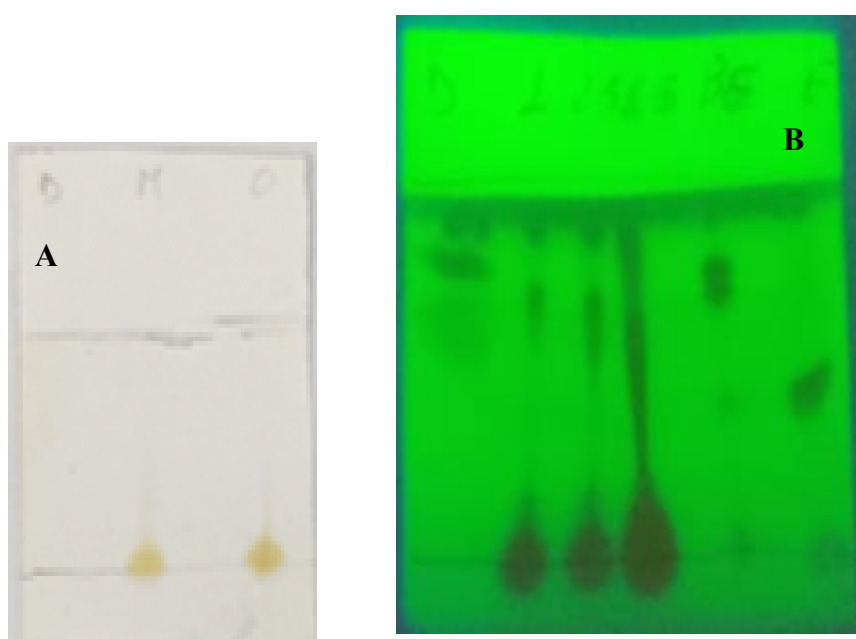


Figure 21. A: the obtained polar aromatic amine is still on the TLC plate base line (yellowish spots). B: TLC plate after the addition of few droplets of ammonia.

4.1.2 Purification with flash chromatography

The reactions crude products were purified by High Performance flash chromatography with a flow rate equal to 35 mL/min. Silica columns (by Teledyne Isco US. (12g and 24g)) were used with EtOAc as solvent A, increasing the gradient of MeOH until 100%. Unfortunately, due to the strong interaction between the aromatic compound amine derivative with the silica inside the column, the CCI-NH₂ purification wasn't achievable by this strategy. In this regard, Figure 22A shows that at the end of the CCI-001 deprotection reaction, just one peak was obtained, which was verified using the LC-MASS spectrometry (exact mass 446.2 m/z), was found to be just the standard CCI-001. On the other hand, the crude product of the successful conjugation was obtained from the first peak of Figure

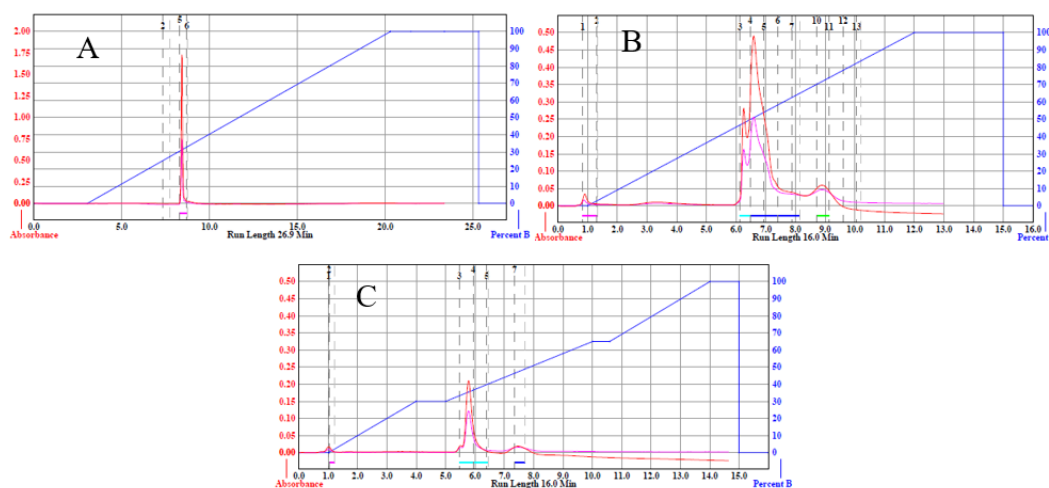


Figure 22. A: result from CCI-001 methyl carbamate deprotection. B: result from unsuccessful linker/CCI-NH₂ conjugation in DMF. C: result from successful linker/CCI-NH₂ conjugation in DMF.

22C, when the 30% of Solvent B was used. While the second small displayed peak in the graph corresponds just to the NHS-PEG7-Mal unreacted during the reaction. One important consideration found involves the tricky chemistry under the CCI-NH₂/linker conjugation. Because, the reaction of NHS esters with amines is strongly pH-dependent: at low pH, the amino group is protonated, and no modification takes place. At higher-than-optimal pH, hydrolysis of NHS is too fast, leading to undesired product as well as lower yield. The optimal pH for this reaction is 8.3-8.5. When hundreds of milligrams of NHS ester are used, as happened during

the second batches of L+D_1 production, the solution tend to acidify over time because of the NHS ester hydrolysis, leading to different products, Figure 22 B. As far as this last outcome is concerned, each one of the three reported peaks were analysed by $^1\text{H NMR}$ in order to understand the nature of the product. The first peak was found to be the degraded linker, the second stands for the L+D_1 that maybe was involved in the maleimide ring degradation and the last one was again the L+D-1 unreacted.

4.1.3 Proton nuclear magnetic resonance ($^1\text{H NMR}$)

The $^1\text{H NMR}$ spectra for all the successful synthesized products were obtained, and they are shown in Figure 23 and Figure 24 paired with the corresponded molecule. The $^1\text{H NMR}$ spectra of the individual compound was used to have the first idea of the outcome.

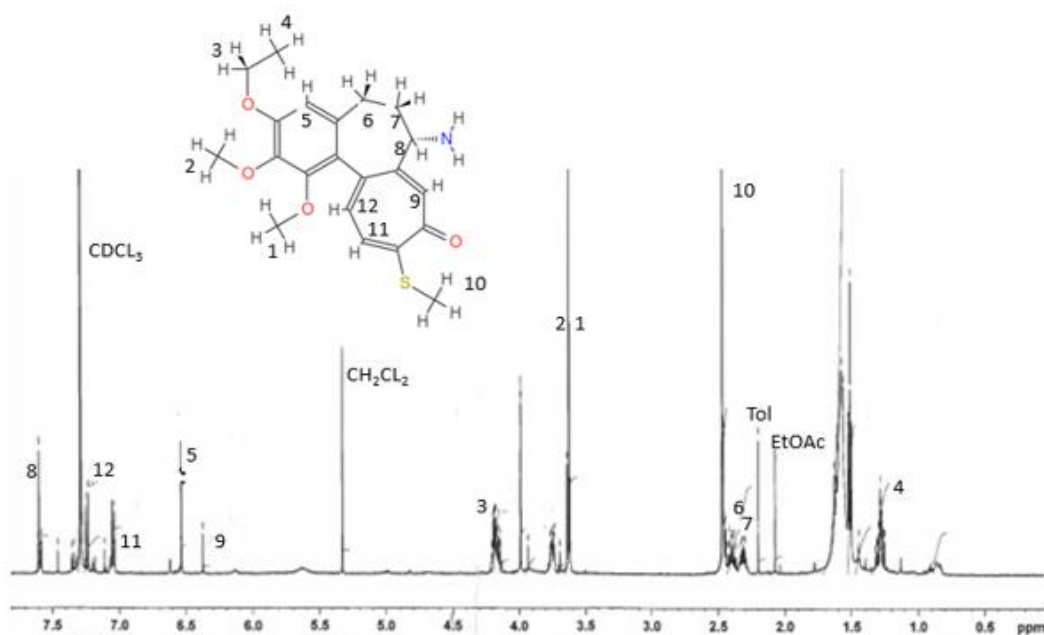


Figure 23. CCI-NH₂ $^1\text{H NMR}$ graph with chemical shifts association.

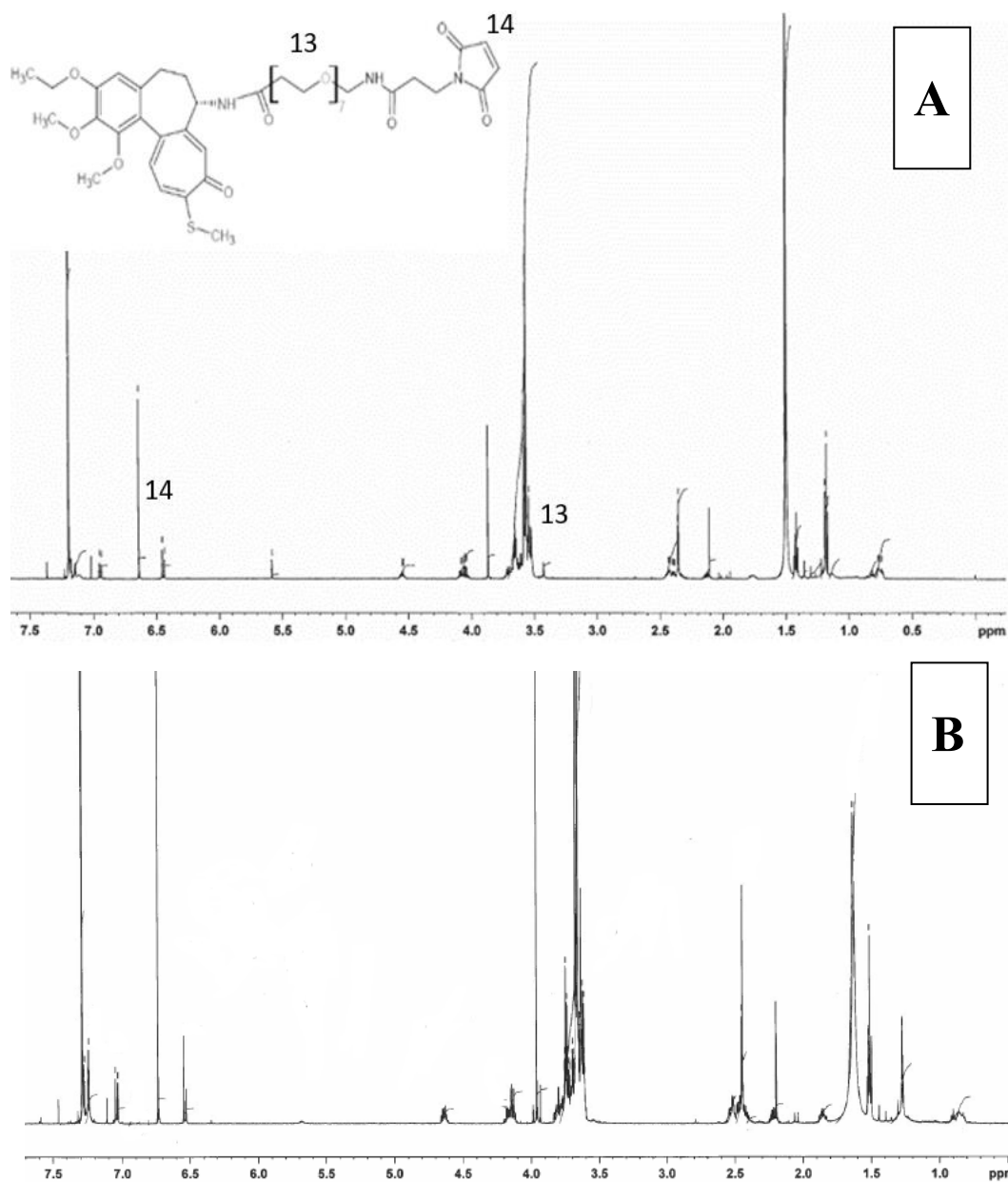


Figure 24. L+D₁ ¹H NMR graph with chemical shifts association. Reaction in THF (A) and in DMF (B).

There are some important points to notice:

- the missing peak 8 after the linker conjugation due to the ‘shield’ effect of the linker molecule.
- Solvents (CH₂Cl₂, Toluene or ethyl acetate) contamination derived by the reaction is reported by the final spectra.

- the integration of the PEG chain peaks (13), when compared to the integration of the peak 11, confirms the reached conjugation.
- regardless of the reaction strategy followed, the final product was the same in both the THF and DMF reactions.

4.1.4 Carbon-13 nuclear magnetic resonance (C-13 NMR)

The C-13 NMR of the CCI-NH₂, when compared to the CCI-001 one, clearly displays the reaction completion as shown in Figure 25.

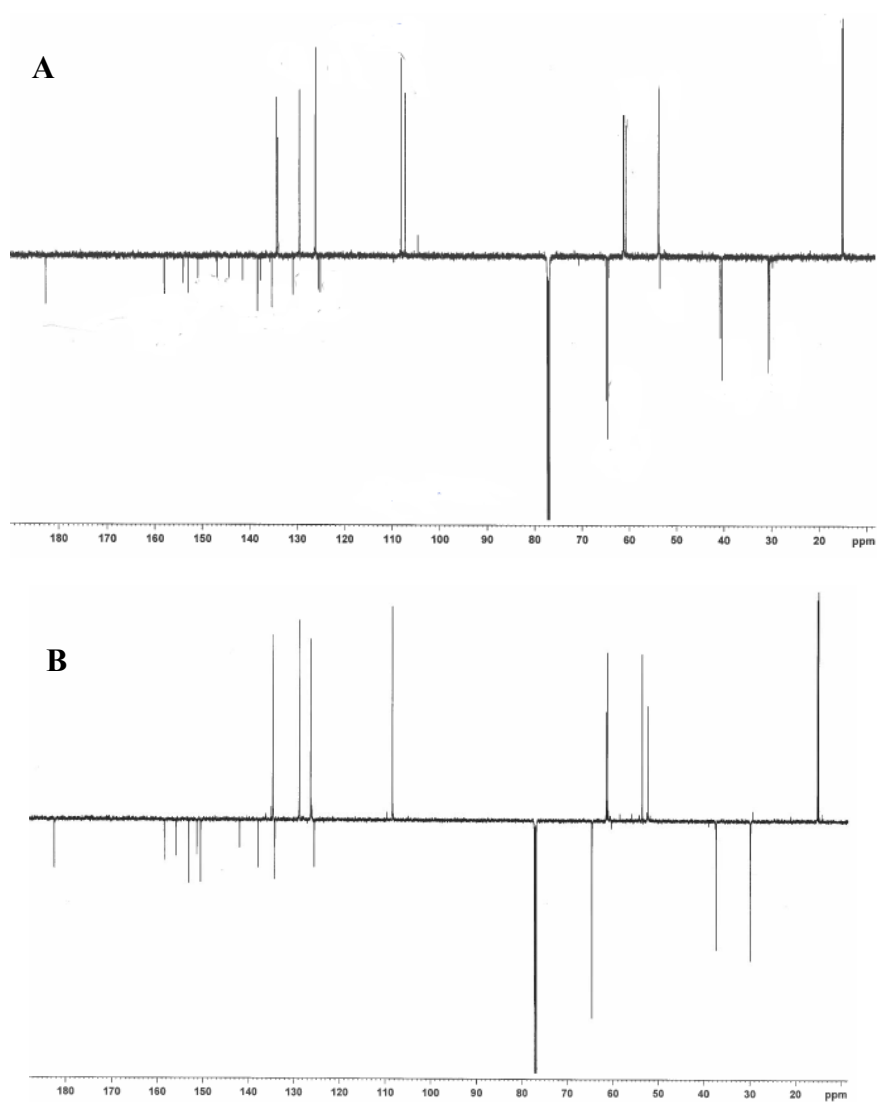


Figure 25. C-13 NMR of CCCI-001 (A) and CCI-NH₂ (B).

4.1.5 Mass spectrometry (MS)

Mass spectrometry, in electrospray ionization mode (Esi), along with the ^1H NMR was used to confirm the reactions outcome. Figure 26A reports the CCI-NH₂ mass spectra. It is evident how, due to the not feasible final purification after the carbamate deprotection reaction, the displayed mass spectra reports several sub-products. Undoubtedly, the harsh reaction conditions were the primary causes of this molecule degradation. However, the most abundant product is still reported. The desired CCI-NH₂, which displays an exact mass of 337.15 u (338.15 m/z as its protonated state) is clearly reported in the graph. On the other hand, in Figure 26B, the expected peak, at 618.263 u, standing for the NHS-PEG7-Mal it doesn't show up among with the other peaks. This outcome could be due to different reasons, such as a mistake in the labelling by the supplier, a too strong ionization method used during the analysis or could be a normal issue speaking of polymeric linkers. Because the exact linker length is unknown, the follow interpretation of the L+D_1 mass spectra become almost impossible. Theoretically, adding to the known linker exact mass provided by the supplier, which was 616.360 u the previous CCI-NH₂ mass, taking into account the hydrolysis of the NHS group (117.042 u) during the binding, the final L+D_1 molecule (C₄₂H₅₈N₂O₁₄S) should have an exact mass of 846.360 u, which is not showed by Figure 26C.

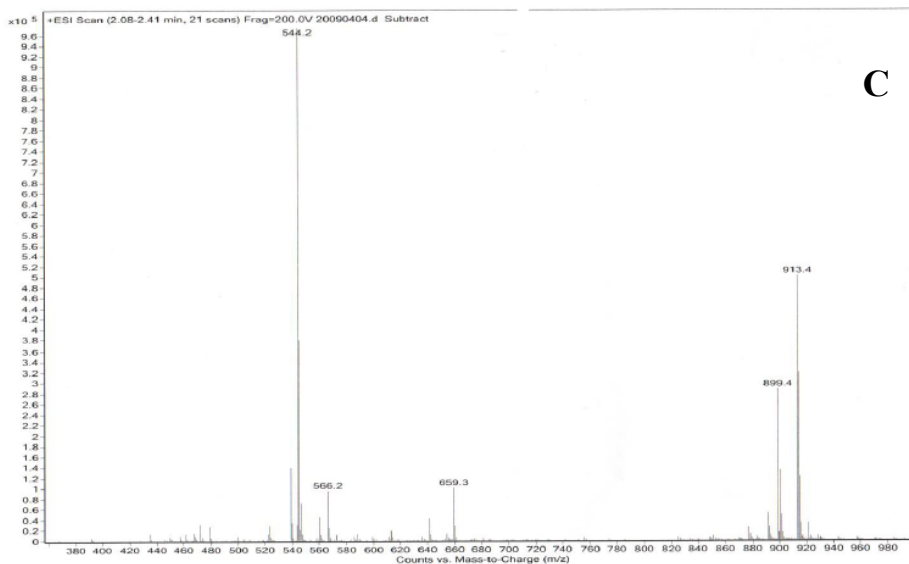
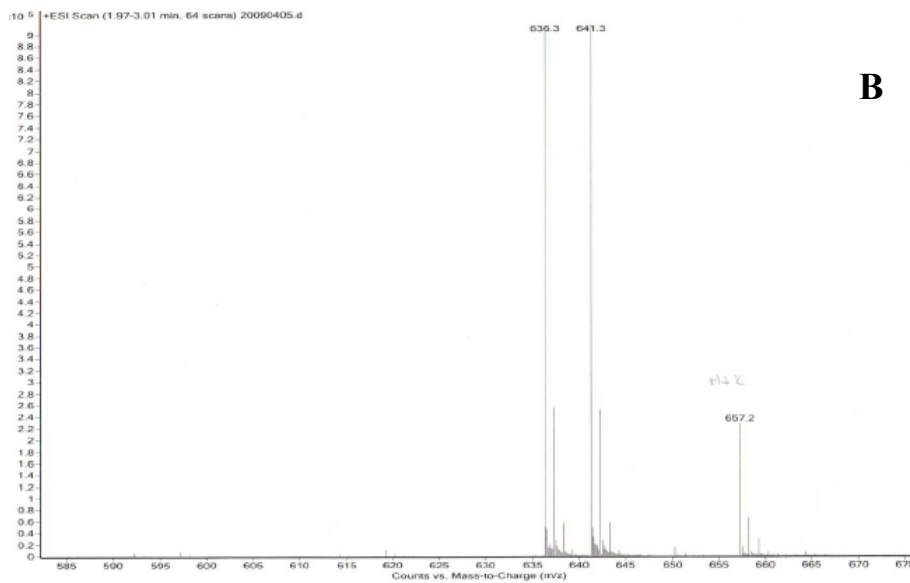
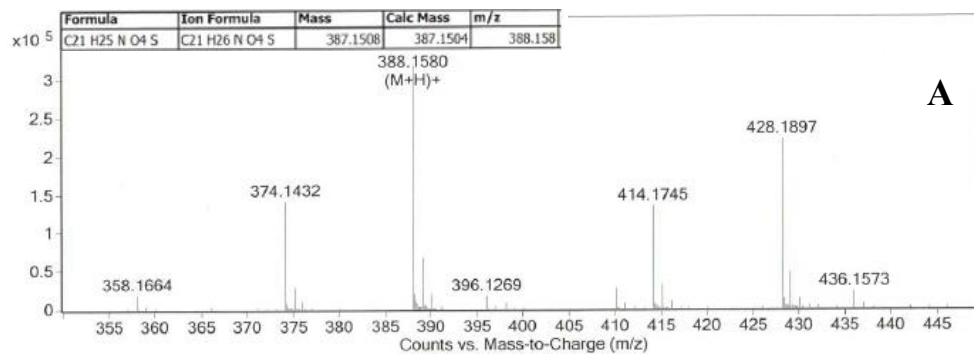


Figure 26. Mass spectra of CCI-NH₂ (A), NHS-PEG₇-Mal linker (B) and L+D₁ (C).

4.1.6 Fourier Transform Infrared Spectroscopy (FTIR)

The infrared spectroscopy was used in order to prove the composition of the obtained products. Mainly, it is fundamental for the monitoring of reaction accomplishment as well as for showing the present functional groups. In this way, Figure 27 reports some association for the more informative peaks. Briefly, peak:

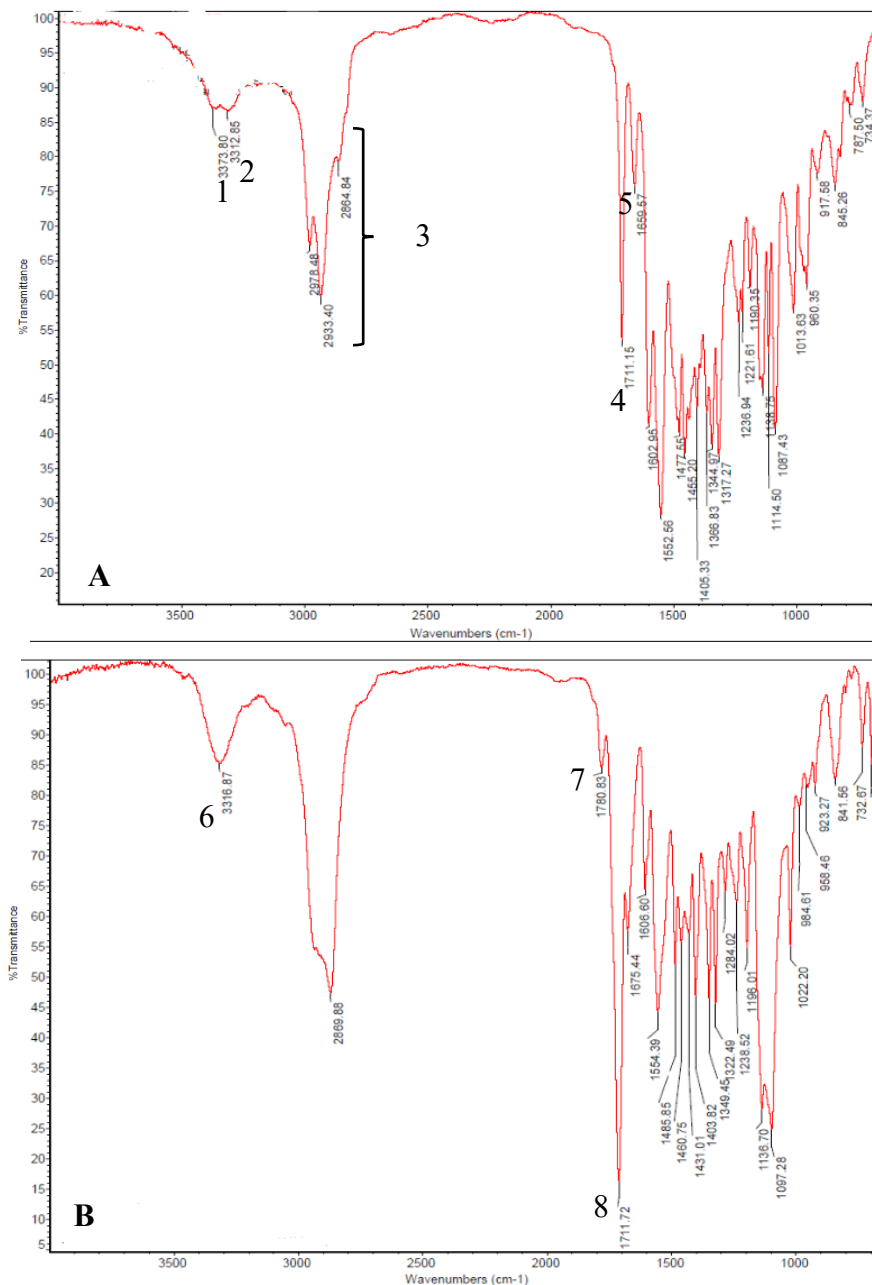


Figure 27. A: FTIR spectra of CCl-NH₂. B: FTIR spectra of L+D₁.

- 1-2: symmetric and asymmetric primary amine stretching, where the asymmetric one has higher energy.
- 3: symmetric and asymmetric aliphatic C-H stretching (2840-3000 cm^{-1}).
- 4: ketone group
- 5: aromatic carbon double bond (C=C).
- 6: secondary ammine stretching after the linker conjugation. The presence of this one peak instead of the previous two peaks confirms the successful outcome.
- 7: maleimide asymmetrical stretching.
- 8: overlapping of the previously ketone detected peak (4) with the maleimide symmetrical stretching.

4.1.7 DAR analysis

Table 7 reports the obtained results for each batch of ADC produced. It is easy to notice how, even if the absolute amount of L+D_1 added for the ADC2 production is more than the one used for the ADC3 production, this last batch had more L+D_1 conjugated to the antibody at the end of the reaction. This results were in accordance with the expectations. The adopted production procedure was the same for all the ADC batches, however, the ADC3 preparation took advantages of a dissolution buffer enriched with EDTA during all the initial steps, not only during the antibody activation as was for the other two batches. The EDTA can prevent the thiol oxidation, which lead to the decrease in L+D_1 conjugation. As described by the procedure section, in order to estimate the ϵ of each compound, the λ_{MAX} was detected. Figure 28 shows the absorbance spectra, within the UV range, for each compound, displaying how the methyl carbamate removal as well as the addition of the pegylated linker didn't affect so much the final λ_{MAX} , which could be considered near to 380 nm each time. In this way, the difference between the L+D_1 and the antibody λ_{MAX} was 100 nm.

Table 7. Summary of the main information about the

Batch	DAR (C_{L+D}/C_{mAb})	L+D_1 molar excess	L+D_1 final concentration
ADC1	0.969	4-fold	10 $\mu\text{g/mL}$
ADC2	1.944	8-fold	20 $\mu\text{g/mL}$
ADC3	2.226	6-fold	25 $\mu\text{g/mL}$

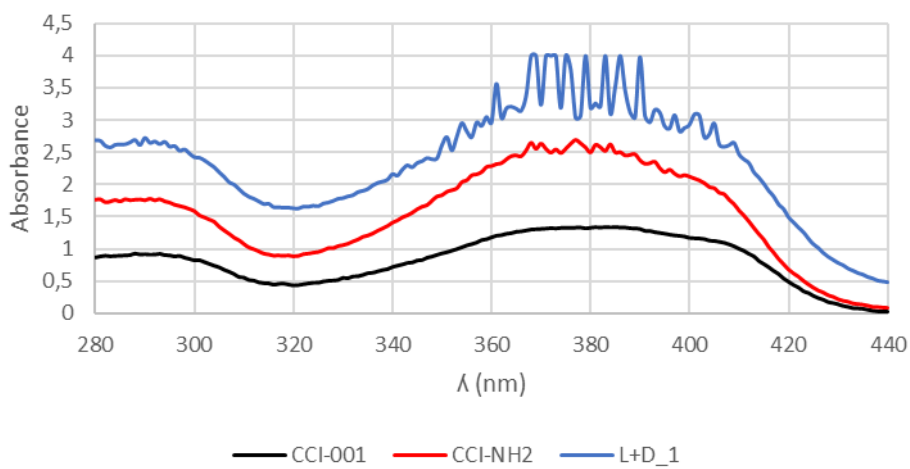


Figure 28. Detected absorbance spectra for the three compounds.

4.1.8 *In-vitro* uptake study

The uptake, comprehensive of the superficial adsorption, was assessed by UV plate reader, observing the dye fluorescence of the. The HCT-116 (EGFR+) and the SW-620 (EGFR-) cell lines were used for this test. As Figure 29 shows, the uptake is higher in the receptor expressing cell lines with a time dependent behaviour. However, even the SW-620 cell line displays a slight absorption due to the other

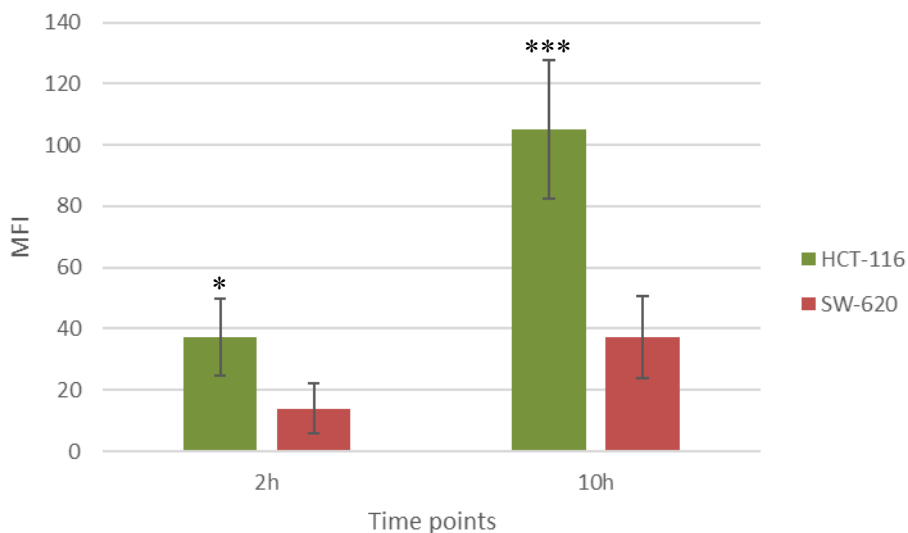


Figure 29. The % of cellular uptake of Cy5 labelled panitumumab after 2 and 10 hours of incubation for the two tested cell lines. Each bar represents average detected fluorescence (%) \pm SD (n=4). Anova test (p = 0.001). * significant at $p < 0.05$, *** significant at $p < 0.005$.

available pathways, reported by the introduction chapter, that could lead to the antibody internalization through non-specific interactions. The Anova test conducted reveal that each of the four data groups is significant different compared to another one.

4.1.9 *In-vitro* cell viability study

The results of *in-vitro* cytotoxicity of CCI-001 versus the cytotoxicity of the synthesized molecules CCI-NH2 and L+D_1 against SW-620, HCT-116 and Panc-1 following 48, 72 hours are reported in Figure 30, while the estimated IC50 values

are reported in Figure 31. As far as the tested ADC1 and ADC2 are concerned, the obtained cell viability values, on the same cell lines, after 92 h incubation are illustrated in Figure 30. As reported, this study was conducted at nanomolar concentrations range for all the treatments, showing how even the newly synthesized molecules were highly cytotoxic at very low concentrations range. The collected results for the CCI-001 cytotoxicity, which was the only treatments not tested in triplicate, were in accordance with the study number 17OL559 carried out by Oncolines™. As far as the ADC case, seems evident how no one of the two tested formulations (ADC1 ADC2) were able to reach the 50% of cell viability. Moreover, there was statistically non-significant difference between the two ADCs (student's t test, $P > 0.05$). Unfortunately, due to a contamination problem, the data for Panc-1 weren't collected in triplicate.

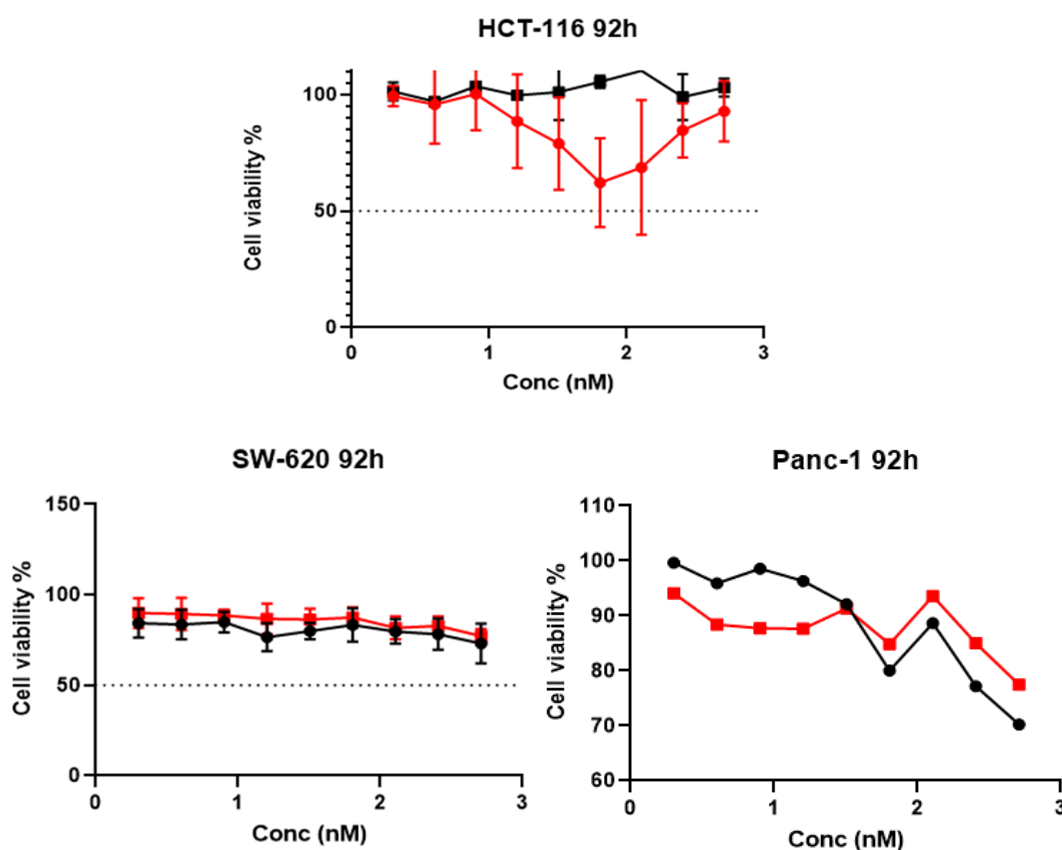


Figure 30. In-vitro cytotoxicity of ADC1 (black circle) and ADC2 (red square) after 92 h incubation.

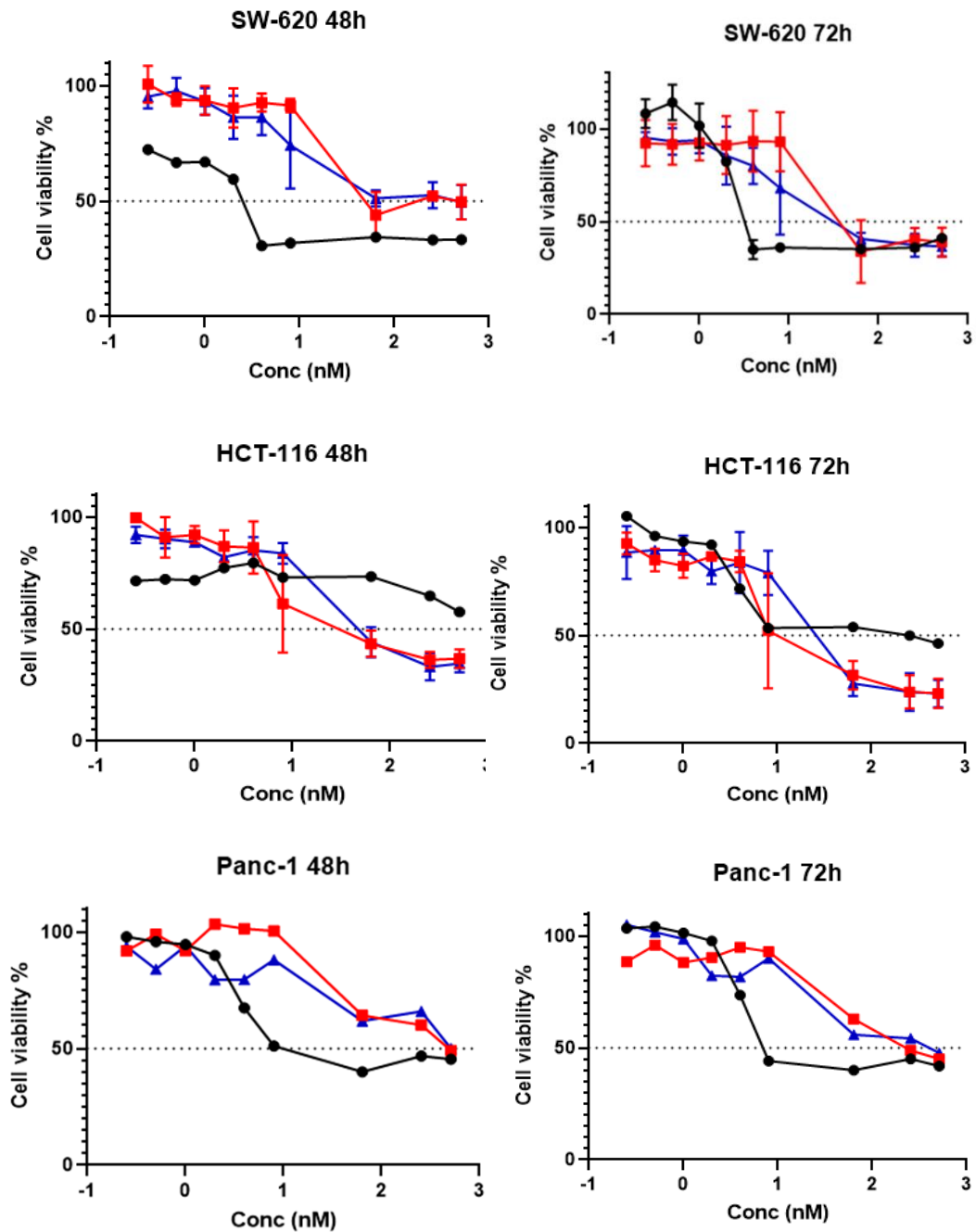


Figure 31. In-vitro cytotoxicity of CCI-001 (black line), CCI-NH2 (red line) and L+D_1 (blue line) on the three studied cell lines. Data represent average \pm SD (n=3) for the HCT-116 and the SW-620 cell lines, while only one repetition is reported for the Panc-1 cell line due to an occurred contamination issue.

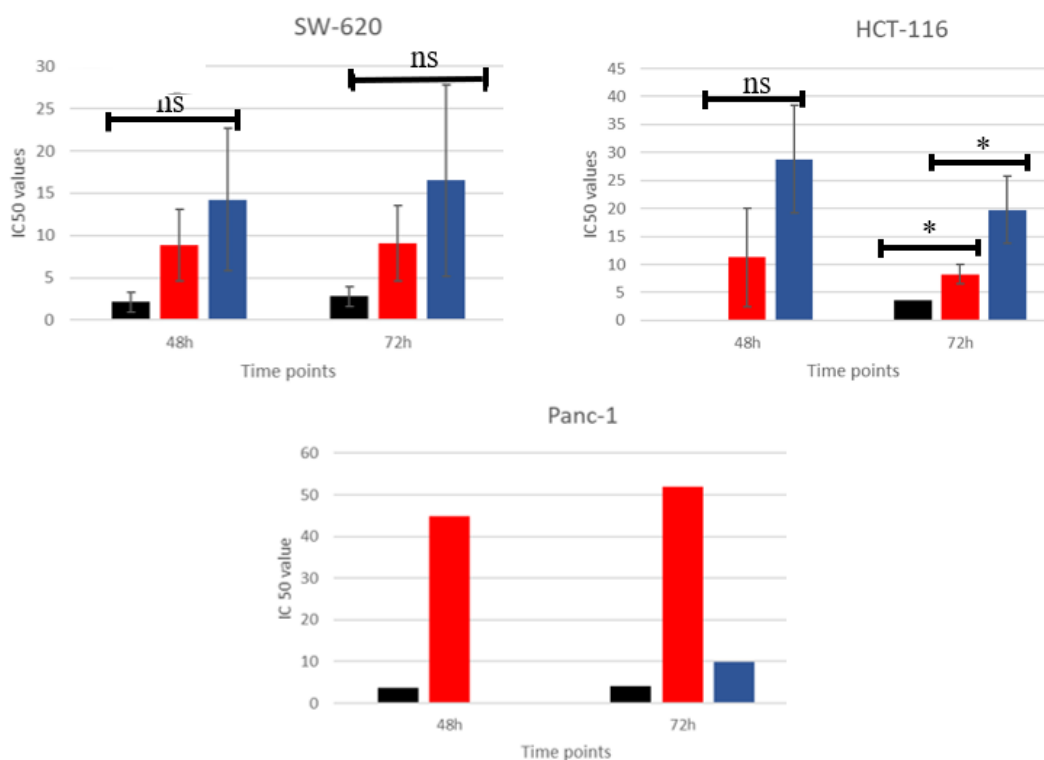


Figure 32. IC 50 values for each treatment on a different cell lines. As the previous graph, the black colour stands for CCI-001, the red one indicates CCI-NH2 and the blue one the L+D_1. Data represent average \pm SD (n=3). * donates statistically significant difference (student's test, $P < 0.05$), while ns donates statistically non-significant (student's t test, $P > 0.05$).

Even though there was no statistic significant difference between the IC50s of the three different treatments, the standard drug was slightly more cytotoxic than the other two molecules. Interestingly, cytotoxicity for the L+D_1 molecule on the Panc-1 was almost affecting as the standard drug, especially if compared with the CCI-NH2. Another consideration takes place realizing that an observable drug effect on the cell lines behaviour was detectable always after at least 48h. Moreover, there was no significant difference in the outcome among the different cell lines as well. Furthermore, the showed cytotoxicity profile as well as the IC50 for the L+D_1 molecule could be lower than the reported one, since the L+D_1 mass spectrometry was showing the presence of some secondary products, which could affect the final molecule potency.

4.1.10 *In-vitro* release study

The *in-vitro* release profile of the L+D_1 molecule from panitumumab was estimated in two different dissolution buffers. However, taking in consideration the dilution factor, the final shape of the release curve was inconclusive. This unexpected behaviour could be related to several reasons such as a non-optimized withdraw strategy or the low sensibility of the used detected method (sensibility of the UV-plate reader $\sim 1 \mu\text{g}$). For all these reasons, Table 8 reports only the final L+D_1 detected concentration outside the bag at the end of 24 hours. The results clearly showed that there was almost no release after one day of buffer incubation. However, the statistical analysis report significant release difference according the different buffer.

Table 8. *In-vitro* final release percentual value of chemically conjugated L+D_1 from panitumumab in different buffers at the end of 24 hours. Each percentage value represents average association (%) \pm SD (n=3). ** donates statistically significant difference (student's test, $P < 0.005$).

Buffer	Initial L+D_1 loaded ($\mu\text{g/mL}$)	Release % average	Standard deviation
BSA (4g/dL)	30	7,50 **	0,305
pH 4.7	30	5,19	0,529

5 Discussion and Conclusion

The main objective of this research was to produce a selective targeted antibody-drug conjugated prepared by chemical conjugation of Panitumumab to a tubulin affected drug, named CCI-001. The final ADC, thanks to its specific antibody, can be internalized only by EGFR containing cells. As far as the biological molecule used in this work, as a monotherapy, it has never showed consistent and durable antitumor efficacy. However, in a combination therapy with other chemotherapeutic agents, the final patient outcome results always considerably improved. To this end, the first task of this work, carried out to readjust the chemical structure of the employed toxic molecule, highlighted the resilience of the methyl carbamate group to be deprotected as well as to undergo to nucleophilic attack by several bases. At the same time, when accomplished, the deprotection seemed to have conferred higher hydrophilicity, preserving the prior cytotoxicity in the nanomolar range. Similarly, once chemically conjugated with the pegylated linker, the new primary amine compound was completely water-soluble (1mg of L+D_1 in 3 mL of DDW). Unfortunately, the final ADC couldn't express improved antigen dependent activity of the drug. Two hypothesis are on the base of this unfavourable outcome. First, the ideally always stable linker adopted for the conjugation, which didn't contain any pH or enzyme sensitive functional groups, which could have led to a fast and reliable payload release. On the other hand, maybe in an *in-vivo* environment this type of system could have shown a sort of liability due to the strong reducing environment within cells, which could lead to the protein degradation. Even a time prolonged ADC administration, which stands for more than just 4 days of treatments, didn't lead to a different result. In the second place, taking advantage of the 2-IT chemical during the conjugation strategy, there was the possibility that newly added sulfuryl groups hindered, on the antibody fab region, the required receptors binding domains, preventing the final mAb recognition as well as the subsequent internalization. Moreover, in this work, the antigen dependent activity of the non-conjugated antibody was successfully assessed. However, there was no experimental evidence to confirm the retained binding ability after the drug conjugation. In this specific case of study, considering unaltered the ADC internalization within the EGFR positive cells, the treatment

efficacy will be related just to the mAb degradation inside the cell since the amine bond between the CCI-NH₂ and the NHS ester is virtually always stable in a biological environment, unless attacked by specific enzymes as amidases. In order to contemplate this case scenario, the release behaviour of the L+D_1 from the antibody has been investigated within two different buffers, with the aim of simulate the biological conditions. The almost absent release found after 24 hours could be the cause of the not effected ADC. Finally, the cytotoxicity of the L+D_1 molecule was assessed within three cell lines, validating its own potency. To sum up all the findings of this work, these proof-of-concept studies encourage further investigation of EGFR-targeted ADCs carrying this newly synthesized compound.

6 Future directions

In this study an initial experimental characterization of the new CCI-001 molecule chemistry as well as an efficient and easy way for the chemical conjugation with an antibody were successfully carried out, leading to an initial *in-vitro* study. However, the shortness of the time spent on this work reserve several improvements, which can be further carried out with the purpose of better develop this theme. The following list reports some of these suggestions for the future work.

- New strategies can be evaluated in order to get done the direct conjugation between the CCI-001 with the linker. Indeed, during the last period of experiments, taking advantage of the organometallic compound (DABAL-Me₃), a yellow sponge like structure was collected from the reaction vial. Unfortunately, the composition of that yellow sponge is still unknown. However, it could worth work in that way, digging the nature of that product, which was hydrophilic.
- An *in-vivo* study of the newly synthesized L+D_1 molecule could be carried out in order to analyse the differences compared to the standard compound, which displays a strong hydrophobic behaviour, limiting the treatment prospects.
- Different linkers, with even different PEG chain length, can be evaluated. Small changes within the PEG chain length result in a huge series of repercussions. For instance, by modulating the cell uptake could increase the dose-limiting aspect, adding less than the 1% of the MWt of the mAb in PEG could lead to an improved plasma pharmacokinetics or avoiding drawbacks in delicate organs such as the liver or the bone marrow [124-125].
- Different linkers with a specific labile motif such as pH, stimuli, acid or enzyme sensitive, if placed in the middle of the pegylated linker could pave the way for a more accurate and predictable release profile. Indeed, being inside the polymeric chain, these types of cleavable motifs don't affect the conjugation reaction chemistry, which it has been already optimized in this work.

- A more complete characterization can be carried out on the obtained ADC1/2/3 taking advantages of different techniques. For instance, the MALDI/TOF analysis to study the mass/charge (m/z) peaks before and after the conjugation, the Mass spectra of the final ADC to better quantify the drug loading and most of all, taking advantage of the Hydrophobic Interaction Chromatography (HIC) as well as the Reversed Phase High-Performance Liquid Chromatography in order to monitor and divide different ratios of payload conjugated within an heterogeneous ADC solution. Such characterization would be the base for allowing an *in-vivo* study using this produced ADC.

7. References

1. Fitzmaurice, C. *et al.* Global, Regional, and National Cancer Incidence, Mortality, Years of Life Lost, Years Lived With Disability, and Disability-Adjusted Life-Years for 29 Cancer Groups, 1990 to 2017. *JAMA Oncol.* **5**, 1749–1768 (2019).
2. Ayala, F. J. & Fitch, W. M. Genetics and the origin of species: An introduction. *Proc. Natl. Acad. Sci. U. S. A.* **94**, 7691–7697 (1997).
3. Vincent, M. Cancer: a de-repression of a default survival program common to all cells?: a life-history perspective on the nature of cancer. *BioEssays News Rev. Mol. Cell. Dev. Biol.* **34**, 72–82 (2012).
4. Zeromski, J. Significance of tumor-cell receptors in human cancer. *Arch. Immunol. Ther. Exp. (Warsz.)* **50**, 105–110 (2002).
5. Kumar Pal, S. & Pegram, M. Epidermal growth factor receptor and signal transduction: potential targets for anti-cancer therapy. *Anticancer. Drugs* **16**, 483–494 (2005).
6. Citri, A. & Yarden, Y. EGF-ERBB signalling: towards the systems level. *Nat. Rev. Mol. Cell Biol.* **7**, 505–516 (2006).
7. Oliveira-Cunha, M., Newman, W. G. & Siriwardena, A. K. Epidermal Growth Factor Receptor in Pancreatic Cancer. *Cancers* **3**, 1513–1526 (2011).
8. Ciardiello, F. & Tortora, G. EGFR antagonists in cancer treatment. *N. Engl. J. Med.* **358**, 1160–1174 (2008).

9. Orth, M. *et al.* Pancreatic ductal adenocarcinoma: biological hallmarks, current status, and future perspectives of combined modality treatment approaches. *Radiat. Oncol.* **14**, 141 (2019).
10. Evolutionary routes and KRAS dosage define pancreatic cancer phenotypes | Nature. <https://www.nature.com/articles/nature25459>.
11. Ying, H. *et al.* Genetics and biology of pancreatic ductal adenocarcinoma. *Genes Dev.* **30**, 355–385 (2016).
12. Hu, Z. I. *et al.* Evaluating Mismatch Repair Deficiency in Pancreatic Adenocarcinoma: Challenges and Recommendations. *Clin. Cancer Res. Off. J. Am. Assoc. Cancer Res.* **24**, 1326–1336 (2018).
13. Distinct epigenetic landscapes underlie the pathobiology of pancreatic cancer subtypes | Nature Communications. <https://www.nature.com/articles/s41467-018-04383-6>.
14. Jiang, H. *et al.* Targeting focal adhesion kinase renders pancreatic cancers responsive to checkpoint immunotherapy. *Nat. Med.* **22**, 851–860 (2016).
15. Daniel, S. K., Sullivan, K. M., Labadie, K. P. & Pillarisetty, V. G. Hypoxia as a barrier to immunotherapy in pancreatic adenocarcinoma. *Clin. Transl. Med.* **8**, 10 (2019).
16. Mahajan, U. M. *et al.* Immune Cell and Stromal Signature Associated With Progression-Free Survival of Patients With Resected Pancreatic Ductal Adenocarcinoma. *Gastroenterology* **155**, 1625-1639.e2 (2018).

17. Nywening, T. M. *et al.* Targeting tumour-associated macrophages with CCR2 inhibition in combination with FOLFIRINOX in patients with borderline resectable and locally advanced pancreatic cancer: a single-centre, open-label, dose-finding, non-randomised, phase 1b trial. *Lancet Oncol.* **17**, 651–662 (2016).
18. Rahn, S. *et al.* Diabetes as risk factor for pancreatic cancer: Hyperglycemia promotes epithelial-mesenchymal-transition and stem cell properties in pancreatic ductal epithelial cells. *Cancer Lett.* **415**, 129–150 (2018).
19. Krüger, A. Premetastatic niche formation in the liver: emerging mechanisms and mouse models. *J. Mol. Med. Berl. Ger.* **93**, 1193–1201 (2015).
20. Wang, S., Huang, S. & Sun, Y. L. Epithelial-Mesenchymal Transition in Pancreatic Cancer: A Review. *BioMed Res. Int.* **2017**, 2646148 (2017).
21. Lee, K. M. *et al.* Class III beta-tubulin, a marker of resistance to paclitaxel, is overexpressed in pancreatic ductal adenocarcinoma and intraepithelial neoplasia. *Histopathology* **51**, 539–546 (2007).
22. Huang, M. *et al.* EGFR-dependent pancreatic carcinoma cell metastasis through Rap1 activation. *Oncogene* **31**, 2783–2793 (2012).
23. Ardito, C. M. *et al.* EGF Receptor Is Required for KRAS-Induced Pancreatic Tumorigenesis. *Cancer Cell* **22**, 304–317 (2012).
24. Rembielak, A. I. *et al.* Phase II Trial of Cetuximab and Conformal Radiotherapy Only in Locally Advanced Pancreatic Cancer with Concurrent Tissue Sampling Feasibility Study. *Transl. Oncol.* **7**, 55–64 (2014).

25. Dunn, G. P., Bruce, A. T., Ikeda, H., Old, L. J. & Schreiber, R. D. Cancer immunoediting: from immunosurveillance to tumor escape. *Nat. Immunol.* **3**, 991–998 (2002).
26. Dong, H. *et al.* Tumor-associated B7-H1 promotes T-cell apoptosis: a potential mechanism of immune evasion. *Nat. Med.* **8**, 793–800 (2002).
27. Pandha, H., Rigg, A., John, J. & Lemoine, N. Loss of expression of antigen-presenting molecules in human pancreatic cancer and pancreatic cancer cell lines. *Clin. Exp. Immunol.* **148**, 127–135 (2007).
28. Tumor-derived Granulocyte-Macrophage Colony-Stimulating Factor Regulates Myeloid Inflammation and T Cell Immunity in Pancreatic Cancer - PubMed. <https://pubmed.ncbi.nlm.nih.gov/22698406/>.
29. Joyce, J. A. & Fearon, D. T. T cell exclusion, immune privilege, and the tumor microenvironment. *Science* **348**, 74–80 (2015).
30. Pardoll, D. M. The blockade of immune checkpoints in cancer immunotherapy. *Nat. Rev. Cancer* **12**, 252–264 (2012).
31. Royal, R. E. *et al.* Phase 2 trial of single agent Ipilimumab (anti-CTLA-4) for locally advanced or metastatic pancreatic adenocarcinoma. *J. Immunother. Hagerstown Md 1997* **33**, 828–833 (2010).
32. Brahmer, J. R. *et al.* Safety and Activity of Anti-PD-L1 Antibody in Patients with Advanced Cancer. *N. Engl. J. Med.* **366**, 2455–2465 (2012).

33. Jacobetz, M. A. *et al.* Hyaluronan impairs vascular function and drug delivery in a mouse model of pancreatic cancer. *Gut* **62**, 112–120 (2013).
34. Hingorani, S. R. *et al.* HALO 202: Randomized Phase II Study of PEGPH20 Plus Nab-Paclitaxel/Gemcitabine Versus Nab-Paclitaxel/Gemcitabine in Patients With Untreated, Metastatic Pancreatic Ductal Adenocarcinoma. *J. Clin. Oncol. Off. J. Am. Soc. Clin. Oncol.* **36**, 359–366 (2018).
35. Özdemir, B. C. *et al.* Depletion of carcinoma-associated fibroblasts and fibrosis induces immunosuppression and accelerates pancreas cancer with reduced survival. *Cancer Cell* **25**, 719–734 (2014).
36. Schnurr, M. *et al.* Strategies to relieve immunosuppression in pancreatic cancer. *Immunotherapy* **7**, 363–376 (2015).
37. Kindler, H. L. *et al.* Gemcitabine plus bevacizumab compared with gemcitabine plus placebo in patients with advanced pancreatic cancer: phase III trial of the Cancer and Leukemia Group B (CALGB 80303). *J. Clin. Oncol. Off. J. Am. Soc. Clin. Oncol.* **28**, 3617–3622 (2010).
38. Yu, M. *et al.* Mitochondrial fusion exploits a therapeutic vulnerability of pancreatic cancer. *JCI Insight* **5**, (2019).
39. Brinkley, W. Microtubules: a brief historical perspective. *J. Struct. Biol.* **118**, 84–86 (1997).
40. Löwe, J., Li, H., Downing, K. H. & Nogales, E. Refined structure of $\alpha\beta$ -tubulin at 3.5 Å resolution¹Edited by I. A. Wilson. *J. Mol. Biol.* **313**, 1045–1057 (2001).

41. Margolis, R. L., Wilson, L. & Kiefer, B. I. Mitotic mechanism based on intrinsic microtubule behaviour. *Nature* **272**, 450–452 (1978).
42. Mitchison, T. & Kirschner, M. Dynamic instability of microtubule growth. *Nature* **312**, 237–242 (1984).
43. Cooper, G. M. Microtubules. *Cell Mol. Approach 2nd Ed.* (2000).
44. Parker, A. L., Kavallaris, M. & McCarroll, J. A. Microtubules and Their Role in Cellular Stress in Cancer. *Front. Oncol.* **4**, (2014).
45. Person, F. *et al.* Prevalence of β III-tubulin (TUBB3) expression in human normal tissues and cancers. *Tumour Biol. J. Int. Soc. Oncodevelopmental Biol. Med.* **39**, 1010428317712166 (2017).
46. Teo, J. *et al.* A Rationally Optimized Nanoparticle System for the Delivery of RNA Interference Therapeutics into Pancreatic Tumors in Vivo. *Biomacromolecules* **17**, 2337–2351 (2016).
47. Stengel, C. *et al.* Class III beta-tubulin expression and in vitro resistance to microtubule targeting agents. *Br. J. Cancer* **102**, 316–324 (2010).
48. Huzil, J. T., Chen, K., Kurgan, L. & Tuszynski, J. A. The Roles of β -Tubulin Mutations and Isozyme Expression in Acquired Drug Resistance. *Cancer Inform.* **3**, 117693510700300030 (2007).
49. McCarroll, J. A. *et al.* β III-tubulin: a novel mediator of chemoresistance and metastases in pancreatic cancer. *Oncotarget* **6**, 2235–2249 (2015).

50. Wani, M. C., Taylor, H. L., Wall, M. E., Coggon, P. & McPhail, A. T. Plant antitumor agents. VI. The isolation and structure of taxol, a novel antileukemic and antitumor agent from *Taxus brevifolia*. *J. Am. Chem. Soc.* **93**, 2325–2327 (1971).
51. Schiff, P. B., Fant, J. & Horwitz, S. B. Promotion of microtubule assembly in vitro by taxol. *Nature* **277**, 665–667 (1979).
52. Wani, M. C. & Horwitz, S. B. Nature as a Remarkable Chemist: A Personal Story of the Discovery and Development of Taxol®. *Anticancer. Drugs* **25**, 482–487 (2014).
53. Rowinsky, E. The Vinca Alkaloids. *Holl.-Frei Cancer Med. 6th Ed.* (2003).
54. Sternlicht, H., Ringel, I. & Szasz, J. Theory for modeling the copolymerization of tubulin and tubulin-colchicine complex. *Biophys. J.* **42**, 255–267 (1983).
55. Martínez, G. J., Celermajer, D. S. & Patel, S. The NLRP3 inflammasome and the emerging role of colchicine to inhibit atherosclerosis-associated inflammation. *Atherosclerosis* **269**, 262–271 (2018).
56. Tropp, B. E. *Molecular Biology: Genes to Proteins.* (Jones & Bartlett Learning, 2008).
57. Ravelli, R. B. G. *et al.* Insight into tubulin regulation from a complex with colchicine and a stathmin-like domain. *Nature* **428**, 198–202 (2004).
58. Kumbhar, B. V., Borogaon, A., Panda, D. & Kunwar, A. Exploring the Origin of Differential Binding Affinities of Human Tubulin Isoforms $\alpha\beta$ II, $\alpha\beta$ III and

- $\alpha\beta$ IV for DAMA-Colchicine Using Homology Modelling, Molecular Docking and Molecular Dynamics Simulations. *PLOS ONE* **11**, e0156048 (2016).
59. Andreu, J. M., Perez-Ramirez, B., Gorbunoff, M. J., Ayala, D. & Timasheff, S. N. Role of the colchicine ring A and its methoxy groups in the binding to tubulin and microtubule inhibition. *Biochemistry* **37**, 8356–8368 (1998).
60. Oakley, B. R., Oakley, C. E., Yoon, Y. & Jung, M. K. Gamma-tubulin is a component of the spindle pole body that is essential for microtubule function in *Aspergillus nidulans*. *Cell* **61**, 1289–1301 (1990).
61. Cosentino, L. *et al.* Synthesis and Biological Evaluation of Colchicine B-Ring Analogues Tethered with Halogenated Benzyl Moieties. *J. Med. Chem.* **55**, 11062–11066 (2012).
62. Lin, C. M. *et al.* Interactions of tubulin with potent natural and synthetic analogs of the antimitotic agent combretastatin: a structure-activity study. *Mol. Pharmacol.* **34**, 200–208 (1988).
63. Banwell, M. G. *et al.* Semisyntheses, X-Ray Crystal Structures and Tubulin-Binding Properties of 7-Oxodeacetamidocolchicine and 7-Oxodeacetamidoisocolchicine. *Aust. J. Chem.* **45**, 1577–1588 (1992).
64. Sharom, F. Complex Interplay between the P-Glycoprotein Multidrug Efflux Pump and the Membrane: Its Role in Modulating Protein Function. *Front. Oncol.* **4**, 41 (2014).

65. Singh, B. *et al.* Colchicine derivatives with potent anticancer activity and reduced P-glycoprotein induction liability. *Org. Biomol. Chem.* **13**, 5674–5689 (2015).
66. Yeh, L.-C. C. *et al.* Effect of CH-35, a novel anti-tumor colchicine analogue, on breast cancer cells overexpressing the β III isotype of tubulin. *Invest. New Drugs* **34**, 129–137 (2016).
67. Abstract 2663: CR42-24, a novel colchicine derivative, a therapeutic for bladder cancer | Cancer Research. https://cancerres.aacrjournals.org/content/78/13_Supplement/2663.
68. Liu, R., Wang, R. E. & Wang, F. Antibody-drug conjugates for non-oncological indications. *Expert Opin. Biol. Ther.* **16**, 591–593 (2016).
69. Shen, J. & Attar, M. Antibody-Drug Conjugate (ADC) Research in Ophthalmology—a Review. *Pharm. Res.* **32**, 3572–3576 (2015).
70. DeVita, V. T. & Chu, E. A history of cancer chemotherapy. *Cancer Res.* **68**, 8643–8653 (2008).
71. Chang, A. J., De Silva, R. A. & Lapi, S. E. Development and characterization of ^{89}Zr -labeled panitumumab for immuno-positron emission tomographic imaging of the epidermal growth factor receptor. *Mol. Imaging* **12**, 17–27 (2013).
72. Mullard, A. 2019 FDA drug approvals. *Nat. Rev. Drug Discov.* **19**, 79–84 (2020).

73. Babcook, J. S., Leslie, K. B., Olsen, O. A., Salmon, R. A. & Schrader, J. W. A novel strategy for generating monoclonal antibodies from single, isolated lymphocytes producing antibodies of defined specificities. *Proc. Natl. Acad. Sci. U. S. A.* **93**, 7843–7848 (1996).
74. Antibody Modification and Conjugation - ScienceDirect.
<https://www.sciencedirect.com/science/article/pii/B9780123822390000200?via%3Dihub>.
75. P, A. & ey. Antibody or Immunoglobulin. *Microbiology Notes*
<https://microbiologynotes.org/antibody-or-immunoglobulin/> (2020).
76. Hocking, C. M. & Price, T. J. Panitumumab in the management of patients with KRAS wild-type metastatic colorectal cancer. *Ther. Adv. Gastroenterol.* **7**, 20–37 (2014).
77. García-Foncillas, J. *et al.* Distinguishing Features of Cetuximab and Panitumumab in Colorectal Cancer and Other Solid Tumors. *Front. Oncol.* **9**, 849 (2019).
78. Yang, B.-B. *et al.* Pharmacokinetic and pharmacodynamic perspectives on the clinical drug development of panitumumab. *Clin. Pharmacokinet.* **49**, 729–740 (2010).
79. NICE Expands Positive Recommendation for Erbitux as First-line Treatment for RAS Wild-type mCRC. *OTS.at*
https://www.ots.at/presseaussendung/OTE_20170302_OTE0001/nice-

expands-positive-recommendation-for-erbitux-as-first-line-treatment-for-ras-wild-type-mcrc.

80. Giannopoulou, E., Antonacopoulou, A., Matsouka, P. & Kalofonos, H. P. Autophagy: novel action of panitumumab in colon cancer. *Anticancer Res.* **29**, 5077–5082 (2009).
81. Wild-type KRAS is required for panitumumab efficacy in patients with metastatic colorectal cancer - PubMed. <https://pubmed.ncbi.nlm.nih.gov/18316791/>.
82. Medicinal Plants and Cancer Chemoprevention. <https://www.ncbi.nlm.nih.gov/pmc/articles/PMC4160808/>.
83. Effects of Drug-Antibody Ratio on Pharmacokinetics, Biodistribution, Efficacy, and Tolerability of Antibody-Maytansinoid Conjugates. - PubMed - NCBI. <https://www.ncbi.nlm.nih.gov/pubmed/28388844>.
84. Adem, Y. T. *et al.* Auristatin Antibody Drug Conjugate Physical Instability and the Role of Drug Payload. *Bioconjug. Chem.* **25**, 656–664 (2014).
85. Hamblett, K. J. *et al.* Effects of drug loading on the antitumor activity of a monoclonal antibody drug conjugate. *Clin. Cancer Res. Off. J. Am. Assoc. Cancer Res.* **10**, 7063–7070 (2004).
86. Tumey, L. N. *et al.* Site Selection: a Case Study in the Identification of Optimal Cysteine Engineered Antibody Drug Conjugates. *AAPS J.* **19**, 1123–1135 (2017).

87. Lewis Phillips, G. D. *et al.* Targeting HER2-positive breast cancer with trastuzumab-DM1, an antibody-cytotoxic drug conjugate. *Cancer Res.* **68**, 9280–9290 (2008).
88. Chari, R. V. J. Targeted cancer therapy: conferring specificity to cytotoxic drugs. *Acc. Chem. Res.* **41**, 98–107 (2008).
89. Gemtuzumab ozogamicin, a potent and selective anti-CD33 antibody-calicheamicin conjugate for treatment of acute myeloid leukemia. - PubMed - NCBI. <https://www.ncbi.nlm.nih.gov/pubmed/11792178>.
90. Zhang, D. *et al.* Catalytic Cleavage of Disulfide Bonds in Small Molecules and Linkers of Antibody–Drug Conjugates. *Drug Metab. Dispos.* **47**, 1156–1163 (2019).
91. Anami, Y. *et al.* Glutamic acid–valine–citrulline linkers ensure stability and efficacy of antibody–drug conjugates in mice. *Nat. Commun.* **9**, 1–9 (2018).
92. Wei, B. *et al.* Discovery of Peptidomimetic Antibody–Drug Conjugate Linkers with Enhanced Protease Specificity. *J. Med. Chem.* **61**, 989–1000 (2018).
93. Lyon, R. P. *et al.* Reducing hydrophobicity of homogeneous antibody-drug conjugates improves pharmacokinetics and therapeutic index. *Nat. Biotechnol.* **33**, 733–735 (2015).
94. β -Glucuronidase-responsive prodrugs for selective cancer chemotherapy: an update. - PubMed - NCBI. <https://www.ncbi.nlm.nih.gov/pubmed/24480360>.

95. Kolodych, S. *et al.* Development and evaluation of β -galactosidase-sensitive antibody-drug conjugates. *Eur. J. Med. Chem.* **142**, 376–382 (2017).
96. Kern, J. C. *et al.* Discovery of Pyrophosphate Diesters as Tunable, Soluble, and Bioorthogonal Linkers for Site-Specific Antibody–Drug Conjugates. *J. Am. Chem. Soc.* **138**, 1430–1445 (2016).
97. Badescu, G. *et al.* Bridging disulfides for stable and defined antibody drug conjugates. *Bioconjug. Chem.* **25**, 1124–1136 (2014).
98. Maruani, A. *et al.* A plug-and-play approach to antibody-based therapeutics via a chemoselective dual click strategy. *Nat. Commun.* **6**, 1–9 (2015).
99. Alley, S. C. *et al.* Contribution of linker stability to the activities of anticancer immunoconjugates. *Bioconjug. Chem.* **19**, 759–765 (2008).
100. Junutula, J. R. *et al.* Site-specific conjugation of a cytotoxic drug to an antibody improves the therapeutic index. *Nat. Biotechnol.* **26**, 925–932 (2008).
101. Li, X. *et al.* Stable and Potent Selenomab-Drug Conjugates. *Cell Chem. Biol.* **24**, 433-442.e6 (2017).
102. Kolb, H. C., Finn, M. G. & Sharpless, K. B. Click Chemistry: Diverse Chemical Function from a Few Good Reactions. *Angew. Chem. Int. Ed.* **40**, 2004–2021 (2001).
103. Nair, D. P. *et al.* The Thiol-Michael Addition Click Reaction: A Powerful and Widely Used Tool in Materials Chemistry. *Chem. Mater.* **26**, 724–744 (2014).

104. Ross, P. L. & Wolfe, J. L. Physical and Chemical Stability of Antibody Drug Conjugates: Current Status. *J. Pharm. Sci.* **105**, 391–397 (2016).
105. Tumeý, L. N. *et al.* Mild Method for Succinimide Hydrolysis on ADCs: Impact on ADC Potency, Stability, Exposure, and Efficacy. *Bioconjug. Chem.* **25**, 1871–1880 (2014).
106. Pk, M. *et al.* Potential mechanisms of target-independent uptake and toxicity of antibody-drug conjugates. *Pharmacology & therapeutics* vol. 200 <https://pubmed.ncbi.nlm.nih.gov/31028836/> (2019).
107. Mahalingaiah, P. K. *et al.* Potential mechanisms of target-independent uptake and toxicity of antibody-drug conjugates. *Pharmacol. Ther.* **200**, 110–125 (2019).
108. Han, S., Kim, C. & Kwon, D. Thermal/oxidative degradation and stabilization of polyethylene glycol. *Polymer* **38**, 317–323 (1997).
109. Friman, S., Egestad, B., Sjövall, J. & Svanvik, J. Hepatic excretion and metabolism of polyethylene glycols and mannitol in the cat. *J. Hepatol.* **17**, 48–55 (1993).
110. Ulbricht, J., Jordan, R. & Luxenhofer, R. On the biodegradability of polyethylene glycol, polypeptoids and poly(2-oxazoline)s. *Biomaterials* **35**, 4848–4861 (2014).
111. Burke, P. J. *et al.* Optimization of a PEGylated Glucuronide-Monomethylauristatin E Linker for Antibody-Drug Conjugates. *Mol. Cancer Ther.* **16**, 116–123 (2017).

112. Lehmann, F. & Scobie, M. Rapid and Convenient Microwave-Assisted Synthesis of Primary Amines via Reductive N - Alkylation of Methyl Carbamate with Aldehydes. *Synthesis* **2008**, 1679–1681 (2008).
113. MacMillan, J. Basic hydrolysis of carbamate to amine in aqueous ethanol. <https://cssp.chemspider.com/article.aspx?id=734> (2014) doi:10.1039/SP734.
114. Full article: Efficient Synthesis of Doxorubicin Melanotransferrin p97 Conjugates Through SMCC Linker. <https://www.tandfonline.com/doi/full/10.1081/SCC-120039494>.
115. Kang, S. & Kim, H.-K. Facile direct synthesis of unsymmetrical ureas from N-Alloc-, N-Cbz-, and N-Boc-protected amines using DABAL-Me₃. *Tetrahedron* **74**, 4036–4046 (2018).
116. Amide Bond Formation Using an Air-Stable Source of AlMe₃. | Request PDF. *ResearchGate*
https://www.researchgate.net/publication/244233963_Amide_Bond_Formation_Using_an_Air-Stable_Source_of_AlMe3 doi:10.1016/j.tetlet.2006.06.004.
117. Gallou, I., Eriksson, M., Zeng, X., Senanayake, C. & Farina, V. Practical Synthesis of Unsymmetrical Ureas from Isopropenyl Carbamates. *J. Org. Chem.* **70**, 6960–6963 (2005).
118. Deokar, H., Chaskar, J. & Chaskar, A. Synthesis and Antimicrobial Activity Evaluation of Novel Oxadiazino/Thiadiazino-Indole and Oxadiazole/Thiadiazole Derivatives of 2-Oxo-2H-benzopyran. *J. Heterocycl. Chem.* **51**, 719–725 (2014).

119. Swenson, R., Raju, N., Estrella-Jimenez, M. & Ramalingam, K. Jte013
Analogues and Methods of Making and Using Same. (2011).
120. Protocols for Lysine Conjugation | Springer Nature Experiments.
https://experiments.springernature.com/articles/10.1007/978-1-62703-541-5_10.
121. Ellmans Test Protocol. 2.
122. Ducry, L. & Stump, B. Antibody-drug conjugates: linking cytotoxic payloads to monoclonal antibodies. *Bioconjug. Chem.* **21**, 5–13 (2010).
123. NHS ester labeling of amino biomolecules. 2.
124. Simmons, J. K., Burke, P. J., Cochran, J. H., Pittman, P. G. & Lyon, R. P. Reducing the antigen-independent toxicity of antibody-drug conjugates by minimizing their non-specific clearance through PEGylation. *Toxicol. Appl. Pharmacol.* **392**, 114932 (2020).
125. Gupta, N. *et al.* Development of a facile antibody–drug conjugate platform for increased stability and homogeneity. *Chem. Sci.* **8**, 2387–2395 (2017).